

2018

Environmental Factors Affecting Methane Cycling in Narragansett Bay

Christopher James McAleer
University of Rhode Island, chris_mcaleer@uri.edu

Follow this and additional works at: <https://digitalcommons.uri.edu/theses>

Terms of Use

All rights reserved under copyright.

Recommended Citation

McAleer, Christopher James, "Environmental Factors Affecting Methane Cycling in Narragansett Bay" (2018). *Open Access Master's Theses*. Paper 1250.
<https://digitalcommons.uri.edu/theses/1250>

This Thesis is brought to you by the University of Rhode Island. It has been accepted for inclusion in Open Access Master's Theses by an authorized administrator of DigitalCommons@URI. For more information, please contact digitalcommons-group@uri.edu. For permission to reuse copyrighted content, contact the author directly.

ENVIRONMENTAL FACTORS AFFECTING METHANE
CYCLING IN NARRAGANSETT BAY

BY

CHRISTOPHER JAMES MCALEER

A THESIS SUBMITTED IN PARTIAL FULFILLMENT OF THE
REQUIREMENTS FOR THE DEGREE OF
MASTER OF SCIENCE
IN
OCEANOGRAPHY

UNIVERSITY OF RHODE ISLAND

2018

MASTER OF SCIENCE THESIS
OF
CHRISTOPHER JAMES MCALEER

APPROVED:

Thesis Committee:

Major Professor Brice Loose

Candace Oviatt

Serena Moseman-Valtierra

Nasser H. Zawia

DEAN OF THE GRADUATE SCHOOL

UNIVERSITY OF RHODE ISLAND
2018

ABSTRACT

Wetlands and estuaries are strong sources of methane to the atmosphere due to high rates of methanogenesis. These environments contain diverse and extensive microbial communities that are responsible for processing organic matter, with tidal flow responsible for exchange between marine, freshwater, and estuarine sources. While most methane is produced in sediment, as methanogenic Archaea generally require anoxic conditions, methane oxidizing bacteria (methanotrophs) regulate emissions in oxygenated waters through the consumption of methane. Therefore, flood tide has the potential to provide wetlands – salt marshes, in particular – with organic matter and methanotrophic communities, creating a unique environment which features the co-occurrence of both methanogenesis and methanotrophy. Ebb tide would then be responsible for the transport of methane and potentially microbial communities to nearby waters. There has been limited research investigating the importance of salt marshes to marine methane cycling.

The objective of this thesis is to study the spatial and temporal distribution of methane in Narragansett Bay and investigate the role of salt marshes in bay cycling under various environmental conditions using stable isotope analysis. This was achieved through incubations of porewater and outlet samples collected from Fox Hill salt marsh in December (7°C water), March (2°C), and May (17°C) during ebb tide, with discrete monitoring of CH₄, CO₂, and CH₄ δ¹³C. Methanogenesis was limited in anoxic samples, largely due to its inhibition by the presence of sulfate reducing bacteria and the lack of sediment in sample vessels, although there was some evidence for the hydrogenotrophic mechanism of production. Oxidation occurred in 7°C and 17°C oxygenated outlet

samples, as well as 17°C marsh porewater samples, though only after a lag period of at least 30 days. The lag likely reflects the presence of facultative methanotrophs in Narragansett Bay, in which methane oxidation occurs only after preferential substrates are consumed. Rates of CH₄ oxidation and microbial respiration, through observed production of CO₂, were significantly correlated with temperature indicating seasonal changes in methane cycling, also evidenced by the lack of activity in all 2°C samples and greater abundance of methanotrophs at 17°C, determined by quantitative PCR. Higher methane oxidation rates in marsh outlet samples reflected the greater degradability of marine organic sources over marsh organic material, indicating that flood tide is crucial for the input of bioavailable organic material to salt marsh microbial communities.

The spatial and temporal distribution of methane was investigated through shipboard samplings from the Providence River to the mouth of Narragansett Bay and the implementation of a time-series study monitoring methane at a fixed location from May to July, respectively. Methane concentrations varied inverse to the salinity gradient, with high concentrations (96 nM) at the river mouth suggesting a significant freshwater source. Freshwater methane was likely the results of wastewater treatment plant effluent and increased methanogenesis due to an absence of sulfate reducing bacteria. Methane concentrations throughout Narragansett Bay were found to be supersaturated with respect to the atmosphere due to freshwater input (including wastewater) and marsh and sediment methanogenesis influence. Principal component analysis of time-series data confirmed the seasonality of methane in Narragansett Bay, as methane concentrations increased with temperature from Spring into Summer as

wind speed decreased. Tidal influence was also evident in time-series data, with an observed anticorrelation between methane and both tidal height and salinity.

The contribution of salt marshes to Narragansett Bay was determined to be $2.4 \times 10^5 \text{ mol year}^{-1}$, computed from data collected continuously by a moored CTD at Fox Hill salt marsh outlet. With the limited methanotrophy that occurred in incubation samples, it is probable that the majority of the methane contribution from salt marshes is emitted rather than oxidized in Narragansett Bay.

ACKNOWLEDGMENTS

First and foremost, I would like to extend a sincere thank you to Brice Loose for his guidance throughout this project and his dedication to teaching in the lab and classroom. I would also like to thank my committee members Candace Oviatt and Serena Moseman-Valtierra for their thoughts and suggestions as to the direction of this project. I would like to give a special thank you to Christiane Uhlig for all her help in the lab and endless support on this project. Thanks also to Brian Heikes for his patience and guidance through my first year of graduate school and beyond.

TABLE OF CONTENTS

ABSTRACT	ii
ACKNOWLEDGEMENTS	v
TABLE OF CONTENTS	vi
LIST OF TABLES	vii
LIST OF FIGURES	viii
CHAPTER 1	1
INTRODUCTION	1
CHAPTER 2	4
REVIEW OF LITERATURE	4
CHAPTER 3	20
MATERIALS & METHODS	20
CHAPTER 4	35
RESULTS & DISCUSSION.....	35
CHAPTER 5	80
CONCLUSION	80
APPENDICES	83
BIBLIOGRAPHY	98

LIST OF TABLES

TABLE	PAGE
Table 1. Experimental design for December 7, 2016 water sample incubation experiments held at 7°C	25
Table 2. Setup for 2°C incubation experiment for March 15, 2017 water samples....	25
Table 3. Experimental setup for water samples collected on May 7, 2017, incubated at 17°C.....	25
Table 4. Measurements from Marsh Outlet and Porewater during each incubation experiment sample collection.....	36
Table 5. Methane oxidation results from incubation experiment samples exhibiting significant decreases in methane.....	42
Table 6. Carbon dioxide rates of production in all incubated sample groups.....	47
Table 7. Particulate organic carbon measurements for all sample groups at incubation start and end. All POC measurements have units $\mu\text{mol L}^{-1}$	55
Table 8. Flow cytometry results, showing bacteria counts for corresponding filter sizes	58
Table 9. Salinity, methane $\delta^{13}\text{C}$, and methane measurements from bay transect, used for linear mixing models	73

LIST OF FIGURES

FIGURE	PAGE
Figure 1. Biochemical pathway for the aerobic oxidation of methane, including required methanotroph enzymes and intermediate products.....	8
Figure 2. Major biological and physical processes within estuaries, with dashed lines indicating salinity gradients, solid lines showing the movement and transformation of organic carbon, and dotted lines representative of CO ₂ flux	11
Figure 3. Cycling of organic carbon in salt marsh ecosystems, where dotted lines represent carbon inputs, solid lines represent biological conversion of carbon compounds, and dashed lines represent the flux of CH ₄ and CO ₂	13
Figure 4. Salt marsh terminal electron receptors ordered by thermodynamic favorability. <i>HS_{ox}</i> refers to oxidized humic substrates.....	13
Figure 5. Theoretical carbon isotopic fractionation in an estuarine environment, with fractionation factors included.....	17
Figure 6. Fox Hill Marsh location in Narragansett Bay, URI/GSO sampling location for methane time series, and sampling sites in Narragansett Bay for April 11, 2017 transect.	22
Figure 7. Fox Hill Marsh porewater and outlet sampling locations.....	22
Figure 8. 7°C filtered marsh outlet methane concentrations (a) and δ ¹³ C (b) during incubation.....	38
Figure 9. 7°C filtered marsh porewater methane concentrations (a) and δ ¹³ C (b) throughout incubation experiment	39

Figure 10. Unfiltered marsh outlet methane concentrations (a) and $\delta^{13}\text{C}$ (b) during 17°C experiment.....	40
Figure 11. 17°C unfiltered marsh porewater methane concentrations (a) and $\delta^{13}\text{C}$ (b) throughout incubation period	41
Figure 12. Projected marsh porewater concentrations (a) and outlet oxidation rates across range of Narragansett Bay temperatures, with indicated measurements, regression, and summer temperature projection	43
Figure 13. Carbon dioxide concentrations for marsh porewater (a) and outlet (b) samples during 7°C incubations	48
Figure 14. Methane concentrations (a) and $\delta^{13}\text{C}$ (b) for unfiltered anoxic marsh porewater samples during 17°C incubation	51
Figure 15. Methane concentrations (a) and $\delta^{13}\text{C}$ (b) for filtered anoxic marsh porewater samples during 17°C incubation	52
Figure 16. Example of H_2S interference on $\delta^{13}\text{C}$ measurements in N_2 -headspace marsh samples from 17°C experiment	55
Figure 17. Dissociation curves from qPCR runs for standards (a) and the 17°C unfiltered marsh sample (b) which exhibited methanotrophy.....	60
Figure 18. Copy numbers for all sample groups exhibiting oxidation.....	62
Figure 19. CH_4 (a), $\delta^{13}\text{C}$ (b), and CO_2 concentrations (c) at URI/GSO sampling location from May to July 2017	65
Figure 20. Temperature (a), salinity (b), and dissolved oxygen (c) at URI/GSO sampling location from May to July 2017	66
Figure 21. Factor loadings for the first three principal components from variables	

shown in Figure 19 and Figure 20.....	67
Figure 22. Normalized variance (bars) and total percent variance (line) for time series principal components	68
Figure 23. Bay survey reference map indicating sampling sites, Fields Point Wastewater Treatment Plant (WTP), and Greenwich Bay (GB) locations.....	69
Figure 24. Surface methane and CO ₂ concentrations (left) and isotope ratios (right) along Narragansett Bay transect.....	70
Figure 25. Linear relationship between measured salinity and methane along West Passage transect.....	71
Figure 26. Model of linear mixing, showing the fractional contributions of river, marsh, and ocean sources to the four interior Narragansett Bay sites. The values on the y-axis are fractions and should sum to one at each site.	73
Figure 27. Methane, methane $\delta^{13}\text{C}$, temperature, and salinity along bay transect with surface (blue) and depth (red) measurements	75
Figure 28. Dissolved oxygen, salinity, and temperature sampled continuously with Seabird moored profile CTD from 12/07/2016 to 01/14/2017, with dashed lines indicating outlet average	77
Figure 29. Mixing diagram of salinity and dissolved oxygen measurements from direct sampling data and linear model results	78

CHAPTER 1

INTRODUCTION

Methane is a potent greenhouse gas that has increased to over 1.8 ppm in the atmosphere (Ciais et al. 2013) due to anthropogenic activity, which accounts for 60% of the global emission sources (Kirschke et al. 2013). The remaining 40% is largely accounted for by the microfauna of freshwater and saltwater wetlands (Kirschke et al. 2013). Methane is produced biologically under anaerobic conditions, where methanogens (microbial methane producers), utilize acetate, carbon dioxide, or single-carbon compounds (Reeburgh 2007), though there is growing evidence for aerobic methane production (Karl et al. 2008; Tang et al. 2014). The two primary sinks for methane produced biologically in aquatic systems are escape to the atmosphere and methanotrophy, in which bacteria are able to utilize methane as their source of growth and energy (Hanson and Hanson 1996). In wetlands, methanogenesis is typically carried out by Archaea associated with the sediment while methanotrophs either consume methane anaerobically in close proximity to methanogens or aerobically in oxygenated waters (Hoehler et al. 1994; Hanson and Hanson 1996). To be bioavailable to methanotrophic bacteria, methane must be released into marsh porewaters and enter adjacent water systems – such as estuaries – through lateral transport.

Coastal wetland and estuary ecosystems act as both a source and sink of carbon by processing organic matter (Canuel and Hardison 2016) through the vast and diverse

microbial communities present (Drake, Horn, and Wüst 2009). These ecosystems are highly impacted by tides, which provide the regions with organic carbon from marine and terrestrial sources and are responsible for high rates of organic matter turnover (Middelburg and Herman 2007). Due to the various sources of organic matter in estuaries, carbon stable isotope analysis is frequently implemented as a tracer for carbon sources and biological activity (Whiticar 1999). Isotope fractionation occurs due to kinetic effects, where microbes preferentially consume the lighter ^{12}C isotope (Hoefs 2009). Therefore, stable isotope analysis is a great technique for monitoring biological processes such as respiration, methanotrophy, and methanogenesis, where the production of carbon dioxide and methane increases the compound-specific $^{12}\text{C}:^{13}\text{C}$ ratio and oxidation decreases the ratio. Because the production of methane is the terminal step in organic matter degradation in anaerobic wetland environments (Bridgman et al. 2013), dissolved methane gas is typically highly depleted in ^{13}C .

The aim of this study was to investigate the role of wetlands in the methane cycling of a coastal estuary – Narragansett Bay – using stable isotope analysis. Recent water sample incubations from Fox Hill salt marsh on Jamestown Island, RI indicated that marshes may be a site of simultaneous methanogenesis and methanotrophy during high tide. It has been shown that a fraction of the methane produced, and possibly the responsible microbial communities, are transported from salt marshes into nearby waters (Matoušů et al. 2017; Atkinson and Hall 1976; Schutte et al. 2016); however, the extent to which wetland biological activity impacts adjacent marine waters has not been well-documented. This was investigated by comparing microbial activity in incubated water samples from several locations in the marsh, using various treatments

as a means of studying the environmental conditions that favor both processes.

Narragansett Bay methane concentrations are supersaturated relative to atmospheric equilibrium; therefore, spatial and temporal measurements were taken to determine potential sources of methane and conditions that impact methane concentrations and stable isotope ratio.

1.1 Objectives

- Collect water samples from Fox Hill salt marsh and incubate them under various treatments to record the conditions that favor methanogenesis and methanotrophy, using stable isotope analysis as a confirmation.
- Compare seasonality of microbial communities through three incubation experiments using water collected at various times throughout the year.
- Use molecular techniques (qPCR – quantitative polymerase chain reaction) to quantify methanotrophs present in marsh.
- Measure CH₄ and CO₂ along the salinity gradient from the Providence River to Block Island Sound to determine potential sources of methane to Narragansett Bay, which is supersaturated with regard to methane concentrations.
- Monitor methane concentrations at fixed location in Narragansett Bay to record temporal changes in methane by season or by varying environmental condition in the bay.
- Capture tidal fluctuations with salinity and dissolved oxygen measurements to estimate overall contribution of salt marshes to Narragansett Bay methane.

CHAPTER 2

REVIEW OF LITERATURE

2.1 Global Importance of Methane

Methane is an important greenhouse gas that accounts for 17% of the total atmospheric radiative forcing, behind only carbon dioxide and water vapor (Myhre et al. 2013). The concentration of methane in the atmosphere has increased by nearly 150% since the industrial revolution and is now over 1.8 ppm (Ciais et al. 2013). Although concentrations are low compared to atmospheric CO₂, methane has a global warming potential roughly 25 times that of CO₂ on a molecule per molecule basis (Ramaswamy and Chen 1997).

Anthropogenic activity is largely responsible for the increase in atmospheric methane, with biomass burning, fossil fuels, agricultural activity, and waste management accounting for roughly 60% of all emission sources (Kirschke et al. 2013). Wetlands by far represent the greatest natural source of methane to the atmosphere at approximately 30% (Kirschke et al. 2013), though there is a great deal of uncertainty as to the amount wetlands contribute due to inaccurate estimates of total surface area and varying flux rates (Melton et al. 2013). The remaining sources of methane include freshwater systems, terrestrial soils, and marine environments – specifically continental shelf regions and estuaries, with a minute fraction from the open ocean (Middelburg et al. 2002).

Methane concentrations in the open ocean are typically close to equilibrium saturation with the atmosphere between 2-3 nM (Reeburgh 2007), while coastal waters can have concentrations several orders of magnitude higher. Sources for methane in coastal systems – specifically estuaries – include sediments, riverine inputs, and marshes (Bange et al. 1994), though concentrations are primarily controlled by river discharge and tidal influence (Grunwald et al. 2009). There are also significant biological constraints leading to a great deal of spatial and temporal variability in methane cycling throughout coastal regions.

2.2 Biological Methane

2.2.1 Methanogenesis

Production of methane in natural systems principally occurs biologically through a process called methanogenesis, though a minute fraction of methane is of thermogenic origin (Reeburgh 2007). Three principal metabolic pathways are utilized by methanogenic Archaea in marine environments, differing in the initial substrate used to produce methane anaerobically (Carpenter, Archer, and Beale 2012). Acetoclastic methanogenesis, which is CH₄ production through acetate fermentation (Equation 1), and hydrogenotrophic methanogenesis, production via carbon dioxide reduction (Equation 2), are two of the pathways in which Archaea are able to produce methane, though substrates required for these reactions – namely acetate and hydrogen – are also utilized by sulfate reducing bacteria that tend to outcompete methanogens (Reeburgh 2007). Methylotrophy represents the third pathway (Equation 3), in which methanogens utilize methylated substrates such as methylamines (Sowers and Ferry 1983), methanol (Carpenter, Archer, and Beale 2012), and dimethylsulfoniopropionate

(DMSP) (Damm et al. 2008). This last pathway has been shown to occur in the presence of sulfate reducing bacteria (Oremland and Polcin 1982) and there is also evidence for production under aerobic conditions (Karl et al. 2008).



Observations of methane supersaturation in the open ocean mixed layer have led to the discovery that methane production can occur in oxygenated environments (Reeburgh 2007), an occurrence known as the “methane paradox.” Karl et al. (2008) determined that methylphosphonate, a form of dissolved organic phosphate produced by phytoplankton, can act as a nutrient source in phosphate-limited waters. Like the methylotrophic pathway, phosphonate is broken down by marine microbes to consume phosphate and release methane as a byproduct (Equation 4), a reaction carried out entirely independent of oxygen (Repeta et al. 2016).



Another process that may be responsible for methane supersaturation is the existence of microanoxic zones, in which anaerobic methanogenic archaea are able to actively produce methane in oxygen-rich waters within anoxic microenvironments. Microanoxic zones can occur within zooplankton guts and fish intestines (Oremland 1979), as well as in suspended and sinking particles like fecal pellets (Marty 1993). Previous studies have shown active in situ methane production from particulate organic matter in aerobic pelagic waters (Karl and Tilbrook 1994) and even identified hydrogenotrophic and methylotrophic methanogens present in sedimenting particulate

matter in the water column (Ditchfield et al. 2012). A potential mechanism has been proposed in which aggregates form in the pelagic zone from phytoplankton and organic detritus (Marty 1993), promoting microbial respiration to occur until anoxic conditions are achieved within the aggregate. Ploug et al. (Ploug et al. 1997) determined that the duration of time in which these aggregates remain anoxic is dependent on the size of the particles; therefore increased methanogenesis occurs as aggregate size increases.

2.2.2 Methanotrophy

2.2.2.1 Anaerobic

Similar to methanogenesis, anaerobic oxidation of methane (AOM) is carried out by microorganisms from the domain archaea referred to as anaerobic methanotrophic archaea (ANME) (Chowdhury and Dick 2013). While the exact mechanism of AOM is unknown, there is evidence that a consortium of methanogens and sulfate reducing bacteria (SRB) are responsible for methanotrophy through ‘reverse methanogenesis’ (Hoehler et al. 1994). The sulfate-methane interface is the transition zone between methanogens and SRBs in the upper marine sediment layer in which sulfate oxidation is favored over methanogenesis due to SRBs outcompeting methanogens for H₂ substrate (Valentine 2011). Under reduced H₂ conditions, ANME oxidize methane to produce carbon dioxide and hydrogen (Equation 5), which is subsequently utilized by SRBs in Equation 6 (Hoehler et al. 1994). This process leads to much of the biologically-produced methane getting oxidized at the oxic-anoxic boundary and acts to regulate the amount of methane escaping to the water column.





2.2.2.2 Aerobic

Aerobic methanotrophs are made up of various groups of methylotrophic bacteria, either obligate or facultative, collectively known as methane oxidizing bacteria (MOB). Obligate methanotrophs utilize methane as a sole carbon and energy source, while facultative methanotrophs possess the ability to grow on other single-carbon and multi-carbon substrates (Hanson and Hanson 1996). All methanotrophs oxidize methane to methanol using methane monooxygenases (MMO), which split oxygen-oxygen bonds and incorporate oxygen into methane to produce methanol (H. Dalton 1991). This is followed by several enzymatic steps to produce formaldehyde (CH_2O) (Anthony 1986), outlined in Figure 1. Two distinct metabolic pathways are involved in the assimilation of carbon following the production of formaldehyde, highlighted in Figure 1 as the ribonucleic acid monophosphate (RuMP) and serine pathways (Hanson and Hanson 1996).

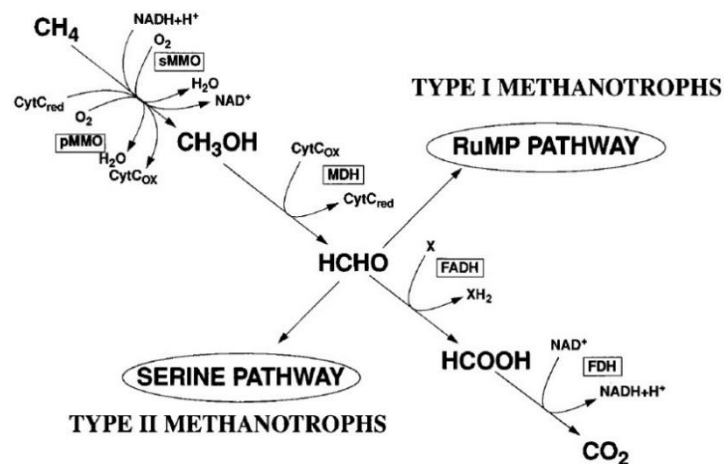


Figure 1. Biochemical pathway for the aerobic oxidation of methane, including required methanotroph enzymes and intermediate products (Hanson and Hanson 1996).

The pathway that is utilized by methanotrophs to assimilate carbon classifies them as either Type I or Type II. Type I methanotrophs, which are the most abundant group, fall into the gamma class of the phylum *Proteobacteria* (family *Methylococcaceae*) and include the genera *Methylococcus*, *Methylobacter*, *Methylomonas*, and *Methylomicrobium* (Semrau, DiSpirito, and Yoon 2010). All Type II methanotrophs are contained within the class *Alphaproteobacteria* (mostly family *Methylocystaceae*) and include *Methylocystis*, *Methylocapsa*, and *Methylocella* (family *Beijerinckiaceae*) (Hanson and Hanson 1996; Dedysh, Knief, and Dunfield 2005). While most methanotrophs fall within the *Proteobacteria* phylum, there have been discoveries of methanotrophs within the phylum *Verrucomicrobia* that are believed to utilize the serine pathway similar to Type II methanotrophs (Semrau, DiSpirito, and Yoon 2010). *Verrucomicrobia* are now categorized into a Type III group of methanotrophs and so far have only been found in extreme environments with high acidities or temperatures (Knief 2015).

Even though methanotrophs are not necessarily closely related within domain Bacteria, a defining characteristic of all methanotrophs is the use of the methane monooxygenase enzyme (Murrell and McDonald 2000). Two forms of this enzyme have been identified within bacteria: particulate MMO (pMMO) that are membrane-bound and soluble MMO (sMMO) present in cytoplasm (Howard Dalton 1980). Shown in Figure 1, sMMO utilizes $\text{NADH} + \text{H}^+$ as the electron donor to oxidize CH_4 to CH_3OH (Hanson and Hanson 1996), while the exact mechanism of oxidation utilized by pMMO for the same reaction is still poorly understood (Semrau, DiSpirito, and Yoon 2010). Although sMMO is better characterized, it is not found in all

methanotrophs. Genes for pMMO have been found in all methanotrophs with the exception of *Methylocella* (Theisen et al. 2005), though it is possible that other species within the *Beijerinckiaceae* family do not utilize pMMO. As pMMO is encoded for by three subunit monomers – α , β , γ – defined as *pmoA*, *pmoB*, and *pmoC*, these subunits are effective markers for functional groups in measurements of abundance and diversity of methanotrophs in environmental samples (Knief 2015).

2.3 Carbon Cycling in Marsh & Estuaries

The production of methane in wetlands and coastal regions is dependent upon the amount and type of available organic matter. Dissolved organic carbon (DOC) and particulate organic carbon (POC) can originate from terrestrial, marine, or in situ (i.e. marsh plants) sources, and tidal estuaries represent the location where these two source materials mix (Middelburg and Herman 2007). Sources of POC and DOC to estuaries include archaea, bacteria, algae, fungi, crustacea, and vascular plants, resulting in a wide variety of carbon compounds available as substrate to methanogens and heterotrophic microbes (Whitehead 2008). Tidal estuaries contain high concentrations of suspended organic matter (particulate and dissolved) (Middelburg and Herman 2007), though it is unclear how much is produced, consumed, and exchanged laterally over time.

Tidal flow, specifically flood tide, is responsible for inputting organic carbon and source material to estuaries and coastal wetlands from marine regions, where organic matter is transformed biologically between various carbon pools. Ebb tide is the period between high tide and low tide, when some fraction of transformed organic matter is transported to coastal waters. Physical processes transporting carbon within

estuaries include water circulation, river and groundwater discharge, salt marsh exchange, tidal flooding, and resuspension of sediment (Canuel et al. 2012), outlined in Figure 2. This depiction also reflects the exchange of CO_2 , in which CO_2 is assimilated via marine phytoplankton and marsh grasses and released through the microbial breakdown of organic material (Canuel and Hardison 2016), though estuaries and wetlands are often found to be net sources of CO_2 to the atmosphere through respiration (Hopkinson and Smith 2005).

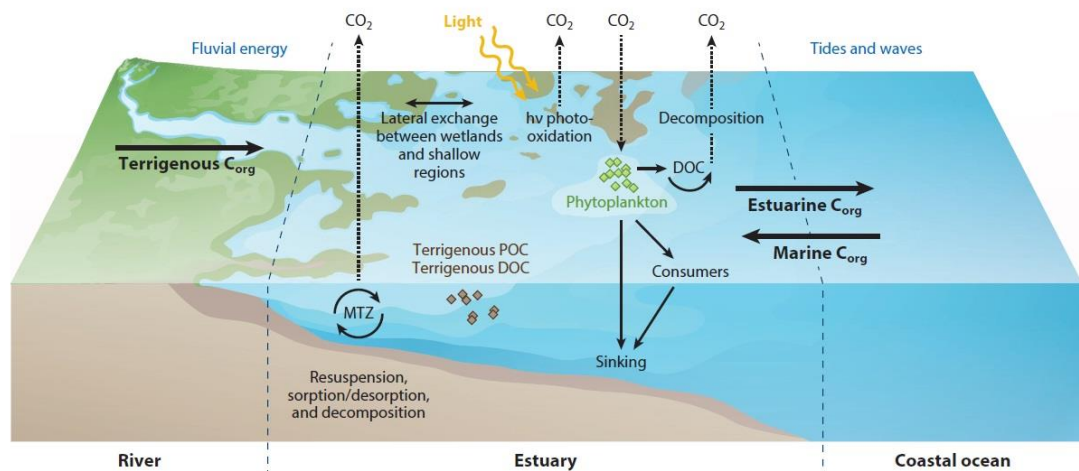


Figure 2. Major biological and physical processes within estuaries, with dashed lines indicating salinity gradients, solid lines showing the movement and transformation of organic carbon, and dotted lines representative of CO_2 flux (Canuel and Hardison 2016).

Though photosynthesis and respiration are certainly the largest microbial processes in estuaries and wetlands, the production of CO_2 is also closely tied in with methane cycling in these regions (Reeburgh 2007). Similar to CO_2 , emissions of CH_4 from coastal systems depend upon the balance between methanogenesis and methanotrophy and the manner through which organic carbon is broken down. Microbes utilize organic carbon as their electron donors for metabolic processes,

though the type of carbon present has a large influence on decomposition (Chanton et al. 2008). Methanogens are largely dependent upon soil stability and plant-derived organic matter (Whiting and Chanton 1993), and there is strong evidence of correlation between methane production and plant productivity rates (Wilmking et al. 2011). New photosynthate from root exudates in the rhizosphere provides substrate to methanogens and heterotrophic microbes alike, and ultimately stimulates CH₄ production (King et al. 2002). The majority of dissolved organic matter in marshes is young compared to the soils present (Chanton et al. 2008), and therefore represents the labile fraction of organic matter. CO₂ and CH₄ produced in wetlands is typically derived from this pool.

The production of methane in salt marshes is dependent upon the initial breakdown of complex molecules by other microbial groups (Drake, Horn, and Wüst 2009). This process is outlined in Figure 3, in which plant polymers are enzymatically degraded to monomers like simple sugars which are consumable by microorganisms with and without oxygen present (Bridgham et al. 2013). As mentioned in the Section 2.2.1, the substrates used in hydrogenotrophic and acetoclastic methanogenesis are preferentially utilized by sulfate reducing bacteria (SRB), as well as microbes using alternate terminal electron receptors (TEA). Although oxygen is the most common TEA, in anoxic environments several other compounds participate in this process that are more favorable than the CH₄ production mechanism, which are outlined in Figure 4. Though the thermodynamic favorability of these compounds supposedly dictates the order with which these compounds will be consumed, microbial communities in

marshes can exhibit utilization of any number of TEA's simultaneously (Bethke et al. 2011).

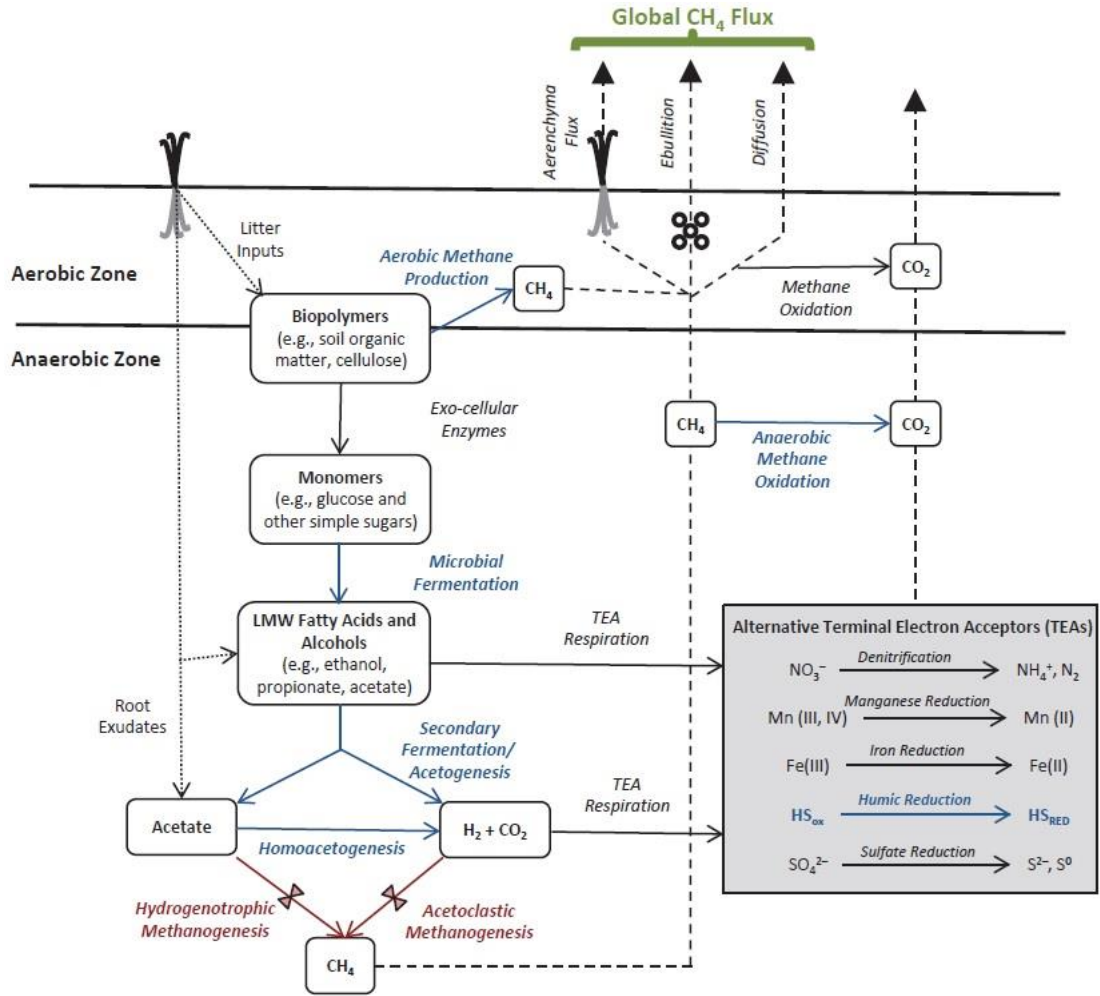


Figure 3. Cycling of organic carbon in salt marsh ecosystems, where dotted lines represent carbon inputs, solid lines represent biological conversion of carbon compounds, and dashed lines represent the flux of CH₄ and CO₂ (Bridgham et al. 2013).

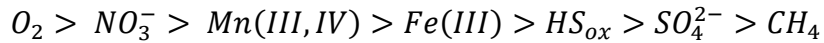


Figure 4. Salt marsh terminal electron receptors ordered by thermodynamic favorability. HS_{ox} refers to oxidized humic substrates.

Upon being produced, CH₄ and CO₂ are transported through wetlands via diffusion, ebullition, and through plants (aerenchyma) (Bridgham et al. 2013). CO₂ tends to be emitted upon reaching the aerobic zone while methane has two major sinks: emission or oxidation by methanotrophs (Hanson and Hanson 1996). Methanotrophy can occur in oxygenated pore waters in aerobic micro-zones surrounding plant rhizosphere systems (Fritz et al. 2011), and rates are highest when soils are completely saturated.

Methanotrophy is important in regulating the amount of methane emitted to the atmosphere from wetlands (Bridgham et al. 2013). Because methanogens reside in the sediment, methane concentrations in marsh pore water are highest at low tide, coinciding with the highest emission rates (Grunwald et al. 2009). Low tide also coincides with the fewest numbers of methane oxidizing bacteria (Sullivan, Selmants, and Hart 2013), as porewater becomes anoxic as oxygenated water flows out with the tide, thus favoring methane production. On the other hand, high tide conditions provide marshes with oxygen as well as methanotrophs, leading to unique environmental conditions that potentially support the co-occurrence of methane producers and consumers.

It has been shown that porewater flow through coastal sediments is responsible for the transport of large amounts of methane to marine waters (Bugna et al. 1996), though most of this input is subject to oxidation upon exiting the sediment (Schutte et al. 2016). Tidal movement causes the entrainment of particles in the flowing water (Uncles and Stephens 1993), resulting in greater amounts of substrate available to marine microbes and likely contributes greater numbers of microbes in water.

Included in these particles are microanoxic zones (Tang et al. 2014), though it is unclear whether these microenvironments remain in marsh porewater or are flushed out into the water column. This would indicate that while methanotrophy is expected to occur on dissolved methane transported from the marsh, methanogenesis may be able to continue within particles flushed out with the tide.

2.4 Stable Isotopes as Biological Tracers

The isotopic composition of carbon compounds in wetlands can provide great insight into carbon cycling, especially with the tracking of methanotrophy and methanogenesis (Whiticar 1999). Isotope fractionation occurs due to the kinetic isotope effect, in which the lighter carbon isotope (^{12}C) is preferentially taken up by microbes over the heavier isotope (^{13}C) (Hoefs 2009). The isotope composition, or isotope ratio ($\delta^{13}\text{C}$) is computed using the following equation, where R refers to the ratio $^{13}\text{C}/^{12}\text{C}$ (Craig 1953):

$$\delta^{13}\text{C} = \left(\frac{R_{\text{sample}}}{R_{\text{standard}}} - 1 \right) * 1000\text{‰} \quad (7)$$

Of the natural production mechanisms for methane, thermogenic methane yields $\delta^{13}\text{C}$ values in the range -50‰ to -25‰ (^{13}C -enriched) while biogenic methane produces $\delta^{13}\text{C}$ values less than -50‰ (depleted in ^{13}C) (Kaplan 2013). Atmospheric methane has an average isotopic signature of -47‰ in the Northern hemisphere, although this can vary by several per mille depending on proximity and type of emission source (Quay et al. 1999).

In biological systems, production of methane from both acetate and carbon dioxide leads to CH_4 depleted in ^{13}C and CO_2 enriched in ^{13}C (Whiticar 1999).

Dissolved and particulate organic matter in estuaries range from -28‰ to -21‰

(Bauer and Bianchi 2011; Loh, Bauer, and Canuel 2006; Raymond and Bauer 2001) depending on the source and class of bioorganic material. Polysaccharides and proteins are more enriched in ^{13}C and therefore have higher $\delta^{13}\text{C}$ (less negative) than lipids due to biosynthesis differences (Hayes 2001). Along these lines, marsh plants tend to undergo less fractionation than terrigenous plants and phytoplankton upon degradation (Ahad et al. 2011; Canuel, Freeman, and Wakeham 1997); therefore, methane and CO_2 produced from marine organic matter degradation has a lower (more negative) $\delta^{13}\text{C}$ than from estuarine sources.

In terms of methanogenesis production mechanisms, methane produced from acetate can yield $\delta^{13}\text{C}$ of -70‰ while hydrogenotrophic methanogenesis can result in isotope ratios lower than -100‰ (M. Elizabeth Holmes et al. 2015). There is also evidence of a seasonal shift in production pathways, with increased acetate concentrations during the summer favoring acetoclastic methanogenesis while hydrogenotrophic production is prevalent the rest of the year (Avery et al. 1999). Figure 5 provides insight into the effects of estuaries processes, outlined in Figure 3, on the $\delta^{13}\text{C}$ of organic matter. Several processes exhibit syntrophy in which no fraction occurs, indicated by the fractionation factor, α , is equal to 1. Methanogenic processes have fractionation factors ranging from 1.04 to 1.09 (M. Elizabeth Holmes et al. 2015), which in turn causes the dissolved CO_2 pool to become more enriched in ^{13}C . Though hydrogenotrophic and acetoclastic methanogenesis effects on $\delta^{13}\text{C}$ is known, the extent to which the methylotrophic pathway fractionates methane is unknown at this time.

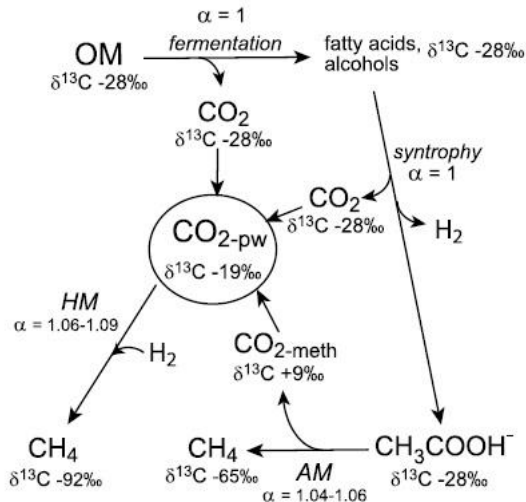


Figure 5. Theoretical carbon isotopic fractionation in an estuarine environment, with fractionation factors included (M. Elizabeth Holmes et al. 2015).

Since methane oxidation results in the formation of CO_2 , fractionation of carbon isotopes produces ^{13}C -depleted CO_2 and ^{13}C -enriched CH_4 , though the impact of methanotrophy on $\delta^{13}\text{C}$ is variable and dependent upon source material, similar to methanogenesis (Sansone, Holmes, and Popp 1999). The balance between methanogenesis and methanotrophy when considering $\delta^{13}\text{C}$ in estuaries has not been established, though the processes are both impacted by tidal and seasonal changes. Carbon stable isotope analysis has been used successfully to describe biological activity with regard to methanogenesis and methanotrophy during incubation experiments (Conrad, Claus, and Casper 2009; Duc, Crill, and Bastviken 2010), therefore making it possible to distinguish between source material and compare various environmental effects on both processes.

2.5 Narragansett Bay

Narragansett Bay is a temperate estuary that covers an area of approximately 342 km^2 across Rhode Island and parts of Massachusetts (Chinman and Scott W.

Nixon 1985). Saline water (~32ppt) from the Atlantic Ocean enters the Bay from the south while riverine and wastewater input provides freshwater from several northern regions, resulting in a salinity gradient across the Bay latitudinally across 45 km. The average depth is 9m, though the bay is divided into the shallower West Passage and deeper East Passage with a maximum depth of 15.2 m (Raposa and Schwartz 2009). Water generally circulates counterclockwise, moving northward through the East Passage and southward through the West Passage (Kincaid, Bergondo, and Rosenburger 2003).

Several regions in Narragansett Bay experience significant extended hypoxia, largely due to nutrient input via runoff and low circulation leading to stratification. These areas include the mouth of the Providence River and Greenwich Bay, with instances of anoxic conditions occurring in bottom waters during summer months. As previously mentioned, these are the conditions that favor methanogenesis; however, there has been limited work carried out with regard to methane biogeochemistry in Narragansett Bay. The majority of methane-related research in Narragansett Bay occurred in the early 1990s, focusing on a permanently anoxic basin of the Pettaquamscutt Estuary along the West Passage (Scranton et al. 1993; Sieburth and Donaghay 1993). These studies found methane concentrations in this location (7 m depth) of 200 nM while, while methane oxidation rates were found to be 1-1.5 nM day⁻¹. Methane production in this region far exceeded oxidation, and some evidence was provided for in situ water column production from microanoxic zones discussed in Section 2.2. It was also theorized that Narragansett Bay methanotrophs are primarily mesophilic while methanogens can be psychrophilic, meaning the latter can

remain active during the winter months (2°C water temperatures). There have been more recent signs pointing to the supersaturation of waters throughout Narragansett Bay, with a variety of sources potentially responsible.

A recent study examined sources of methane to the German Bight (North Sea), suggesting that wastewater, salt marshes, and rivers all contribute to high dissolved methane concentrations (Osudar et al. 2015). In the case of the Hudson Estuary, these sources together have been shown to contribute 6.23×10^7 mol year⁻¹ to adjacent marine waters (de Angelis and Scranton 1993); however, it is not clear how these contributions are partitioned between sources. Much of the Narragansett Bay coastline is dominated by salt marshes, which take up an approximate area of 11.5 km² (Raposa and Schwartz 2009). Narragansett Bay experiences semidiurnal tides with marsh tidal ranges of approximately 1m. With approximately 12 hours of outgoing tide per day, marshes, with their high methanogenesis rates, could represent a significant source of methane to Narragansett Bay.

Samples collected from Fox Hill Salt Marsh, located on Jamestown Island along the West Passage, is an area that recently indicated the potential for co-occurrence of methanogenesis in and methanotrophy in oxic waters (Christiane Uhlig 2016). As previously discussed, seawater exchange between estuaries and adjacent wetlands can transport methane (Atkinson and Hall 1976), and Fox Hill is a source of methane to the atmosphere (Martin and Moseman-Valtierra 2015). This study seeks to examine the details of microbial processes and seasonality to better understand their contribution to methane cycling in estuaries, specifically across Narragansett Bay.

CHAPTER 3

MATERIALS & METHODS

3.1 Study Sites

Seawater was collected for incubation experiments at Fox Hill Salt Marsh of Jamestown Island in Narragansett Bay on 07 December 2016, 15 March 2017, and 09 May 2017. Water was sampled from a porewater well, installed in low marsh sediment and positioned approximately 2 m from a tidal creek, and from the tidal creek outlet into Narragansett Bay (Figure 6). The porewater well was constructed of PVC pipe with a screen at the base and openings positioned every 0.1 m from the base to the midpoint. The well extended 1 m down into the sediment, with roughly 0.05 m exposed above the marsh surface. Water initially present in the porewater well was removed prior to sampling, in order to remove effects from gas exchange and capture water samples most representative of porewater outflow.

Samples for the incubation experiments were collected starting 1 hour after high tide and lasting approximately four hours, starting with the pore water and ending at the creek outlet. The tidal creek outlet was sampled directly from the outflowing water, with an approximate depth of 1.5 m. Temperature, salinity, and dissolved oxygen measurements were additionally obtained with a YSI Professional Plus probe (YSI, OH).

Two other datasets were constructed during the course of this project, including a bay transect and a time series of methane concentrations in Narragansett

Bay. The time series samples were collected in a single location from 18 May 2017 to 19 July 2017 with a sampling frequency of two days per week. The sampling time occurred independently of tidal and weather conditions. Seawater samples were obtained at the University of Rhode Island Graduate School of Oceanography (URI GSO) dock from the upper third of roughly 3 m deep water. The bay transect was carried out on 10 April and 11 April 2017 from the mouth of the Providence River to the mouth of Narragansett Bay along the West Passage, indicated by Figure 6. A URI-owned vessel was utilized to carry out the transect over the two-day span. Six stations were established for sample collection and YSI measurements during the transect, where bottom and surface waters were sampled for later methane measurements. Samples were stored cool and measured 12 hours after collecting.

A Seabird SBE 37-SMP-ODO MicroCAT Conductivity, Temperature, and Optical Dissolved Oxygen Recorder (Moored CTD) was placed underwater at the Fox Hill marsh outlet during the 07 December 2016 sampling. The instrument continuously sampled from 07 December 2016 until 19 January 2017 to capture fluctuations in salinity, temperature, and dissolved oxygen during tidal cycles. All data were downloaded from the instrument hard drive once the Seabird CTD was removed from the outlet locations and returned to the lab.

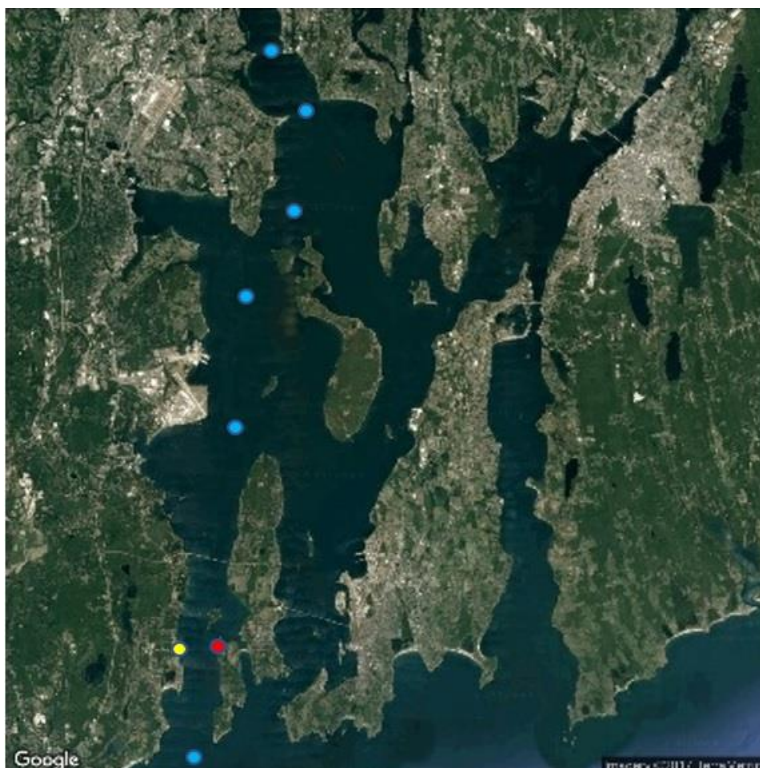


Figure 6. Fox Hill Marsh location in Narragansett Bay (red), URI/GSO sampling location for methane time series (yellow), and sampling sites in Narragansett Bay for April 11, 2017 transect (blue).



Figure 7. Fox Hill Marsh porewater (red) and outlet (yellow) sampling locations.

3.2 Incubation Experiments

Water samples from Fox Hill salt marsh were collected and incubated under various treatments to record the conditions that favor methanogenesis and methanotrophy. Samples were collected using a Masterflex E/S portable peristaltic pump with silicone tubing. Multi-layer foil gas sampling bags (1000mL capacity, Restek Corporation), which have proven to be successful vessels for sample collection (Uhlig and Loose 2017), were utilized to collect and incubate seawater samples from Fox Hill Salt Marsh. Sample bags were equipped with polypropylene valves consisting of a hose connection and sampling port with replaceable septum for use with syringes. Prior to filling sample bags, several steps were taken to prevent contamination by air and microbes. First, water was flushed from the well for several minutes to ensure samples were devoid of all microbial communities outside of those present in the marsh porewater. All bubbles were removed from filters and tubing to prevent ambient air from entering sample bags and eventually contributing to gas headspace with bags. Bags from marsh porewater were then filled with 600-900mL at a sampling rate roughly equal to the well-filling rate.

Upon returning to the lab, bags were injected with a 100ml headspace of either hydrocarbon free zero air (ZA, Airgas) or N₂ gas (Airgas) depending on the corresponding treatment (Tables 1-3). All bags from December 7th and March 15th, as well as six May 7th samples, were also spiked with 15mL of 2500ppmv methane standard, with a known $\delta^{13}\text{C}$ ratio of $-23.9 \pm 0.2\text{‰}$ (Isometric Instruments). The methane spike was introduced in order to maintain methane concentrations in marsh porewater samples and was computed using the series of calculations outlined in

Equations 8 & 9. Bags were then weighed to determine the total water volume for each sample. All samples were held at constant temperature for the entire incubation period, with the incubation temperature corresponding to in situ temperature.

3.2.1 Experimental Treatments

Filled sample bags were given treatments to test various environmental effects on salt marsh microbial communities, outlined in Tables 1-3. The use of hydrocarbon free and nitrogen gas in the headspace of each sample was intended to study the microbial responses to oxygenated and low oxygen environments, respectively. A nitrogen headspace was only used for marsh pore water samples, as microbes present in the marsh were accustomed to greater variability in oxygen on a daily basis. It was expected that methanogenesis would be promoted by the nitrogen headspace, while methanotrophy was promoted by the oxygen present in hydrocarbon free headspace (Reeburgh 2007). Given the relevance of aerobic methanogenesis in current research (Tang et al. 2014), several other treatments, including inhibitor use and filtration, were utilized to test whether aerobic methane production could be promoted in Fox Hill Salt marsh samples. All experimental treatments in incubation experiments were applied in triplicate to water samples.

Treatment Group	Sample Location	Headspace	Filtered/ Unfiltered	Additional Treatments
1	Marsh Outlet	Zero Air	Filtered	CH ₄ Spike
2	Marsh Pore Water	Zero Air	Filtered	CH ₄ Spike
3	Marsh Pore Water	Zero Air	Filtered	CH ₄ Spike, BES (25mM)
4	Marsh Pore Water	Zero Air	Filtered	CH ₄ Spike, NaOH (0.2 M)
5	Marsh Pore Water	Nitrogen	Filtered	CH ₄ Spike

Table 1. Experimental design for December 7, 2016 water sample incubation experiments held at 7°C.

Treatment Group	Sample Location	Headspace	Filtered/ Unfiltered	Additional Treatments
1	Marsh Outlet	Zero Air	Unfiltered	CH ₄ Spike
2	Marsh Pore Water	Zero Air	Filtered	CH ₄ Spike
3	Marsh Pore Water	Zero Air	Unfiltered	CH ₄ Spike
4	Marsh Pore Water	Zero Air	Unfiltered	CH ₄ Spike, NaOH (0.2 M)
5	Marsh Pore Water	Nitrogen	Unfiltered	CH ₄ Spike

Table 2. Setup for 2°C incubation experiment for March 15, 2017 water samples.

Treatment Group	Sample Location	Headspace	Filtered/ Unfiltered	Additional Treatments
1	Marsh Outlet	Zero Air	Filtered	CH ₄ Spike
2	Marsh Outlet	Zero Air	Unfiltered	CH ₄ Spike
3	Marsh Pore Water	Zero Air	Unfiltered	None
4	Marsh Pore Water	Nitrogen	Filtered	None
5	Marsh Pore Water	Nitrogen	Unfiltered	None
6	Marsh Pore Water	Nitrogen	Unfiltered	NaOH (0.2 M)

Table 3. Experimental setup for water samples collected on May 7, 2017, incubated at 17°C.

2-Bromoethane sulfonate (BES) was used during the December 7th incubation experiment as a treatment to control for methanogenesis, as it is a structural analogue of methyl-coenzyme M and inhibits the production of methane (Nozoe 1997). Conrad et al. (2009) determined that complete inhibition of methane production occurred only when BES was applied at concentrations greater than 20mM. Therefore, enough BES was added in our experiment to produce total sample BES concentrations of 25mM. This treatment was designed to isolate the effects of methanotrophy if there was observed co-occurrence of methanogens and methanotrophs.

Micro-anoxic zones, as well as sediment size effects, were accounted for through the use of filtered and unfiltered water samples from marsh porewater and outlet samples. Because the cutoff for micro-anoxic zones was found to be 5 μ m, GF/D filters (2.7 μ m pore size, Whatman) were used in conjunction with plastic filter holders (Whatman) attached directly to tubing shown in Figure 8. All samples from the 7°C experiment were filtered to eliminate the possibility of micro-anoxic zone effects, while filtered and unfiltered water samples were used for the 2°C and 17°C incubations to study the effects of sediment size on methane cycling. Porewater samples with an oxygen headspace were filtered and unfiltered for the 2°C samples, while all samples from the 17°C experiments were unfiltered with the exception of N₂-headspace porewater and a ZA-headspace outlet sample group. The filtered and unfiltered 2°C porewater samples were expected to distinguish between the presence and absence of micro-anoxic zones. Filtration was used in the 17°C experiment to study the effects of varying particle sizes on both methanogenesis and methanotrophy.

Flow cytometry was used as a means of obtaining microbial cell counts from marsh porewater and comparing the effects of filter pore size on cell counts. Water samples were collected from Fox Hill Marsh wells on November 14, 2016 and filtered at 20 μ m, 2.7 μ m, and 0.2 μ m pore size. 1.9ml filtered water was aliquoted from each sample bottle and fixed with 100 μ L formaldehyde. 1ml of fixed sample was then combined with 100 μ L SYBR Green I solution and allowed to incubate for 20 minutes to ensure proper intercalation between the dye and DNA. Duplicates were prepared and all six samples were then run on a BD Influx Cell Sorter/Flow cytometer through the University of Rhode Island Marine Science Research Facility. DNA was detected at the 530/40 nm fluorescence signal for SYBR Green.

Sodium hydroxide (NaOH) was employed as a killed control for microbial activity in all three experiments. Enough 10M NaOH was added until seawater pH was above 12, which represents the upper limit of the pH range of which bacteria are able to survive (Magen et al. 2014). The NaOH volume ranged from 7ml to 12ml depending on the total seawater volume per bag. Seawater pH was confirmed through the use of pH strips, using a syringe with a hypodermic needle to extract the required sample volume (several drops) from bags and dispense directly on the strips. Due to the effects of pH on seawater CO₂ concentrations (Schulz et al. 2009), NaOH treated samples were used only as a control for methane isotopes.

3.2.2 Methane and carbon dioxide measurements

A cavity ring down spectroscopy (CRDS) greenhouse gas analyzer (Picarro G2201-*i*) was used to measure methane and carbon dioxide isotopes discretely during incubation experiments. Gas headspace subsamples were removed from sample bags

with syringes and injected directly into a Small Sample Isotope Module (SSIM) coupled to the analyzer. 0.5 to 15ml subsample volumes were injected depending on the expected concentration of the analyte and origin of the samples. Duplicate measurements were carried out for each sample bag, though additional measurements were taken if the relative error exceeded 2% from the mean. CH₄ and CO₂ gas concentrations were reported as partial pressures with units of ppm, while δ¹³C was reported with the standard units per mille (‰).

A dilution factor was required to account for the cavity volume of the SSIM, as all subsample injections were diluted with zero air in order to completely fill the 20mL cavity. The pressure difference between ambient air and SSIM were corrected for through the use of a dilution factor calculation, shown in Equation 8.

$$Dilution\ Factor = \frac{V_{SSIM} * P_{SSIM}}{V_{sample} * P_{atm}} \quad (8)$$

The dilution factor was computed using the SSIM cavity volume (V_{SSIM}), subsample injection volume (V_{sample}), atmospheric pressure (P_{atm}), and SSIM pressure (P_{SSIM}). The true gas concentration (P_{CH_4}) was calculated as the product of the dilution factor and Piccaro concentration output for both CH₄ and CO₂. Corrections were not required for δ¹³C measurements.

Seawater sample methane concentrations were computed from gas measurements using the Bunsen coefficient (β) for methane (Yamamoto, Alcauskas, and Crozier 1976), the ideal gas law, and sample volumes obtained from sample mass and densities. Final concentrations of methane were calculated based on previously obtained series of equations (Magen et al. 2014):

$$[CH_4] = \frac{P_{CH_4} * \beta * V_{gas}}{R * T * V_{water}} \quad (9)$$

Where P_{CH_4} (atm) was the methane partial pressure calculated using the dilution factor, β was Bunsen coefficient for methane, R was the Ideal Gas constant ($0.08206 \text{ L}\cdot\text{atm}\cdot\text{K}^{-1}\cdot\text{mol}^{-1}$), V was volume (L), and T was temperature (K). Carbon dioxide concentrations were calculated similarly to methane, with the exceptions of β specific to CO_2 (Weiss 1974) and P_{CO_2} in place of methane-specific constants.

Gas standards were run concurrently with samples to calibrate sample measurements and account for instrument drift and daily fluctuations due to ambient temperature and pressure differences. CH_4 , CO_2 , and $\delta^{13}\text{C}$ were calibrated using 2,500ppmv CH_4 standard (-23.9‰ & -66.5‰; Isometric Instruments), 250ppmv standard (-38.3‰; Isometric Instruments), and a mixed standard with 1000ppmv CH_4 and 4000ppmv CO_2 (Airgas). $\delta^{13}\text{C}$ for carbon dioxide was not calibrated for, as isotope ratios were not supplied for the Airgas standards.

Methane oxidation and carbon dioxide production rates were computed using the first order reaction:

$$r_{ox} = k * [\text{CH}_4] \quad (10)$$

Where the rate constants, k , were obtained as the negative slope of the linear regression of the natural log CO_2 or CH_4 molar quantities and incubation time. The rate constants for samples exhibiting methane oxidation were computed from the start of methanotrophy rather than the incubation start period.

3.2.3 Particulate Organic Carbon Determination

Samples for particulate organic carbon analysis (POC) were collected in acid-washed 1L sample bottles and brought to the lab. Samples were then immediately prepared for particulate organic carbon determination according to published

procedures (Pike and Moran 1997). Briefly, 500ml samples were vacuum-filtered through acid-washed polysulfone (Gelman) filter holders onto pre-combusted Whatman GF/F filters (pore size of 0.7 μ m). Filters were then dried, acidified for 24 hours using 12M HCl, and dried again before being stored at -80°C until analysis.

Measurement of total organic carbon in each sample was carried out on an Exeter Analytical CE-440 CHN analyzer. Filters were cut in half with acetone-washed forceps, enclosed in tin sleeves, and finally packed into nickel capsules as per the requirements of the instrument manufacturer prior to analysis. Calibration curves were produced using the standard acetanilide (99%, MilliporeSigma), with the molecular weight 135.17g/mol and known carbon content of 71.1%. POC content were calculated using equation (1) for each sample, where x = carbon (μ mol), y =CHN carbon counts, and m and b refer to the slope and intercepts of the standard curve. POC concentrations were then obtained by dividing by GF/F filter volume. Blanks were run to correct for carbon content in GF/D filters and nickel capsules.

$$x = \left(\frac{y-b}{m}\right)/V_{sample} \quad (11)$$

3.2.4 DNA Extractions

Sterile Sterivex-GP 0.22 μ m filters (EMD Millipore Corporation) were attached directly to tubing and filtered with 500-2000mL to ensure sufficient cellular material was collected for methanotroph quantification (Vigneron et al. 2017). Samples were collected from both Fox Hill Marsh locations in agreement with the filtration methods outlined in Tables 1-3 during for each incubation experiment.

DNA was extracted from Sterivex filters using the MO BIO PowerWater DNA Isolation and Qiagen DNeasy PowerWater kits. The procedure was carried out

according to the manufacturer's protocols, with the modification that the filter membranes were first manually removed from the Sterivex filter cartridges. The bead beating method was utilized to mechanically free cellular material from filter membranes and aid in cell lysis (Kolb et al. 2003). Additionally, lysis buffer was warmed to 55°C to dissolve all components and increase yields. Following several wash steps, sample DNA was eluted and dissolved into 80µL TE buffer.

DNA concentrations were quantified for each sample using an Invitrogen Qubit 2.0 fluorometer. Samples were diluted by 1:100 in a working solution of 200µL Qubit double-stranded DNA High Sensitivity buffer with added dye. A two-point standard curve was generated using 0ng/mL and 500ng/mL DNA standards and sample DNA concentrations were computed internally.

3.2.5 Quantitative Real-Time PCR

pmoA genes from marsh and outlet samples were amplified using the primer pair pmoA189F-mb661r. PCR mixtures were prepared in 20µL reaction volumes using 10µL SsoFast EvaGreen Supermix with Low ROX (BioRad), 100nM of each primer, and 10ng of Bovine Serum Albumin (BSA). Several experiments were run to determine the optimal primer and DNA concentrations for *pmoA* amplification. BSA was added to prevent inhibition of gene amplications (Kreader 1996). EvaGreen was selected opposed to the more commonly used SYBR Green Supermix due to lower levels of PCR inhibition (Eischeid 2011) and previous success with *pmoA* quantification in environmental samples (Bornemann et al. 2016).

A Stratagene Mx3000P qPCR Thermocycler was used for qPCR analysis. All samples were run in triplicate. Three stages were defined as part of the temperature

program in accordance with previously established programs specific to EvaGreen reaction mixtures (Bornemann et al. 2016). A denaturation step at 98°C was implemented for 2 minutes in the first stage, followed by 40 cycles of annealing and extension at 98°C for 6 seconds and 60°C for thirty seconds. Dissociation curves were obtained after the third stage, in which temperature was increased by 0.5°C from 60°C to 95°C. Melt curves were used in conjunction with gel electrophoresis to correlate sample DNA with standard results.

In order to calculate copy numbers for *pmoA* genes in samples, calibration curves were generated using a 10-fold serial dilution of the cleaned-up PCR product. Final gene copy numbers were computed using on Equation 12, where [DNA] was the extracted DNA concentration ($\text{ng } \mu\text{l}^{-1}$), qPCR was the instrument output (copies), V_{ext} was the 80 μl extraction volume, m_{DNA} was the 2ng of sample or standard used for qPCR reactions, and V_{sample} was the sample volume originally filtered through Sterivex cartridges (ml). To confirm successful amplification of *pmoA* genes, standard melt curve temperatures were correlated with literature values.

$$\frac{\text{Copies}}{\text{ml}} = \frac{[\text{DNA}] * \text{qPCR} * V_{\text{ext}}}{m_{\text{DNA}} * V_{\text{sample}}} \quad (12)$$

3.2.5.1 Standard Preparation

The qPCR standard was selected based on results from incubation experiments. A single marsh sample from the 7°C experiment exhibiting oxidation was used as the standard due to the likely presence of methane oxidizing bacteria. The 25 μL PCR reactions were carried out using the above procedure for only the chosen standard DNA. The 17.5 μL Agencourt AMPure XP paramagnetic bead solution (Beckman

Coulter) was added to the PCR product and was mixed by pipetting. PCR products were incubated at room temperature and placed on the magnet (Magnetic Particle Concentrator, Life Technologies) for 5 minutes. The supernatant was then removed and pellets were washed twice with 80% ethanol. The supernatant was again removed and products were left open to dry. Pellets were subsequently resuspended in 30mL RO water and placed on the magnet. 27 μ L of DNA-containing supernatant was removed and transferred to a clean PCR tube. An agarose gel was run using 2 μ L cleaned up product to ensure the successful removal of primer dimer products in the standard.

3.3 Data Analysis

All calibrations, analyses, and figure generation were processed using MATLAB R2015b and RStudio version 3.3.2. Principal Component Analysis (PCA) was used to compute variance for the Narragansett Bay time series data to determine potential correlations between variables over the two-month span. Temperature, salinity, methane concentration, dissolved oxygen, wind speed, and mean lower low water (MLLW) height data were used in the PCA, and the first three principal components were recorded and defined. A linear mixing model was constructed through matrix inversion calculations to compare relative methane contributions of various sites across Narragansett Bay, using in situ marsh measurements and Bay transect data.

Data from the moored CTD was used to compute the fraction of porewater present in outgoing water. Average salinity and dissolved oxygen values were calculated for both outgoing and incoming tidal flow. A mixing plot of salinity and

dissolved oxygen was then constructed with flood and ebb tide values along with porewater values from the 7°C sampling. The least squares method was then used to compute the fractions of marsh porewater and Narragansett Bay water present in outgoing water. The fraction of marsh porewater was applied to methane concentrations from the marsh and scaled up to include all Narragansett Bay salt marshes. This was achieved through using the salt marsh area estimate of 11.3 km² (Raposa and Schwartz 2009) across Narragansett Bay with an approximate average depth of 1 m. Annual contributions of methane were then determined by approximating 12 hours for the average daily outflow of water from marshes.

CHAPTER 4

RESULTS & DISCUSSION

4.1 Salt Marsh Biogeochemistry

Methane concentrations ranged from 394nM to 504nM in marsh porewater samples collected for incubation experiments. Methane increased with temperature (Table 4), possibly indicating a seasonal dependence, while carbon dioxide concentrations and methane $\delta^{13}\text{C}$ changed minimally in the porewater from December to May. Outlet CO_2 and CH_4 changed very little from 2°C to 7°C, but increased by over 150% during the May sample collection. Methane $\delta^{13}\text{C}$ in outlet samples correlated with temperature, similar to porewater methane concentrations. The stability of porewater $\delta^{13}\text{C}$ throughout the three sampling dates indicates that methanogenesis occurs via the same mechanism during this time span. The low $\delta^{13}\text{C}$ of -80‰ would suggest that hydrogenotrophic methanogenesis is the primary mechanism (M. Elizabeth Holmes et al. 2015), though $^{13}\text{CH}_4$ is much more depleted in our study than in previous porewater measurements (Avery et al. 1999). This would indicate that similar sources are utilized across this span as well, with the low isotopic signatures representative of marine sources rather than estuarine sources (Sansone, Holmes, and Popp 1999). Although $\delta^{13}\text{C}$ in the porewater stayed relatively stable, the outlet $\delta^{13}\text{C}$ trends likely indicate that the influence of the salt marsh on Narragansett Bay increases with temperature, reflecting the seasonality of methane cycling.

Date	Sample Location	Temperature (°C)	Salinity (ppt)	Dissolved Oxygen (μmol/kg)	CH ₄ (nM)	CH ₄ δ ¹³ C (‰)	CO ₂ (μM)
12/7/2016	Porewater	6.8	28.5	28.7	430±12	-81.4	1630±50
	Outlet	7.7	31.89	288.6	21.4±0.4	-62.1	22±1
3/15/2017	Porewater	2.2	25.08	20.1	394±3	-81.1	1628±1
	Outlet	2.7	32.2	316.6	24.7±0.5	-57.2	22.4±0.4
5/7/2017	Porewater	11.9	11.34	20.4	504±8	-80.2	1607±13
	Outlet	13.4	30.97	271.8	35.2±0.2	-67.4	33.2±0.6

Table 4. Measurements from Marsh Outlet and Porewater during each incubation experiment sample collection.

Methane concentrations shown in Table 4 are fairly low compared to previous porewater measurements, with studies reporting values as high as 472mM in salt marsh porewater samples (Parkes et al. 2011). Though this is nearly three orders of magnitude higher than our findings, it is significant that methane in the current study was measured shortly after high tide, when porewater concentrations are expected to be lowest due to dilution with seawater and the presence of oxygen (Grunwald et al. 2009). A preliminary sampling of methane in Fox Hill salt marsh porewater in November 2016 yielded concentrations of 764±2 nM during flood tide, which would suggest that this same trend is evident in Narragansett Bay marshes. It would also be conceivable that porewater methane concentrations approach the millimolar range at low tide, though sampling location, porewater depth, and organic matter input certainly influence methane levels throughout salt marshes (Parkes et al. 2011). Carbon dioxide concentrations are in agreement with porewater values from previous studies (LaZerte 1981; Parkes et al. 2011; Guo et al. 2016) and as mentioned above remain fairly constant across each sampling date.

4.2 Incubation Experiment Results

4.2.1 Methane Oxidation

Microbial activity with regard to methane was surprisingly inactive throughout the majority of samples. Of the three incubation experiments, only three treatment groups exhibited definitive changes in methane concentrations. The decrease in methane was accompanied by an increase in $\delta^{13}\text{C}$, indicating that biological oxidation was responsible for the methane turnover (Valentine et al. 2001; Reeburgh et al. 1991). Figures 8, 10, and 11 show the confirmation of methanotrophy, though all samples exhibited a significant period of inactivity, which is discussed in more detail in Section 4.2.1.1.

The 7°C filtered outlet samples represented the only treatment group to exhibit oxidation through the first two incubation experiments (7°C and 2°C). Because of the methane spike, dissolved methane concentrations in the outlet were similar to marsh concentrations. The added methane resulted in outlet $\delta^{13}\text{C}$ starting at approximately -25‰ and porewater $\delta^{13}\text{C}$ of -35‰. Figure 8(a) indicates the breakdown of methane from 400nM to 180nM with the corresponding increase in $\delta^{13}\text{C}$ to -10‰ in Figure 8(b) for the filtered outlet samples, though this only occurred after a span of 54 days. A similar study determined that the diversity of microbes decreases while the abundance of methanotrophs increases during long incubations in the presence of excess methane (C. Uhlig et al. 2017). Given the long incubation time, it is probable that the microbial communities in our samples were significantly evolved by the time oxidation occurred. Over the same period, all marsh porewater samples had constant methane

concentrations and isotope ratios, including those with BES added and nitrogen headspace, shown Figure 9 as well as in Appendix A.

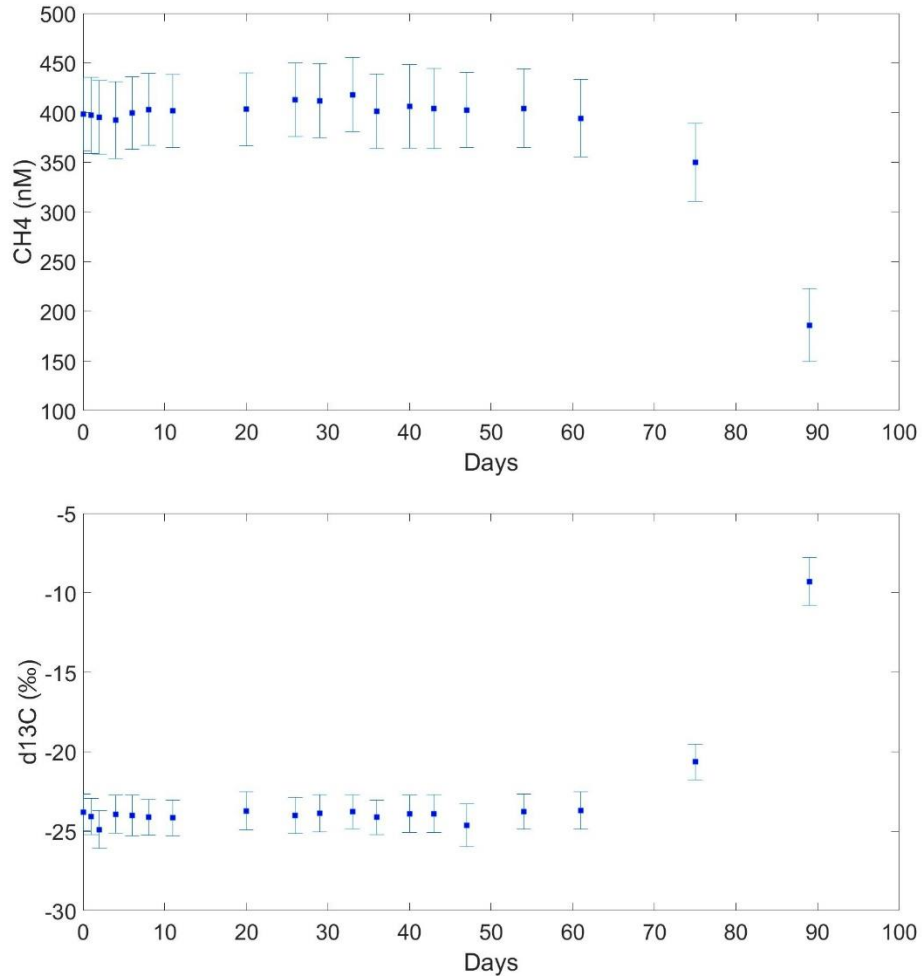


Figure 8. 7°C filtered marsh outlet methane concentrations (a) and $\delta^{13}\text{C}$ (b) during incubation.

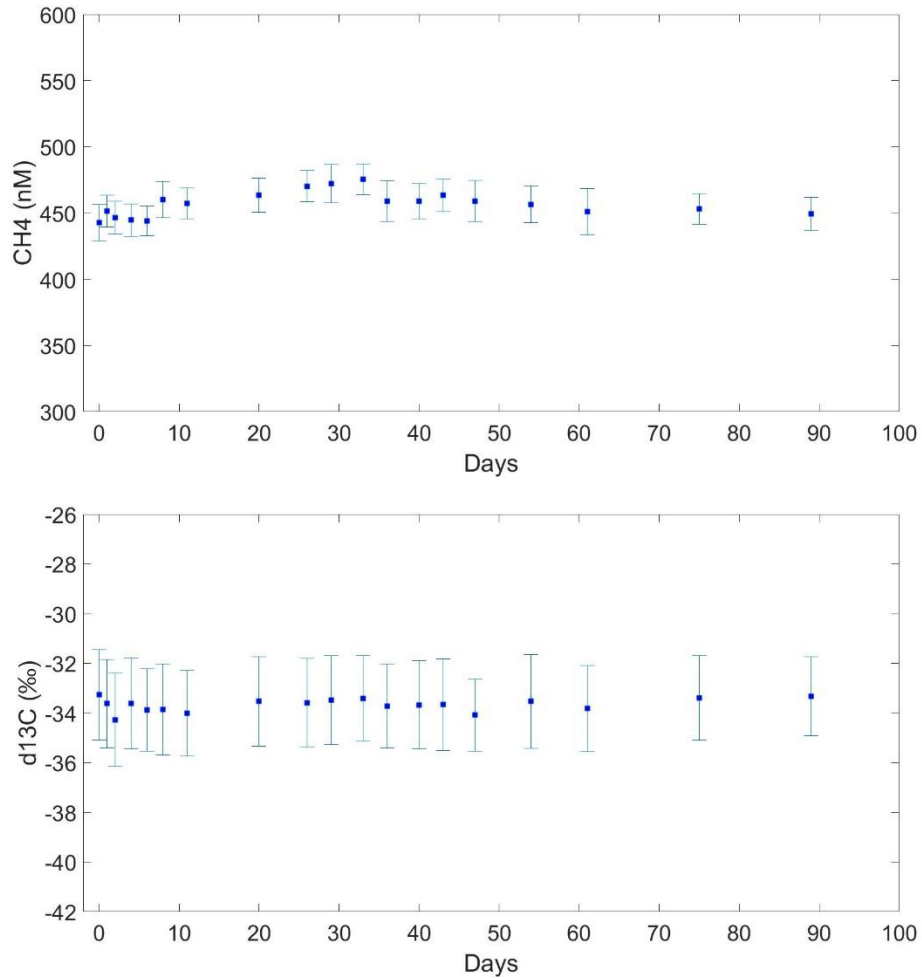


Figure 9. 7°C filtered marsh porewater methane concentrations (a) and $\delta^{13}\text{C}$ (b) throughout incubation experiment.

The 17°C incubation experiment featured two out of three oxygenated sample groups to exhibit methane oxidation, specifically the unfiltered outlet (Figure 10) and marsh porewater samples (Figure 11). In contrast, filtered outlet samples did not exhibit a methane decrease under oxic conditions. The effect of filter pore size on methane oxidation in estuarine samples was first considered by de Angelis & Scranton (1993), who found that methane oxidation rates decreased as filter pore size decreased. These findings may be supported by results in this study (Table 5), in that oxidation rates in unfiltered samples are nearly double those of filtered samples. However, as

both outlet samples also differed in incubation temperature and were collected separately, it is not clear whether differing oxidation rates are due to filtration or not. There is some evidence of increased methanotroph activity with greater suspended particulate matter (Abril, Commarieu, and Guérin 2007), which would be consistent with 17°C unfiltered outlet samples under the assumption that unfiltered samples had greater combined DOC and POC content.

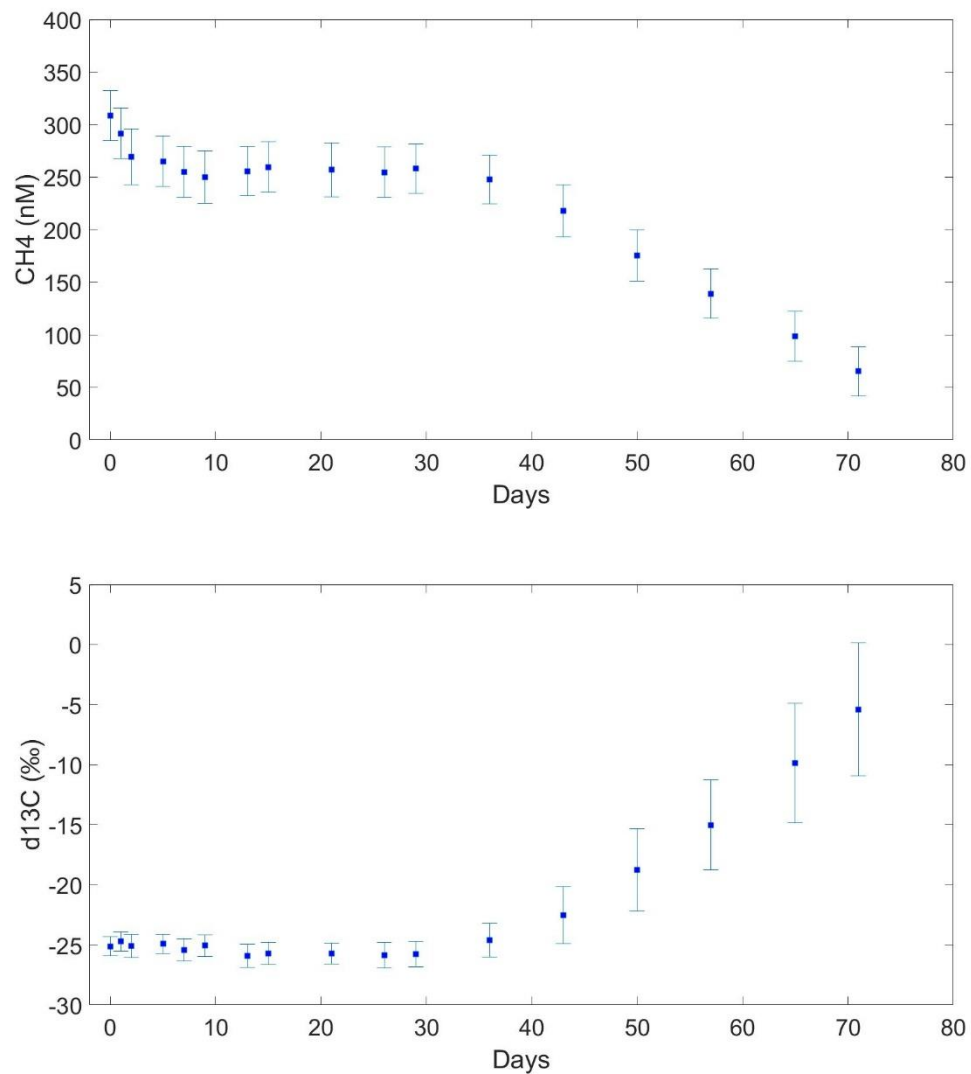


Figure 10. Unfiltered marsh outlet methane concentrations (a) and $\delta^{13}\text{C}$ (b) during 17°C experiment.

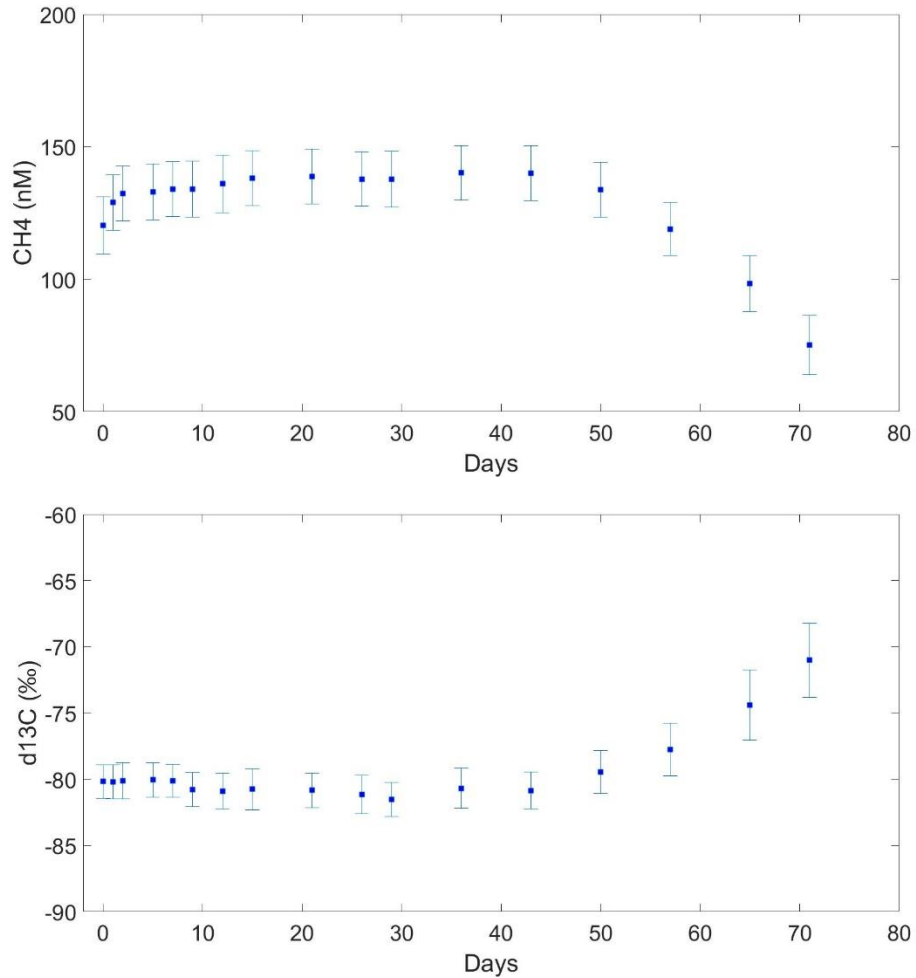


Figure 11. 17°C unfiltered marsh porewater methane concentrations (a) and $\delta^{13}\text{C}$ (b) throughout incubation period.

Results indicate that methane oxidation occurs more readily in the marsh outlet rather than the porewater. Oxidation rates are also significantly higher in the outlet than in the porewater, which could indicate higher numbers of methanotrophs or less inhibition of methanotrophs, discussed in further detail in Section 4.2.1.1. The oxidation rates for outlet samples were $6.4 \pm 0.6 \text{ nM d}^{-1}$ and $15 \pm 5 \text{ nM d}^{-1}$ for 7°C and 17°C, respectively, which are comparable to results from the 1993 study carried out in Narragansett Bay (Scranton et al. 1993). This study found oxidation rates up to 10 nM in the oxycline of the Pettaquamscutt Estuary, approximately 2 miles south of Fox Hill

Salt Marsh on the opposite shore of the West Passage. Methane concentrations in this region were found to be on average 600nM (Scranton, Donaghay, and Sieburth 1995), similar to the concentrations in the Fox Hill Marsh porewater but significantly higher than the outlet concentrations. High oxidation rates in our outlet samples were probably the result of the added methane spikes and may not reflect in situ rates of oxidation. However, results here indicate that if methane concentrations in the water were to increase (i.e. during warmer periods), methane oxidation will increase as well. The fact that oxidation rates in the marsh porewater were low despite high methane concentrations supports the idea that methanotrophy is controlled or inhibited by other factors present in the marsh

Temperature (°C)	Date	Sample Location	Treatment	Oxidation Rate (nM/day)	Days Before Oxidation Start
7	12/7/2016	Outlet	Filtered, ZA	6.4±0.6	54
17	5/15/2017	Outlet	Unfiltered, ZA	15±5	32
17	5/15/2017	Marsh	Unfiltered, ZA	0.71±0.02	38

Table 5. Methane oxidation results from incubation experiment samples exhibiting significant decreases in methane.

The influence of temperature on methanogenesis and methanotrophy are very well documented (Pulliam 1993; Bange et al. 1994; Lofton, Whalen, and Hershey 2014). Outlet sample oxidation results are consistent with findings that microbial processes double in rate for every 10°C temperature increase (Atlas and Bartha 1998), providing evidence for the seasonal dependence of methane cycling in the region. A great deal of research has been dedicated to this seasonality in estuaries, with highest

production rates (and thus concentrations) occurring in late summer and lowest over the winter when temperatures are at a minimum (Osudar et al. 2015; Gelesh et al. 2016). Although incubation experiments were not carried out using samples collected from summertime, calculated oxidation rates and in situ methane concentrations from all three experiments indicate that these variables would peak during the summer as well. Assuming there is a linear relationship between temperature and rates of methanotrophy, oxidation rates could reach 30nM/day during the highest outlet water temperatures while methane concentrations could reach 60nM and 640nM for the marsh outlet and porewater, respectively, during ebb tide (Figure 12).

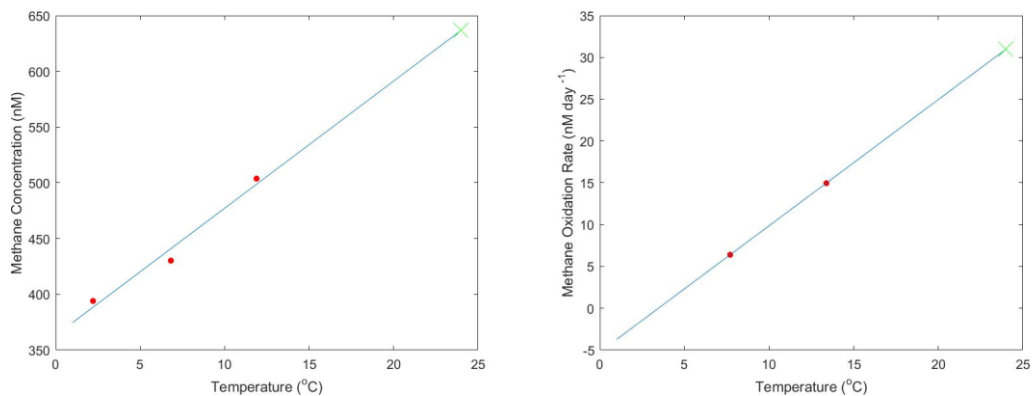


Figure 12. Projected marsh porewater concentrations (a) and outlet oxidation rates across range of Narragansett Bay temperatures, with indicated measurements (red dots), regression (blue line), and summer temperature projection (green x).

The lack of activity with the 2°C incubation samples implies that there is likely a temperature threshold for methanotrophs. For comparison purposes, methanotrophy in the cold waters of the Arctic Ocean (Damm et al. 2008; E. Damm et al. 2010; Damm et al. 2015) indicate that methane oxidation occurs at low rates at temperatures even lower than those used in our experiments. However, it is possible that methanotrophs and other microbial groups of Narragansett Bay have significantly

diminished metabolic rates at low temperatures, to the point where no methane-related activity was evident. Not all microbial processes were inhibited by the low temperatures, as CO₂ was produced throughout the 2°C experiments and SRB were still active in the anoxic samples (evidenced in subsequent sections). Methanotrophs have been shown to be sensitive to temperature changes in temperate regions (Matoušů et al. 2017), and therefore it is probable that their activity rates are at a minimum during winter. As there is no evidence for anaerobic methanotrophy in our samples, the case can be made that most methane produced in Fox Hill Marsh was emitted rather than oxidized. Because methane concentrations in the Marsh porewater remained high during winter, shown in Table 4, methanogenesis still continues throughout the year though there is evidence of temperature dependence of production rates in the upper portion of Fox Hill salt marsh (Martin and Moseman-Valtierra 2015).

4.2.1.1 Oxidation Lag Phase

In all samples exhibiting oxidation, methane concentrations did not begin to decrease until at least 32 days into the incubation period (Table 5). Although initially this lag was attributed to an adjustment period in which microbes were getting accustomed to their new environment (Valentine et al. 2001; Magen et al. 2014), the waiting period before oxidation occurred was longer than was documented in previous studies (Kosiur and Warford 1979). Kinetic effects due to temperature were likely responsible for the longer lag in the 7°C outlet samples (Atlas and Bartha 1998). There was no indication that the oxidation start day was correlated with POC content, methanotroph population numbers, or even oxidation rates (Table 5).

There are several hypotheses as to what factors were responsible for the significant lag time and the lack of oxidation in general. One possibility is that the methane oxidizing bacteria present in Narragansett Bay are facultative, in that they are able to utilize other substrates besides methane as a carbon source. Species of both *Alphaproteobacteria* and *Gammaproteobacteria* groups have been shown to consume single carbon compounds besides methane (Trotsenko and Murrell 2008). Species of the genus *Methylocella* in particular represent the only known methanotroph group capable of utilizing multi-carbon substrates. *Methylocella* species have been proven to utilize compounds like acetate, malate, and succinate, and may even prefer these compounds to methane (Dedysh, Knief, and Dunfield 2005). This group of compounds is abundant in wetlands due to their participation in major biological processes (Im et al. 2011); therefore, there is a strong possibility that facultative methanotrophs like *Methylocella* species are responsible for the oxidation lag.

Similar to methane, organic acids and ethanol can occur in wetlands via oxidation or anaerobic degradation, specifically through the decomposition of plant tissues and release through root systems (M. Elizabeth Holmes et al. 2015). Organic acids such as propionic acid can occur in marsh porewater at millimolar concentrations (Küsel et al. 2008), and have been shown to decrease or even inhibit methane oxidation at these concentrations (Wieczorek, Drake, and Kolb 2011). As propionic acid has not been found to be consumed by methanotrophs, it is possible that it inhibits methane oxidation via toxicity (Dedysh, Knief, and Dunfield 2005). Propionic and acetic acid can be detrimental to cellular membranes at high (greater than 1mM) concentrations (Russell 1992) and therefore could contribute to the

delayed methane-related activity in our samples. Given that this toxicity is not limited to methanotrophs and carbon dioxide concentrations increased during all experiments, suggesting that microbial respiration was not inhibited, it is more likely that facultative methanotrophy or competition between microbes was responsible for the lag instead of toxicity. Compared to other wetland and marine microbes, methanotrophs are historically regarded as slow growing (Osudar et al. 2015), meaning even with an energy source it takes longer to build up methanotroph communities.

4.2.2 Carbon Dioxide Production

Throughout the three incubation periods, carbon dioxide concentrations increased in all oxygenated samples bags (Table 6). This can be attributed to ongoing respiration under oxic conditions, as micro-organisms present continue the breakdown of organic material. Unlike the samples exhibiting methane oxidation, carbon dioxide in marsh samples began increasing within the first several days of the incubation period. Outlet samples tended to increase linearly throughout the incubation period while marsh porewater samples increased linearly for the first 30 days before leveling off, potentially due to a limited amount of labile organic material. As marine organic material tends to be more readily consumed than marsh organic material (Chen, Goni, and Torres 2016), a higher percentage of organic carbon in marsh outlet samples are directly available to microbes than in the porewater.

Temperature (°C)	Treatment	CO ₂ Production Rate (mM/Day)
7	Filtered Outlet - ZA - CH ₄ Spike	0.53±0.04
	Filtered Marsh - ZA - CH ₄ Spike	3.1±0.2
	Filtered Marsh - ZA - BES - CH ₄ Spike	2.2±0.5
	Filtered Marsh - N ₂ - CH ₄ Spike	1.34±0.07
2	Unfiltered Outlet - ZA - CH ₄ Spike	0.54±0.03
	Filtered Marsh - ZA - CH ₄ Spike	2.03±0.08
	Unfiltered Marsh - ZA - CH ₄ Spike	2.1±0.2
	Unfiltered Marsh - N ₂ - CH ₄ Spike	0.81±0.04
17	Filtered Outlet - ZA - CH ₄ Spike	0.60±0.08
	Unfiltered Outlet - ZA - CH ₄ Spike	0.5±0.2
	Unfiltered Marsh - ZA	3.9±0.5
	Filtered Marsh - N ₂	-0.62±0.08
	Unfiltered Marsh - N ₂	-0.6±0.3

Table 6. Carbon dioxide rates of production in all incubated sample groups.

CO₂ production rates show significant differences between outlet and marsh samples (Table 6). Production rates for outlet sample range from 0.5 to 0.6mM day⁻¹, while marsh sample production rates exceeded 2mM day⁻¹. Increased production rates in the marsh could reflect the higher amount of carbon present as well as a larger initial community of consumers. Results indicate a rapid phase of consumption followed by a slowdown of growth, caused by diminishing supply of available carbon. Slow sustained growth by heterotrophs in outlet samples indicate that initial population numbers were low while DOC concentrations were high. While the outlet sample production rates remain fairly constant through the three experiments, oxygenated marsh porewater samples had production rates that correlated significantly with temperature. 2°C marsh porewater production rates were 2mM day⁻¹, while the 7°C and 17°C samples produced CO₂ at a rate of 3.1±0.2mM day⁻¹ and 3.9±0.5mM day⁻¹.

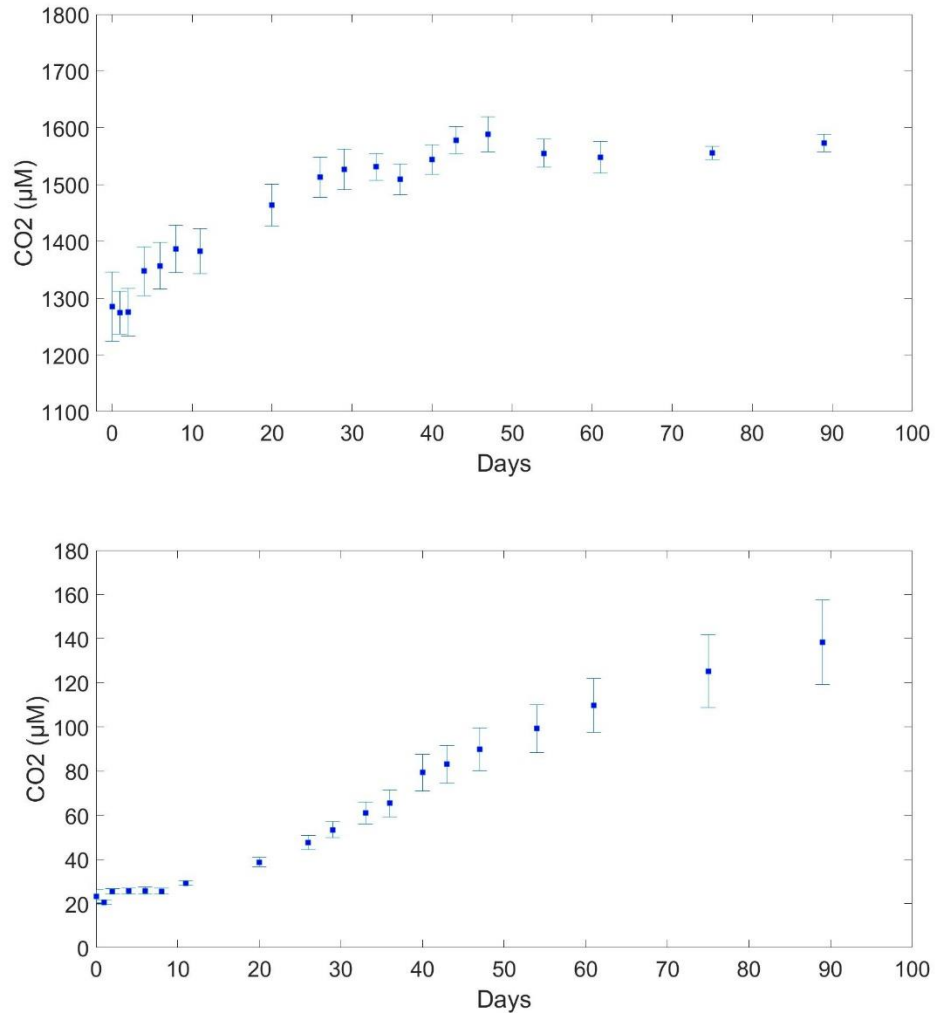


Figure 13. Carbon dioxide concentrations for marsh porewater (a) and outlet (b) samples during 7°C incubations.

As indicated by Table 6, both filtered and unfiltered porewater samples at 2°C produced CO₂ at approximately the same rate, indicating that all respiration occurring in the marsh utilized organic material from the <2.7μm size class. This trend was also evident in 17°C marsh outlet samples, which means that most CO₂ produced via respiration is derived from the pool of smaller-size of organic carbon, likely DOC. These findings indicate that this is the preferred size fraction for respiration across Narragansett Bay, similar to previous research (Lapoussière et al. 2011).

The negative rates of CO₂ production in 17°C anoxic marsh samples signify a breakdown of carbon dioxide. Given that CO₂ is a substrate for hydrogenotrophic methanogenesis, it is possible that CO₂ in our experiment is consumed by methanogens. It has been shown that hydrogenotrophic methanogens tend to account for the majority of methane production from fall through spring, while acetoclastic methanogens dominate during summer months when acetate concentrations are high (Avery et al. 1999). Since acetate fermentation produces carbon dioxide and methane, hydrogenotrophic methanogenesis is the likely mechanism in Fox Hill salt marsh porewater.

4.2.3 Methanogenesis

There was limited evidence for methane production during any of the three incubation periods. The possibility for micro-anoxic zones existing in oxygenated waters was not evidenced in the experiments, as there was no increase in methane observed in any samples with oxygen-containing headspace added. The 2°C incubation experiment indicated no statistical differences between filtered and unfiltered samples, as well as no difference between oxic and anoxic samples.

As previously mentioned, methanogens are expected to be less temperature dependent than methanotrophs. However, there was a significant difference between anoxic samples from the 17°C experiment, highlighting kinetic effects with methanogenesis similar to methanotrophy and respiration (Segers 1998). While the filtered 7°C and unfiltered 2°C anoxic samples did not exhibit any methane-related activity, the 17°C unfiltered N₂-headspace samples showed a net increase in methane concentrations and corresponding decrease in δ¹³C, shown in Figures 14 and 15.

Though not always expected to decrease with production (Whiticar 1999), methane becoming more depleted in ^{13}C would suggest the consumption of highly fractionated organic material (Conrad, Claus, and Casper 2009). Methane is expected to have a $\delta^{13}\text{C}$ signature reflective of source material and therefore largely dependent upon the production pathway. Methane produced from CO_2 via the hydrogenotrophic pathway, yields a $\delta^{13}\text{C}$ more depleted in ^{13}C than CH_4 produced via acetate fermentation (M. Elizabeth Holmes et al. 2015). The decrease in $\delta^{13}\text{C}$, coupled with a negative production rate in carbon dioxide reflecting net CO_2 decrease, confirm that methane produced in the 17°C samples occurred via the hydrogenotrophic pathway.

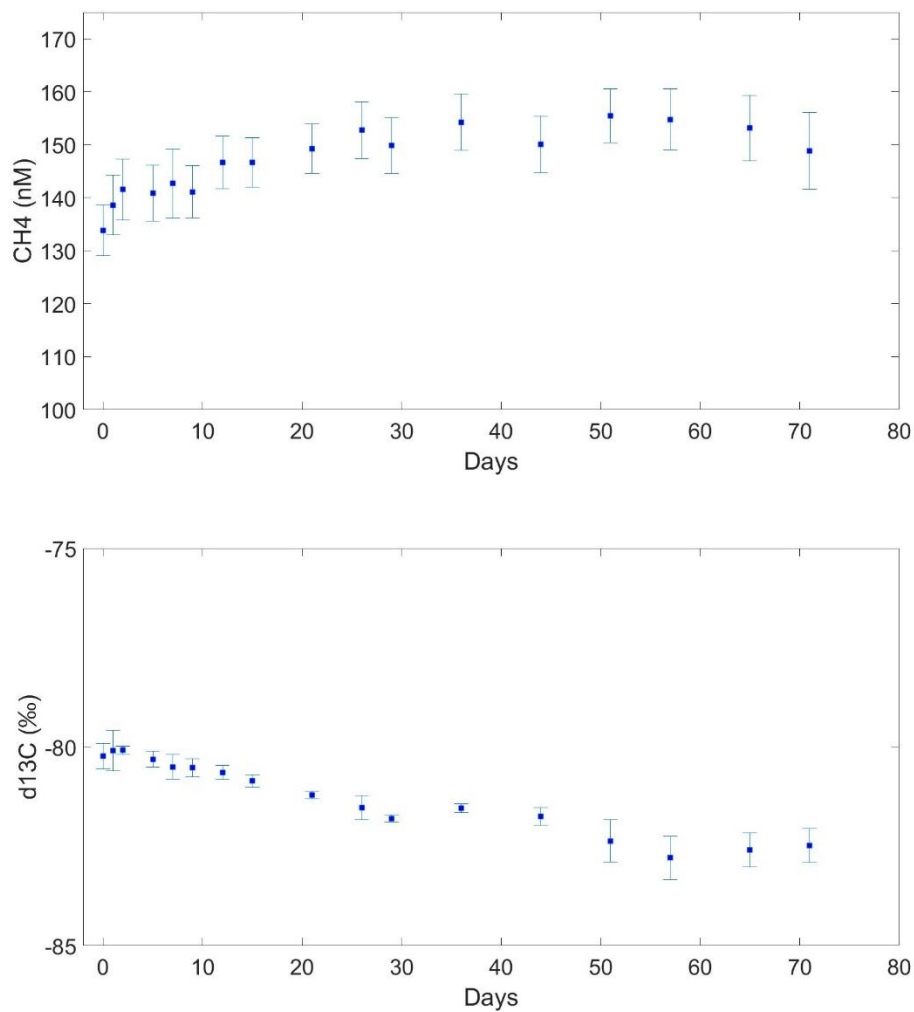


Figure 14. Methane concentrations (a) and $\delta^{13}\text{C}$ (b) for unfiltered anoxic marsh porewater samples during 17°C incubation.

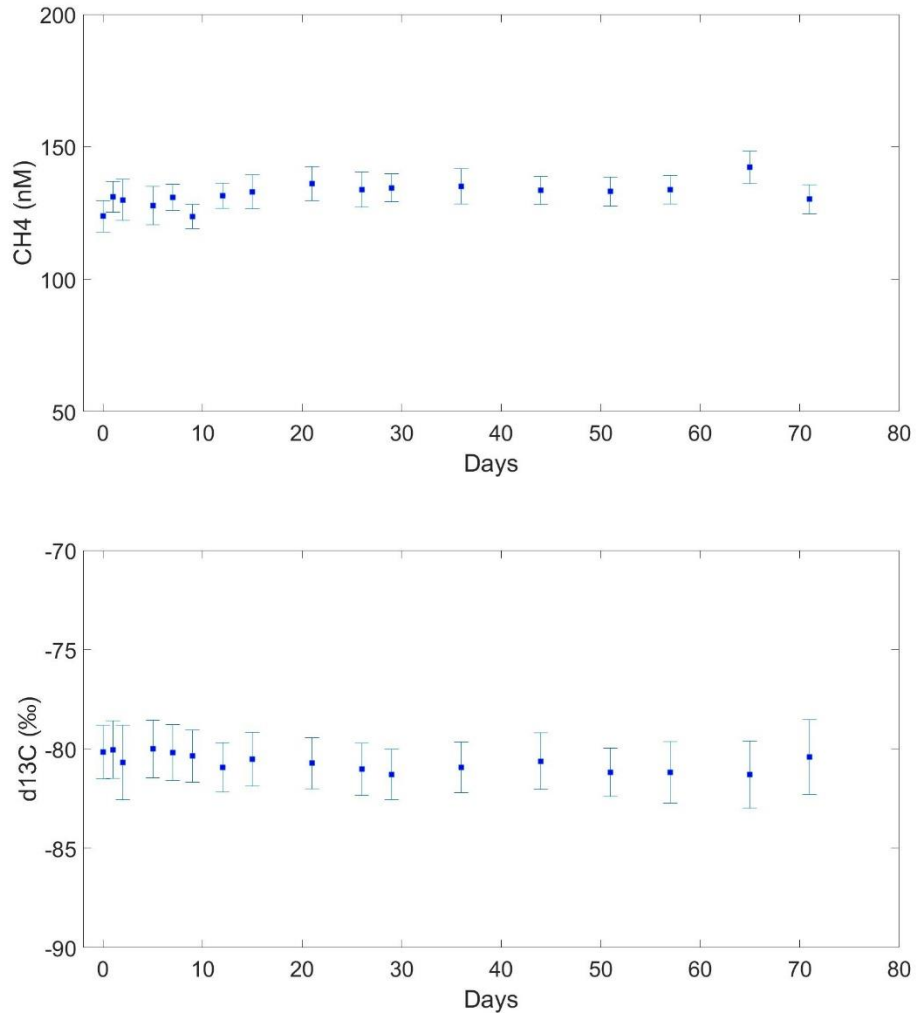


Figure 15. Methane concentrations (a) and $\delta^{13}\text{C}$ (b) for filtered anoxic marsh porewater samples during 17°C incubation.

It appears that methane production and CO₂ production display similar characteristics. The preferential removal of lighter organic carbon compounds results in residual ¹³C-enriched substrate in the marsh. The residual organic material is also typically less readily broken down (Canuel and Hardison 2016); therefore, it is possible that much of the organic matter utilized by methanogens and consumers alike is introduced to microbes through tidal influx, though the relationship between methanogenesis and plant productivity is already well established (Whiting and

Chanton 1993). Fatty acids and alcohols are more readily broken down than marsh grass detritus (primarily cellulose and lignins) (Cifuentes and Salata 2001), further providing evidence for the importance of recently produced organic matter in both CH₄ and CO₂ production. For salt marshes like Fox Hill, tidal influence is essential for the turnover of organic matter, providing marsh microbial communities with substrate.

While the microorganisms that carry out respiration can be free-floating, the archaea responsible for methane production tend to have a close relationship with sediment and particulate matter (Wüst, Horn, and Drake 2009). This is evident in the incubation samples, as no filtered marsh samples with N₂ gas headspace exhibited increases in methane. Filtering samples using 2.7µm pores excluded the 5µm threshold for micro-anoxic zones (Magen et al. 2014) as well as larger POC compounds that may play a role in housing methanogenic archaea. The unfiltered treatment appears to have been successful at capturing methanogens; however, since methane concentrations level off after the initial 30 days it is possible that either conditions were not favorable in our water samples or available organic matter was used up within the 30-day period. It has been shown that the majority of methane production occurs within the sediment (Reeburgh 2007), indicating that methanogens were likely stressed by remaining in suspension within the sample vessels, which limited production and potentially diminished the community size.

Apart from the argument for non-ideal incubation conditions, results indicate that methanogens were significantly affected by sulfate-reducing bacteria (SRB). Although sulfur compounds were not directly measured in this study, Picarro greenhouse gas analyzer CO₂ δ¹³C measurements can exhibit significant interference

by hydrogen sulfide (H₂S) gas (K. Malowany et al. 2015). Measurements of $\delta^{13}\text{C}$ for carbon dioxide throughout incubation experiments were abnormally low, indicative of H₂S interference. Hydrogen sulfide is the results of the reduction of sulfur (sulfate) by SRB. These bacteria utilize sulfate as a source of energy under hypoxic conditions as required to oxidize organic material (Clarke 1953). This reaction occurs readily in salt marshes in low oxygen conditions and is favored over methanogenesis, which uses the same substrates. The $\delta^{13}\text{C}$ results shown in Figure 16 indicate that this region is dominated by SRB that outcompete methanogens.

The Picarro G2201-*i* CRDS CO₂ isotopic signals are especially impacted by H₂S, to the point where a linear relationship has been found between H₂S concentrations and $\delta^{13}\text{C}$. One particular study found that H₂S concentrations of 20ppmv yielded $\delta^{13}\text{C}$ values around -600‰, even though the known $\delta^{13}\text{C}$ was -16‰ (K. Malowany et al. 2015). The 2°C and 7°C experiments showed $\delta^{13}\text{C}$ values of -100‰ to -200‰; however, the $\delta^{13}\text{C}$ of 17°C N₂-headspace samples read from -400 ‰ to -800‰ at times. As CO₂ isotope ratios this low have never been recorded (M. Elizabeth Holmes et al. 2015), this must be the result of H₂S. The fact that the interference in O₂-headspace samples disappeared after several days reiterates that H₂S was the cause. The $\delta^{13}\text{C}$ found in the present study would indicate the H₂S concentrations were in excess of 20ppmv, which translates to an inhibition of CH₄ production and methanogen communities with much smaller populations than SRB communities. Because of this interference, CO₂ $\delta^{13}\text{C}$ results were not able to be reported in this study even after steps were taken to remove H₂S from subsamples (K. Malowany et al. 2015).

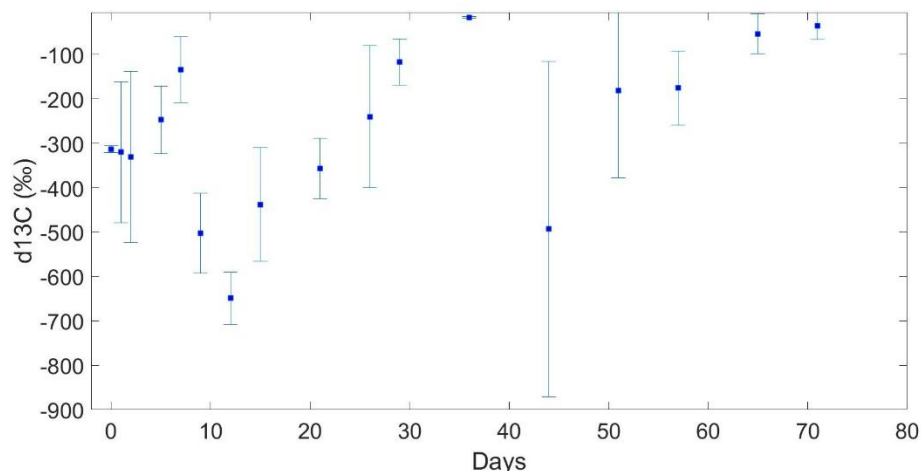


Figure 16. Example of H₂S interference on δ¹³C measurements in N₂-headspace marsh samples from 17°C experiment.

4.2.4 Particulate Organic Carbon

Temperature	Treatment	Starting POC	Final POC
7	Filtered Outlet - ZA - CH ₄ Spike	3.93	9.42
	Filtered Marsh - ZA - CH ₄ Spike	3.40	8.17
	Filtered Marsh - ZA - BES - CH ₄ Spike	3.40	19.79
	Filtered Marsh - N ₂ - CH ₄ Spike	3.40	5.52
2	Unfiltered Outlet - ZA - CH ₄ Spike	23.61	7.96
	Filtered Marsh - ZA - CH ₄ Spike	6.55	19.15
	Unfiltered Marsh - ZA - CH ₄ Spike	43.90	9.32
	Unfiltered Marsh - N ₂ - CH ₄ Spike	43.90	11.72
17	Filtered Outlet - ZA - CH ₄ Spike	9.07	14.08
	Unfiltered Outlet - ZA - CH ₄ Spike	10.78	13.02
	Unfiltered Marsh - ZA	7.23	10.64
	Filtered Marsh - N ₂	6.38	10.75
	Unfiltered Marsh - N ₂	7.23	17.29

Table 7. Particulate organic carbon measurements for all sample groups at incubation start and end. All POC measurements have units μmol/L.

POC concentrations varied greatly depending on the time of year and location at which sampling took place (Table 7). As expected, filtered samples had lower starting POC than unfiltered samples, although this observation did not correlate with

final POC content. The final organic carbon concentrations for the 7°C and 17°C were higher than the starting concentrations for all treatment groups. The 2°C unfiltered sample bags had much higher starting POC concentrations than all other experiments and decreased by the end of the incubation period in all but the filtered marsh samples. The high POC concentrations could be the result of a toxic algae bloom that occurred throughout Narragansett Bay the week prior to sampling in the marsh, as bloom conditions tend to generate large amounts of particulate carbon (Chalmers, Wiegert, and Wolf 1985). This could also be attributed to more difficulties with removing larger sediment from sample vessels. The unfiltered marsh and outlet POC samples decreased significantly through the incubation experiment, potentially due to particulate carbon material more readily consumed opposed to plant material. Based on carbon dioxide production rates (Table 6) it is plausible that respiring microbes were able to utilize carbon from the POC pool if the high POC concentrations reflected labile organic matter sources, like phytoplankton detritus following bloom conditions.

In many cases, POC of outlet samples exceeded those from the marsh porewater. This could reflect the particle size selected for by the filtration methods. Unfiltered samples contained all particles smaller than 100 μm , while all filtered samples contained particles smaller than 2.7 μm . As marsh porewater typically consists of particles greater than 100 μm (Moskalski and Sommerfield 2011), it is reasonable that POC concentrations below this threshold are similar between the marsh and outlet. The low starting POC content of the 7°C samples may simply indicate that samples were collected closer to flood tide, as ebb tide water contains higher

concentrations of DOC and POC opposed to flood tide (Moskalski and Sommerfield 2011).

Another possible explanation is that the filtration of small sample volumes (1-2 L) through glass fiber filters may result in the retention of dissolved organic carbon (DOC) despite the 0.7 μ m filter pore size. One particular study found final POC concentrations to erroneously contain over 35% DOC at low sample volumes (Abdel-Moati 1990). The solution to this issue is to increase the filtration volume to at least 100L (Moran et al. 1999); however, this was not feasible in our experiments given the tidal dependence of the experiments and the slow sampling rates.

All samples that exhibited methanotrophy also experienced increases in POC. As these samples were also positive for carbon dioxide production, the increase in POC may result from the aggregation of DOC and detritus (Biddanda and Pomeroy 1988), which is feasible given the duration of all three incubation periods. There appears to be no correlation between methane oxidation and POC concentrations, indicating that this pool is not directly impacted by methane cycling. Larger particles may be more important in housing microbes, as studies have found that oxidation rates increase with increasing filter pore sizes during sample collection (de Angelis and Scranton 1993). One particular study suggested that methanotrophs are surface active, as rates of methane consumption in bacteria were increased by the addition of 2 μ m particulate matter (Weaver and Dugan 1972). The idea that smaller size fraction of POC (<2 μ m) are important to microbes may indicate that small particles provide increased nutrients, stimulation or enhancement of oxidation, or even the adsorption of inhibiting compounds and competing microbes (Weaver and Dugan 1972). The

assumption from our results is that outlet samples POC had proportionally smaller size fraction relative to porewater samples, potentially explaining why multiple outlet samples exhibited methane oxidation relative to marsh porewater samples.

4.2.5 Microbiology of Incubation Samples

An initial question in the filtration of marsh water samples was if they would restrict the number of microbes able to pass through into sample vessels. Although the 2.7 μm pore size was well above the 0.2 μm cutoff for bacteria (Salonen, Kairesalo, and Jones 2012), significant buildup of sediment was observed with every filter use to the point of water flow being impacted. To test whether the 2.7 μm filter was limiting the passage of bacteria, samples from marsh wells were collected on November 14, 2016 for analysis by flow cytometry. Results from flow cytometry indicate that there is no significant difference in cell count between the 2.7 μm and 20 μm filters (Table 8). It appeared that the GF/D filters used were successful in filtering out microanoxic zone-containing particles without restricting the bacteria communities able to be sampled. These results also provided total bacteria counts for marsh porewater samples, though it is probable that community numbers are generally highly variable throughout the year

Filter pore size (μm)	Bacteria count (cells/ml)
0.2	4.29 \pm 0.13E04
2.7	3.12 \pm 0.89E06
20	3.16 \pm 0.88E06

Table 8. Flow cytometry results, showing bacteria counts for corresponding filter sizes.

Molecular tools were applied to further characterize the bacterial community with respect to the presence of methanotrophs. Melt curve analysis indicates that *pmoA* genes were successfully amplified by the selected primer pair, shown in Figure 17 with the standard template. Amplification of the standard template resulted in a single dissociation peak of 83°C (17a), which was then used as the reference melting temperature to confirm amplification of the correct gene in all samples. Previous results indicate that the primer pair A189f/mb661r yields PCR products with melt curves in the 82-83°C range, consistent with our standard results and indicating that the correct product was amplified. The *pmoA* gene, with a sequence of 510 base pairs (Kolb et al. 2003), was also confirmed in the standard by gel electrophoresis.

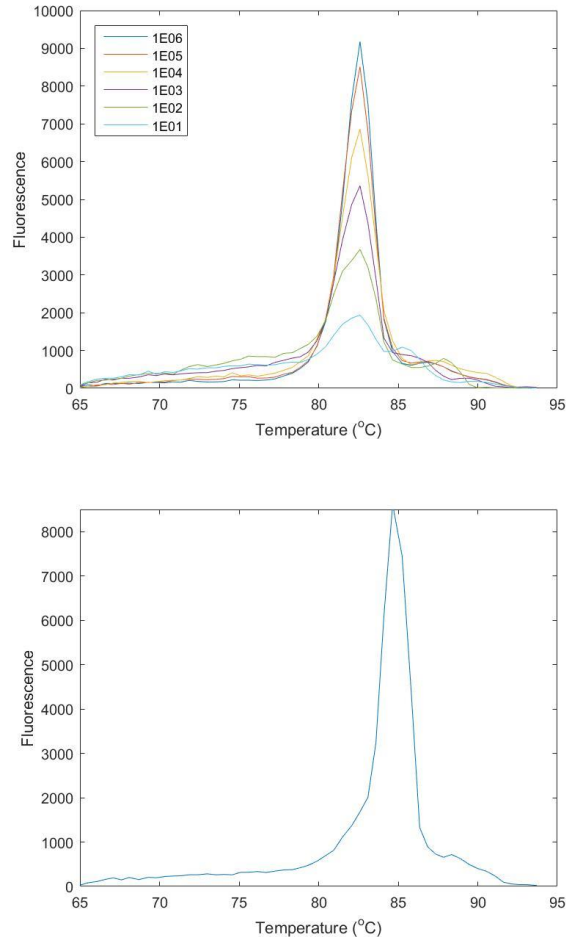


Figure 17. Dissociation curves from qPCR runs for standards (a) and the 17°C unfiltered marsh sample (b) which exhibited methanotrophy.

Most samples with hydrocarbon-free (oxygenated) headspaces were confirmed by qPCR dissociation curves to express the *pmoA* gene and thus have methanotrophs present. However, in most cases the correct peak was accompanied by one or multiple peaks at different temperatures. Typically primer-dimer peaks are reflected below 80°C in melt curve analysis, due to their being smaller sized products than the 510-base pair *pmoA* genes (Kolb et al. 2003). This was an issue in early qPCR runs along with amplification inhibition; however, a re-purification step was implemented that led to improved amplification of samples, discussed in Appendix B. Given that the

multiple peaks displayed in most samples were greater than this 80°C threshold, it is likely that non-specific amplification was prevalent during PCR reactions opposed to primer-dimer artifacts (Bourne, McDonald, and Murrell 2001). The outlet samples in particular all contained a peak at 88°C, both in the samples collected directly from the marsh and those collected at the end of the incubation experiments. Because of this nonspecific amplification, copy numbers were not computed for the majority of samples in this study.

While qPCR was unsuccessful at accurately and precisely quantifying copy numbers of *pmoA* in all incubation samples due to false positives associated with nonspecific amplification (Ruiz-Villalba et al. 2017), qPCR dissociation curves and gel electrophoresis did confirm that there were methanotrophs present in Fox Hill Salt Marsh throughout the year. Figure 18 shows the computed copy numbers for the three sample groups that exhibited oxidation, in which both 17°C samples had higher bacteria counts than the 7°C sample. While the copy numbers agree with previous findings of the positive impact temperature has on microbial culture growth (Atlas and Bartha 1998), copy numbers do not correlate with oxidation rates, as the 17°C unfiltered marsh samples had the lowest oxidation rates. However, given the increased lag time in the 17°C porewater samples compared to outlet samples, it is likely that a greater percentage of methanotrophs in marsh porewater samples were facultative. This would make sense, given the high concentrations of small organic acids and alcohols typically present in salt marshes (Dedysh, Knief, and Dunfield 2005; Im et al. 2011).

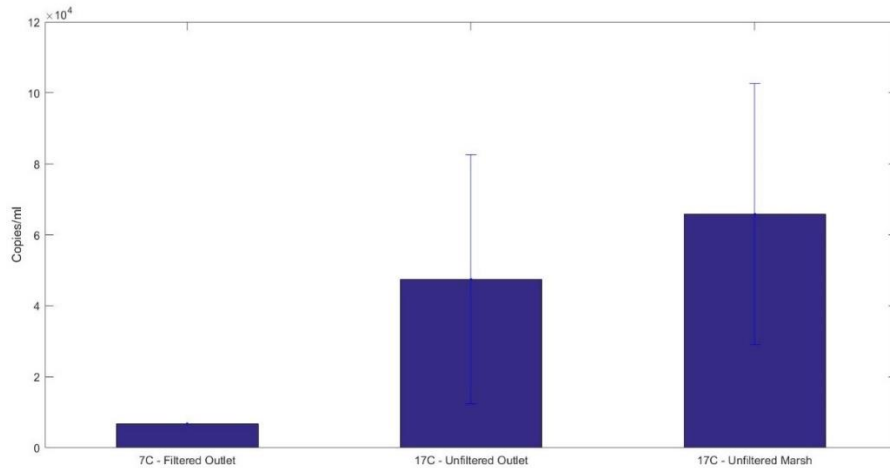


Figure 18. Copy numbers for all sample groups exhibiting oxidation.

Theoretically, there are two *pmoA* copies per cell (S. Stolyar et al. 1999; Sergei Stolyar, Franke, and Lidstrom 2001) so the true methanotroph counts are approximately half of the copy numbers displayed above. The flow cytometry data (Table 8) reflect marsh porewater bacteria counts of approximately 3×10^6 cells ml^{-1} , while in situ methanotroph cell counts were roughly 2×10^3 cells ml^{-1} . This translates to a methanotroph abundance of 0.07% of the total bacteria present in the marsh, which is comparable to water column abundance (Bornemann et al. 2016) but much lower than typical soil abundance (Kolb et al. 2003). These results provide evidence for the lag in incubation time and the proposed slow growth of Narragansett Bay methane oxidizing bacteria.

It is suspected that the nonspecific amplification in most samples is largely due to low target gene abundance, as it is clear that methanotrophs were either inhibited in incubation samples or took a great deal of time to develop due to their slow growth relative to other microbial groups (Osudar et al. 2015). However, the computed copy numbers also may not reflect the true methanotroph populations of Fox Hill marsh

porewater and outlet. *Methylocella*, the most well-documented genus of facultative methanotrophs, do not possess pMMO enzymes and only utilize the sMMO. Since our qPCR experiments only involved the *pmoA* primer pair, copy numbers belonging to the *Methylocella* genus were not computed. In the future, it would be beneficial to use *pmoA* and *mmoX* primers for qPCR, as *mmoX* genes encode the soluble methane monooxygenase enzyme and quantification of *Methylocella* would be possible.

4.3 Narragansett Bay Methane: Time Series

The two-month time series showed temporal variability across all measurements as the water temperature increased from Spring into Summer (Figures 19 and 20). Methane concentrations ranged from 7nM to 20nM, which agrees with previous measurements in similarly shallow coastal sections of estuaries (Osudar et al. 2015). Water temperature rose from 14°C in May to 24°C in July, which would result in approximately 3.0nM and 2.5nM CH₄, respectively, if waters were at equilibrium saturation with the atmosphere (Yamamoto, Alcauskas, and Crozier 1976). Dissolved oxygen measurements were undersaturated with respect to the atmosphere by 10-20%, likely reflecting high rates of microbial respiration (Lee et al. 2015).

As methane concentrations increased, $\delta^{13}\text{C}$ decreased with the rising temperature. The isotope ratio on average is more ¹³C-depleted than the average Narragansett Bay water (see Section 4.4), with $\delta^{13}\text{C}$ around -58‰ at this location. Though lateral transport could provide this area with methane, it is more likely that methane is produced in the sediment, given the shallow depth of this site and sediment type (Wüst, Horn, and Drake 2009). These results confirm the findings from the incubation experiments, in that methane concentrations increase with water

temperature due to higher production rates. Carbon dioxide concentrations over this two-month period are highly variable, though over the entire dataset concentrations trend down.

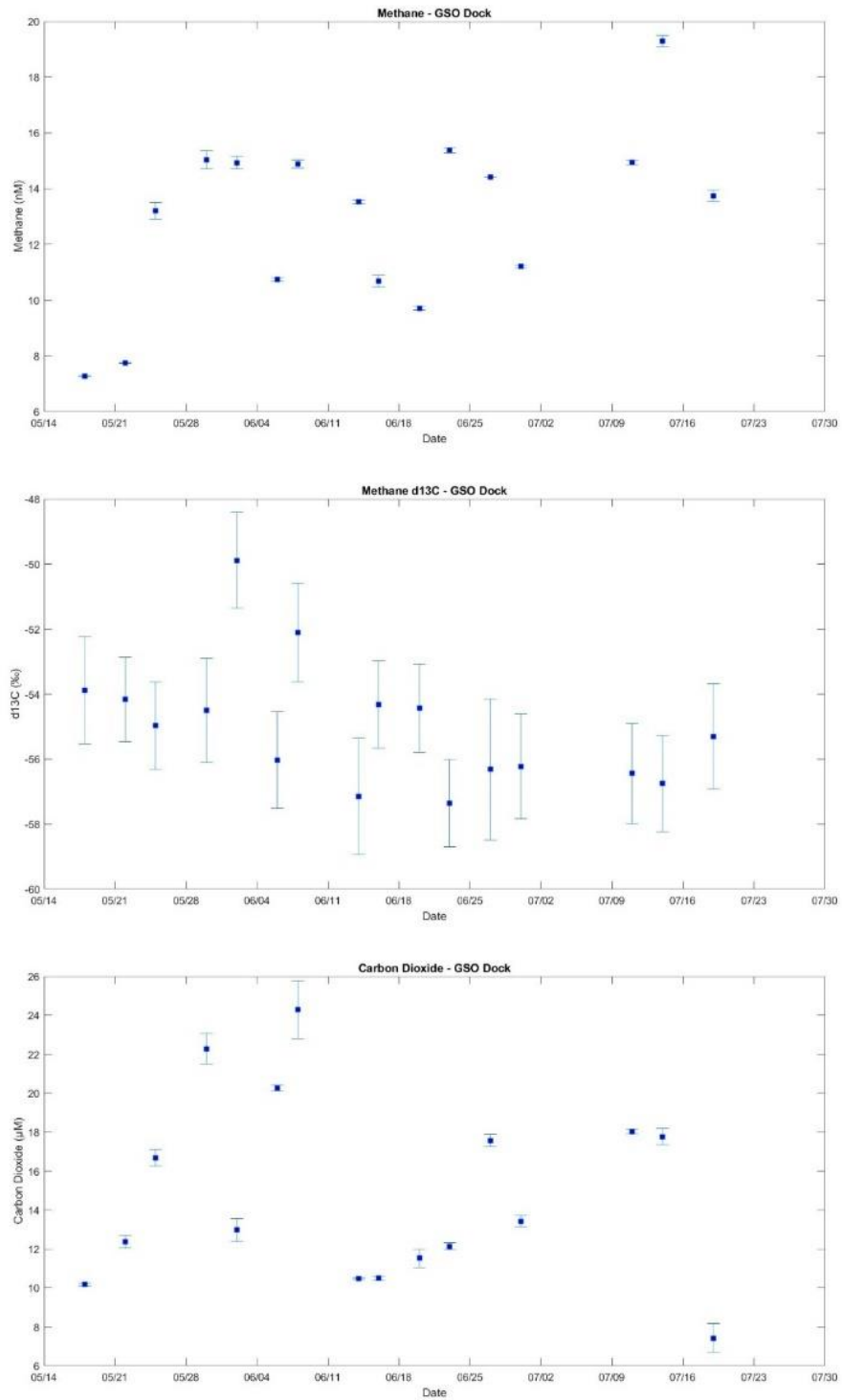


Figure 19. CH₄ (a), δ¹³C (b), and CO₂ concentrations at URI/GSO sampling location from May to July 2017

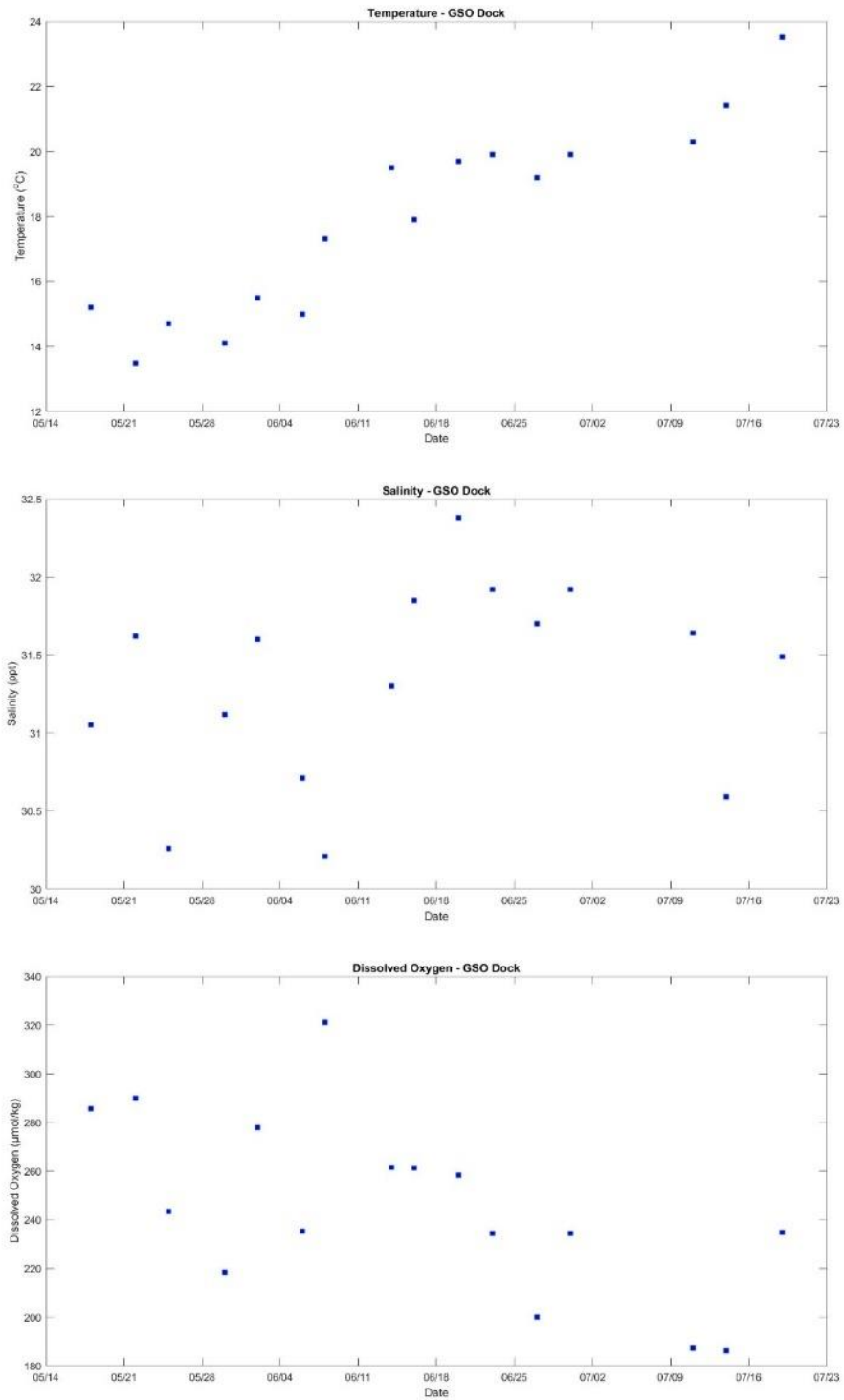


Figure 20. Temperature (a), salinity (b), and dissolved oxygen at URI/GSO sampling location from May to July 2017.

The principal component loadings in Figure 21 reflect the observations made in Figures 19, 20, and Appendix C, as the first principal component (PC1) shows methane and temperature anticorrelated with wind speed, $\delta^{13}\text{C}$, and CO_2 . This component can be explained temporally, in that wind speed decreased as temperature increased from Spring into Summer. This also confirms that in situ production in the sediment was responsible for increasing methane concentrations, evidenced by the decreasing $\delta^{13}\text{C}$. Figure 22 shows that 42% of the data variance can be explained by this seasonal shift.

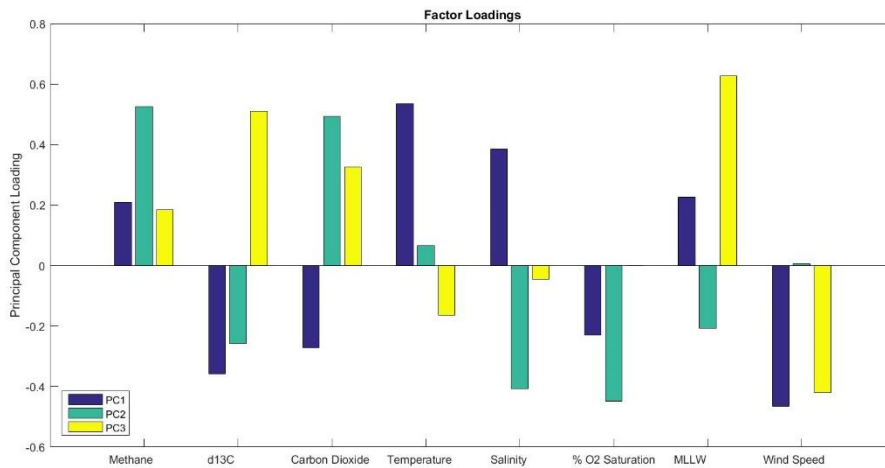


Figure 21. Factor loadings for the first three principal components from variables shown in Figure 19 and Figure 20.

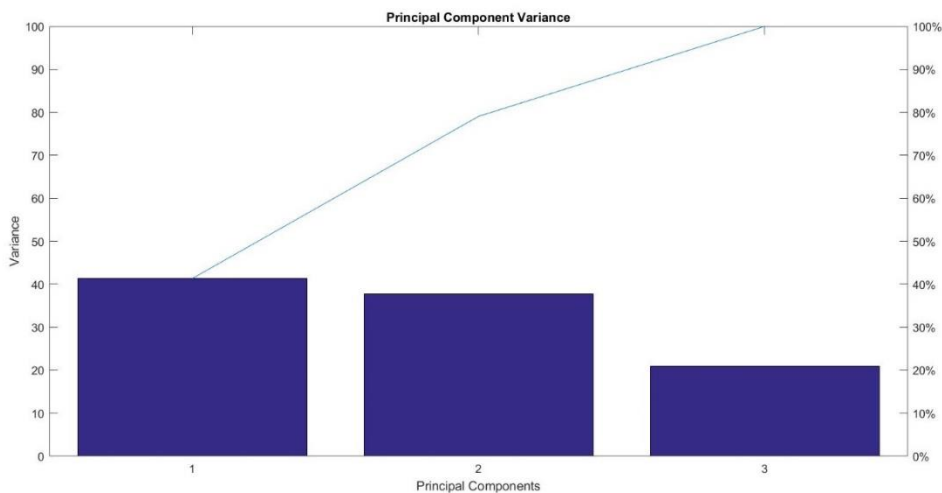


Figure 22. Normalized variance (bars) and total percent variance (line) for time series principal components.

Approximately 38% of the time series data variance (PC2) can be explained by tidal influence, as methane varies inversely to salinity and MLLW. Methane concentrations were higher and $\delta^{13}\text{C}$ lower following low tide when salinity and water levels decreased. Similar to previous findings (Grunwald et al. 2009) and in situ Fox Hill marsh measurements, rates of methane production were highest at low tide opposed to high tide. Another finding within the second principal component was that carbon dioxide and oxygen saturation were strongly anticorrelated, which may indicate that respiration, like methanogenesis, is tidally dependent. Though not measured in this experiment, emission rates for both greenhouse gases likely peak with low tide in Narragansett Bay, given the shorter water column leading to increased vertical transport and decreased lateral transport (Yang et al. 2017).

The third component (PC3) accounts for 20% of the variance and indicates a correlation between methane $\delta^{13}\text{C}$ and MLLW and anticorrelation with wind speed. This principal component reflects the effects of two major processes on methane

isotope ratios. Even though the production of methane results in low isotope ratios (depleted in ^{13}C), tidal influx into Narragansett Bay dilutes methane $\delta^{13}\text{C}$ with $^{13}\text{CH}_4$ enriched waters of the Atlantic Ocean, which on average has an isotopic signature of -45‰ (Yu et al. 2015; Keir et al. 2005). At the same time, gas transfer increases quadratically with wind speed (Wanninkhof 1992), which means that a relatively insoluble gas like methane experiences increased emissions with increased wind speed. Although biological fractionation has been thoroughly discussed in this study, fractionation also occurs with gas transfer; ^{12}C is more likely to be emitted than the heavier ^{13}C due to the kinetic isotope effect and therefore, aquatic methane $\delta^{13}\text{C}$ increases (^{13}C -enriched) with higher sustained wind speeds.

4.4 Narragansett Bay Survey



Figure 23. Bay survey reference map indicating sampling sites, Fields Point Wastewater Treatment Plant (WTP), and Greenwich Bay (GB) locations.

Results from the bay survey show that methane concentrations along the West Passage are highest at the mouth of the Providence River and lowest approaching the mouth of Narragansett Bay. This would indicate that there is a strong freshwater source for methane in Narragansett Bay, similar to previous findings in similar environments (Osudar et al. 2015; de Angelis and Scranton 1993; Scranton and McShane 1991). Methane $\delta^{13}\text{C}$ generally increases moving southward toward the mouth of the bay; however, there was a strong signal recorded at Station 4 (-60‰), 15km from the river. Although results show a significant freshwater source, this site likely has a more proximal source of methane in the form of production in the sediment or from nearby Greenwich Bay (indicated in Figure 23). Carbon dioxide concentrations are also highest at the mouth of the Providence river at 17 μM and decrease to 12-14 μM south of Station 1. The $\delta^{13}\text{C}$ for CO_2 suggests that organic matter in the upper bay is more ^{13}C -depleted than in the lower bay.

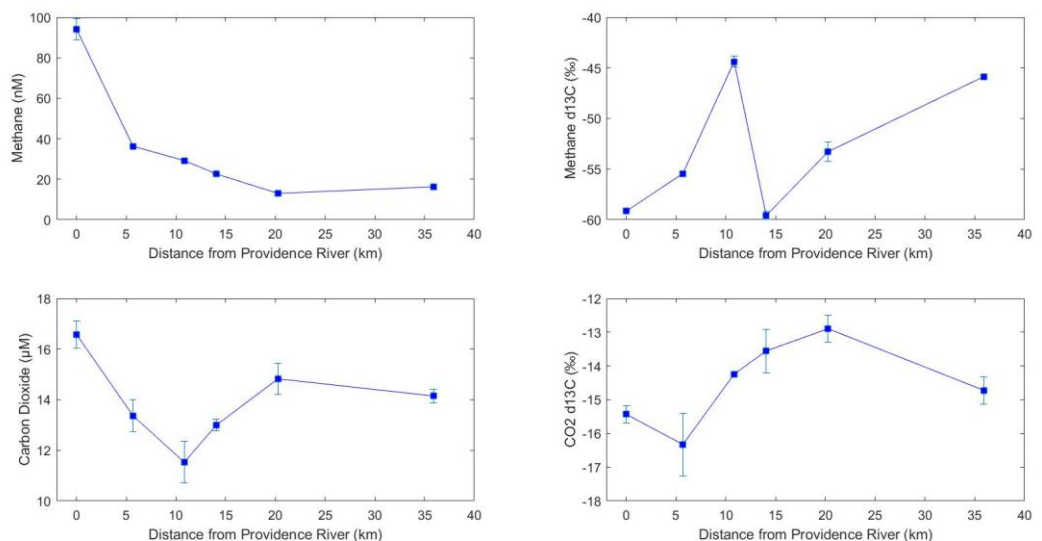


Figure 24. Surface methane and CO_2 concentrations (left) and isotope ratios (right) along Narragansett Bay transect.

There are two factors that could contribute to the high concentrations of methane measured in the Providence River. First, methane production in freshwater occurs much more readily than methanogenesis in salt water. Salinity is an inhibitor of methanogens due to the presence of sulfate, as sulfate reducing bacteria utilize similar substrates to methanogens and outcompete methanogens over resources (Reeburgh 2007). Figure 25 shows the relationship between methane and salinity established by the transect data, and a multiple linear regression indicates that methane concentrations at the freshwater endmember are roughly 150nM. A second contributor to high riverine methane levels could be the presence of wastewater treatment plants.

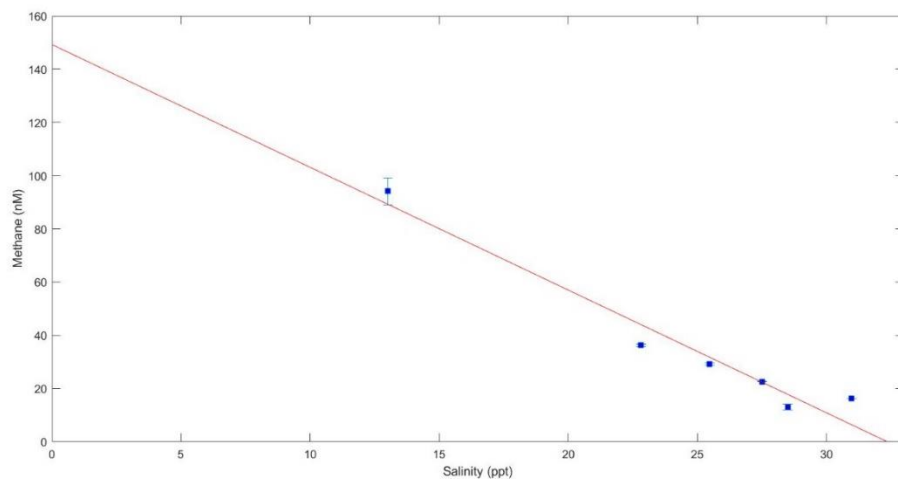


Figure 25. Linear relationship between measured salinity and methane along West Passage transect.

Situated near the mouth of the Providence River are three wastewater treatment plants, the largest of which is located at Fields Point close to Station 1. Wastewater treatment plants have been shown to be sources of methane to both to the atmosphere and adjacent waters. While tertiary treatment upgrades at Narragansett Bay treatment plants have successfully reduced nitrogen inputs in the Bay by over 50% (Schmidt

2014), it is likely that methane input is still an issue. It has even been theorized that anaerobic treatment (tertiary) will lead to large discharge rates of dissolved methane (Liu et al. 2014). A recent study determined that methane concentrations were higher downstream of plants than upstream, though in some cases effluent had lower methane concentrations than downstream sampling sites (Alshboul et al. 2016). This indicates that plants contribute to methane concentrations directly and indirectly, and a linear relationship between methane and organic material in wastewater has now been established. Therefore, it is probable that plants in Narragansett Bay discharge a combination of methane and methane precursors in the form of dissolved organic matter.

The addition of wastewater effluent to river discharge in the bay would likely increase methane significantly without lowering $\text{CH}_4 \delta^{13}\text{C}$ to levels observed in wetlands. All organic material in marshes has undergone a great deal of fractionation (M. Elizabeth Holmes et al. 2015) and therefore is depleted in ^{13}C . As organic material from wastewater effluent is not necessarily as depleted in ^{13}C , this would explain why $\text{CH}_4 \delta^{13}\text{C}$ measured at Sites 1 and 2 is not as low as expected with a production site. The Edgewood Shoals area, adjacent to Station 1, contains a gyre with long residence times and poor water quality. One particular study modeled the dispersion of nutrients released from Fields Point, finding that particles were either entrained in the Edgewood gyre or were transported southward (Kincaid 2012). On top of this, water from the Pawtuxet travels northward along the shore, further providing the area around station 1 with nutrients and possibly methane as well. Likely the combination of

freshwater production, low circulation, and the input of wastewater contribute to the high methane concentrations in upper Narragansett Bay.

Location	Salinity (ppt)	CH ₄ δ ¹³ C (‰)	CH ₄ (nM)
River (Site 1)	13.01	-59.16	96.5
Marsh & Sediment	30.97	-67.38	35.2
Ocean (Site 6)	30.98	-45.86	13.2
Site 2	22.82	-55.44	36.3
Site 3	25.48	-44.38	29.2
Site 4	27.51	-59.59	22.6
Site 5	22.82	-53.28	13.5

Table 9. Salinity, methane δ¹³C, and methane measurements from bay transect, used for linear mixing models.

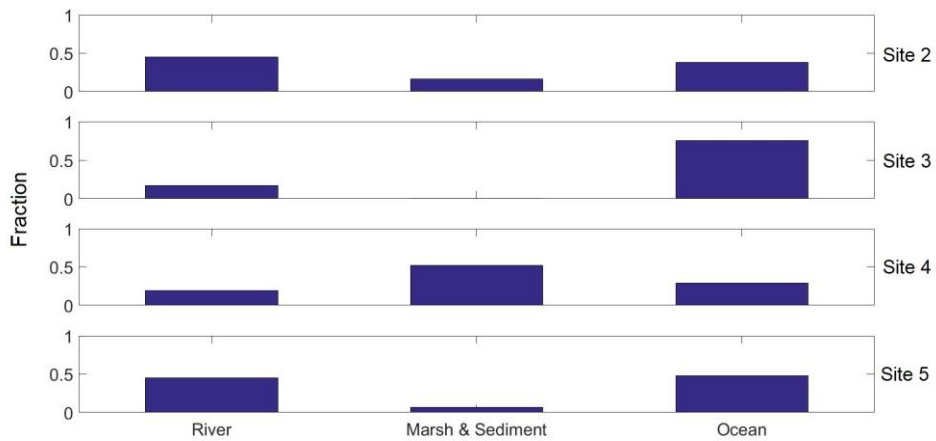


Figure 26. Model of linear mixing, showing the fractional contributions of river, marsh, and ocean sources to the four interior Narragansett Bay sites. The values on the y-axis are fractions and should sum to one at each site.

To assess the relative contributions of methane sources to the four interior bay sampling locations, a model of linear mixing was constructed utilizing three primary sources as inputs to the tracer composition that we observed at each sample site. The sources were riverine input, marine input, and a combined marsh and sediment source. The model was constrained by salinity and CH₄ δ¹³C measurements, and the end member values in each source are listed at the top of Table 9. Methane itself was not

used as a source constraint, because of its tendency to also be affected by gas exchange; the isotopic ratio on methane can also be affected by gas exchange, but the effect is small enough to be neglected (M.E. Holmes et al. 2000). The model of linear mixing yields fractions ($0 \leq f_i \leq 1$) for each individual source, and the final constraint on the matrix inversion was included by requiring the fractions from each source to sum to one, which acts as a conservation constraint. With three constraints, the linear mixing model can be solved by direct matrix inversion to yield the fractional contribution from riverine, marine, and marsh/sediment sources. Additionally, we imposed a constraint that the fraction of each source be greater than or equal to zero, as a negative fraction has no physical interpretation in this case.

We evaluated the fit quality of the model by computing the residuals or model-minus-data misfit for the water mass fractions. The fractions should sum to 1, within an uncertainty 0.05 (Karstensen and Tomczak 1998). Results from the model, are shown in Table 9 and Figure 26, indicate that lateral movement of methane accounts for much of the methane variability within Narragansett Bay. The $\text{CH}_4 \delta^{13}\text{C}$ at station 4 is the lowest of all surface samples with -59.6‰, followed by station 2 at -55.4‰. Site 2 is in close proximity to the mouth of the Providence River, which accounts for the high methane concentrations and low $\delta^{13}\text{C}$. Site 4 has the lowest surface $\text{CH}_4 \delta^{13}\text{C}$ of all stations sampled at -59.6‰, and our model indicates that production in marsh and sediments are responsible for this value.

Figure 27 reflects surface and depth measurements for methane, temperature, and salinity, showing that salinity and temperature measurements are consistent at depth while methane is not. Methane was expected to have increased concentrations at

depth due to sediment production; however, this is only true of Sites 4 and 5. Site 3, located just north of Prudence Island, is influenced most by marine sources, as the surface $\delta^{13}\text{C}$ of -45% is similar to Atlantic Ocean values (Yu et al. 2015). Methane concentrations are roughly 30nM at the surface and 15nM at depth with lower $\delta^{13}\text{C}$ at depth (-50%). Because of the significantly lower salinity at the surface, it is likely that riverine input is responsible for the high methane concentrations while marine sources dilute the $\delta^{13}\text{C}$ at this site. In general, these results indicate incoming seawater is responsible for replenishing $^{13}\text{CH}_4$ through mixing. As water circulates northward along the East passage and southward along the West passage of Narragansett Bay (Kincaid, Bergondo, and Rosenburger 2003), Site 3 is positioned at the intersection between the two. Therefore, it would make sense that Station 3 has a methane $\delta^{13}\text{C}$ equivalent to incoming seawater at Station 6.

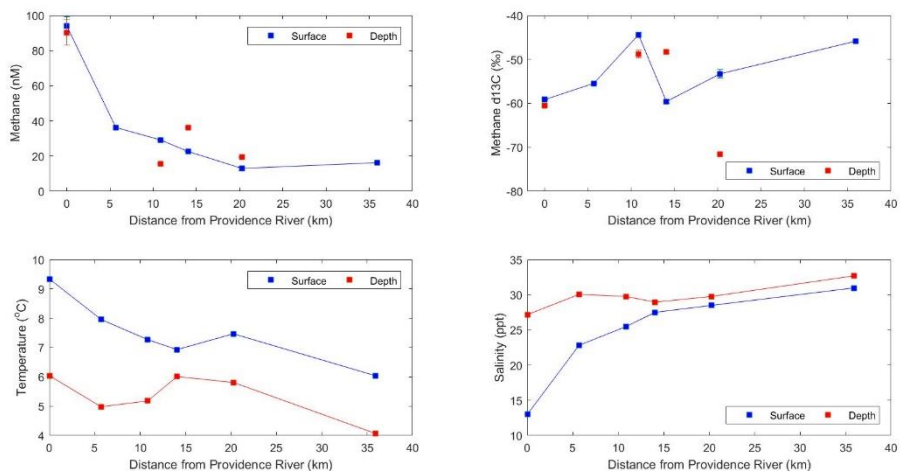


Figure 27. Methane, methane $\delta^{13}\text{C}$, temperature, and salinity along bay transect with surface (blue) and depth (red) measurements

Site 5 has a much lower $\delta^{13}\text{C}$ at depth than at the surface, with the two measurements differing by nearly -20% . There is evidence for bottom sediment type

being important in the contribution of methane from depth to surface waters. Organic rich sediments have been shown to be stronger sources of methane (de Angelis and Scranton 1993), while sandy sediments tend not to contribute methane to adjacent waters (Scranton and McShane 1991). This region in Narragansett Bay has been surveyed for sediment type, with studies indicating a compositional makeup of clay and silt (Raposa and Schwartz 2009), suggesting that methane production from the sediment is a distinct possibility at Site 5. According to the matrix inversion model, methane production in the sediment does not account for the surface measurements and instead the site is influenced most by marine and freshwater sources.

Site 4 had the highest marsh and sediment signal in the model, but direct depth measurements suggest that bottom sediment was not responsible for the depleted ^{13}C . It is significant that this sampling site is adjacent to Greenwich Bay, a small sub-estuary along the West passage of Narragansett Bay with a long history of anthropologic impact (Pesch et al. 2012). Nearly two thirds of the land surrounding the Greenwich Bay is developed, and therefore runoff represents a major issue in this part of the bay. With surface runoff comes issues like bacterial pollution, chemical pollution – nitrogen especially –, eutrophication, and anoxic conditions (Lake and Brush 2015). Given this history, Greenwich Bay is a likely source of methane production, as methane is the terminal step in organic matter degradation (Rudd and Hamilton 1978) and the combination of anoxia with organic matter favors methanogenesis. This production site corresponds well to our model results and direct observations of site 4.

4.5 Salt Marsh contribution to Narragansett Bay

Measurements from the Seabird moored profile CTD and dissolved oxygen meter are shown in Figure 28, with daily variability in DO, salinity, and temperature reflecting the semidiurnal tidal cycle of Narragansett Bay. High tides are represented by peaks in dissolved oxygen and salinity and troughs in temperature measurements. Dissolved oxygen ranged by $50 \mu\text{mol kg}^{-1}$ while salinity only differed by 0.5ppt from high tide to low tide. In this study, we made the assumption that salinity and dissolved oxygen in the outlet decreased due to mixing with marsh porewater, as the porewater end members were 28.5 ppt and $28.7 \mu\text{mol kg}^{-1}$, respectively.

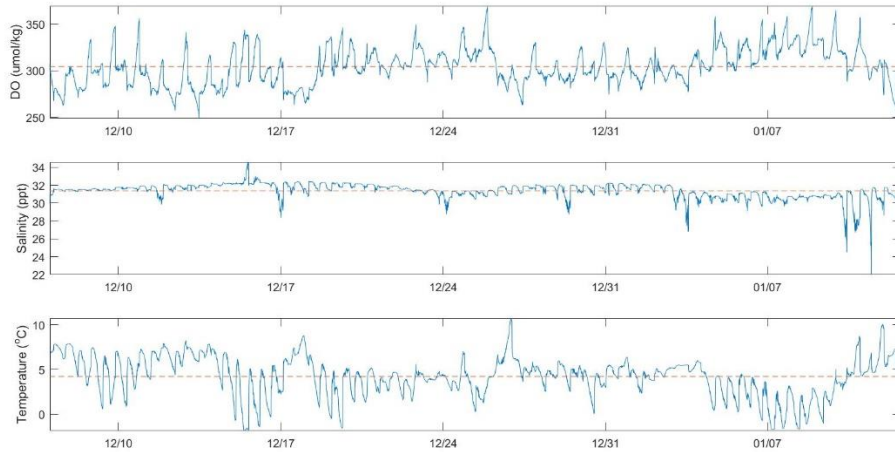


Figure 28. Dissolved oxygen, salinity, and temperature sampled continuously with Seabird moored profile CTD from 12/07/2016 to 01/14/2017, with dashed lines indicating outlet average.

The mixing diagram in Figure 29 indicates that direct measurements of salinity and dissolved oxygen from marsh porewater and outlet samples agree well with calculations from the least-squares results. The coefficient of determination for the linear mixing model in Figure 29 was 0.9962, with the computed value differing by

0.41% for salinity and 3.57% for dissolved oxygen. Least-square results yielded methane concentrations of 41.3nM at the marsh outlet where the Seabird was placed. Although the salinity and dissolved oxygen fit well with the mixing diagram, the calculated methane concentration is significantly higher than the measured value of 21.4nM during the December 7, 2017 sampling of the marsh. We make the assumption here that the difference between the two values, 19.9nM, was lost to gas exchange.

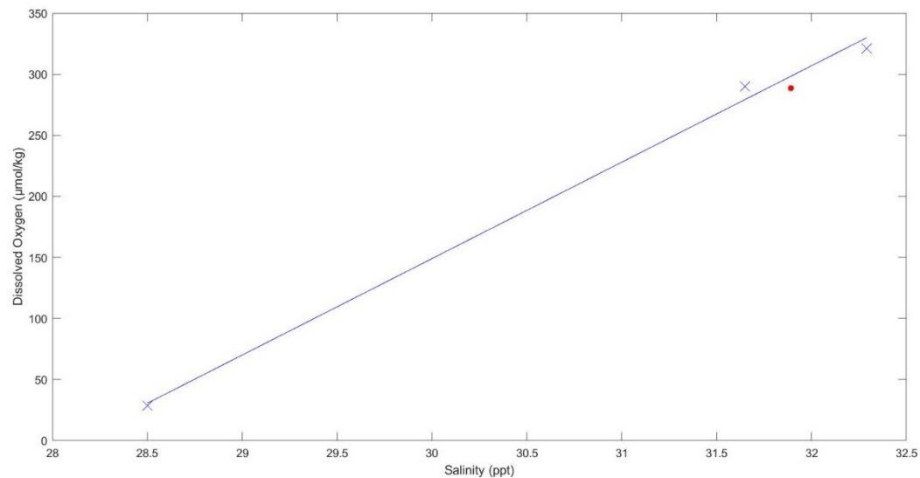


Figure 29. Mixing diagram of salinity and dissolved oxygen measurements from direct sampling data ('x') and linear model results ('red point').

Scaling up these results, our data would suggest that $2.4 \times 10^5 \text{ mol year}^{-1}$ methane flows from Narragansett Bay marshes via porewater during ebb tides, portioned between marine waters and the atmosphere. Given the significant lag in oxidation that occurred with marsh outlet water samples, the majority of the methane contribution from marshes may be emitted to the atmosphere rather than oxidized. The $2.4 \times 10^5 \text{ mol year}^{-1}$ contribution of marshes may be small compared to riverine sources in Narragansett Bay, as a similar study computed a contribution of 1.24×10^7

mol CH₄ year⁻¹ from the Hudson River, NY to marine waters (de Angelis and Scranton 1993), though this is a much larger scale.

CHAPTER 5

CONCLUSION

Marsh environments have been shown to be the strongest natural source of methane to the atmosphere. However, their contribution to adjacent waters is not well-established. This study aimed to investigate the role wetlands play in Narragansett Bay methane cycling and study the conditions that favor methanogenesis, methanotrophy, or the cooccurrence of the two within Fox Hill salt marsh. Stable isotope analysis was used throughout the study to confirm both processes, as well as trace sources of methane throughout Narragansett Bay. Methane concentrations in Fox Hill marsh porewater ranged from 400nM-500nM during all ebb tide samplings, while the $\delta^{13}\text{C}$ values below -80‰ confirmed the biological production of methane in this location. A significant correlation was observed between methane concentrations and temperature, indicating seasonal differences in methane production with highest concentrations predicted to occur during the summer.

There was limited evidence of methane production occurring in porewater incubations, indicating that most Archaea reside in the sediment and are not flushed out of the marsh with the tide. Confirming this statement, there was no evidence of methanogenesis in outlet samples nor was there indication of this marsh containing aerobic methanogens. Methanotrophy was expected to be a major sink for methane in all oxygenated waters; however, stable isotope analysis only confirmed its occurrence in three samples and a significant lag time occurred before methane consumption

occurred. The lag was predicted to be due to facultative methanotrophs, specifically those belonging to genus *Methylocella*, which preferentially utilized other common marsh compounds over methane. Aerobic methanotrophs are also likely to be transported to the marsh from Narragansett Bay, as oxidation in outlet samples occurred more readily and exhibited significantly higher oxidation rates than the porewater sample. Seasonally, as methane concentrations increased with temperature, methane oxidation and methanotroph numbers increased as well.

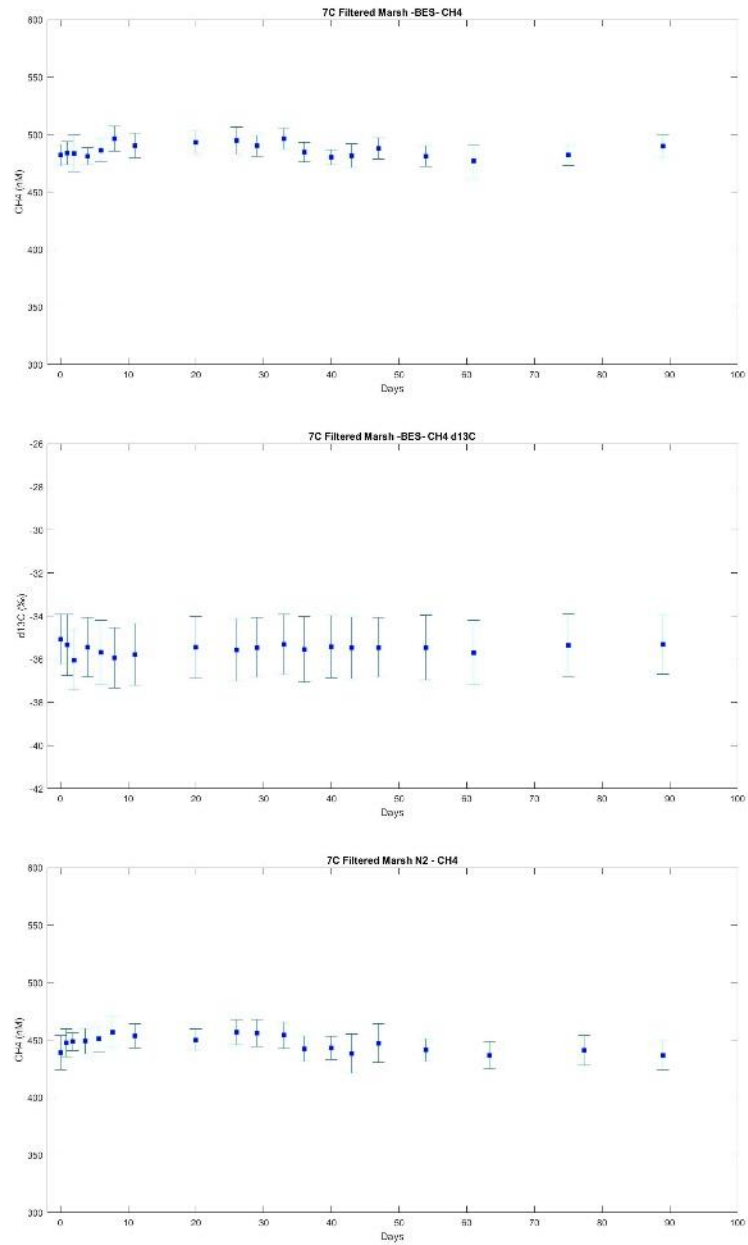
Narragansett Bay was found to be supersaturated relative to atmospheric equilibrium methane concentrations (~12nM), with strong riverine input (including wastewater treatment), bottom sediment production, and marsh outflow found to be responsible, though the relative contribution of sources depended on sampling location throughout the Bay. In general, methane concentrations in Narragansett Bay were most dependent upon temperature and tides, though there is a significant salinity gradient latitudinally that is anticorrelated with methane. Our findings suggest that marshes throughout Narragansett Bay contribute approximately 2.4×10^5 mol CH₄ annually to Narragansett Bay.

A significant limitation in our study was the lack of summertime incubation experiments, as the trends of this study indicate highest oxidation and production rates should occur when temperatures are also highest. In order to gain a complete picture of Narragansett Bay methane cycling, it would also be beneficial to conduct incubations of Narragansett Bay water samples, specifically along the transect outlined in this study. This would provide more information about the nature of Narragansett

Bay methanotrophs and whether the inhibition observed during the incubation experiments is limited to Fox Hill salt marsh or if it is widespread throughout the bay.

APPENDICES

Appendix A Incubation Experiment



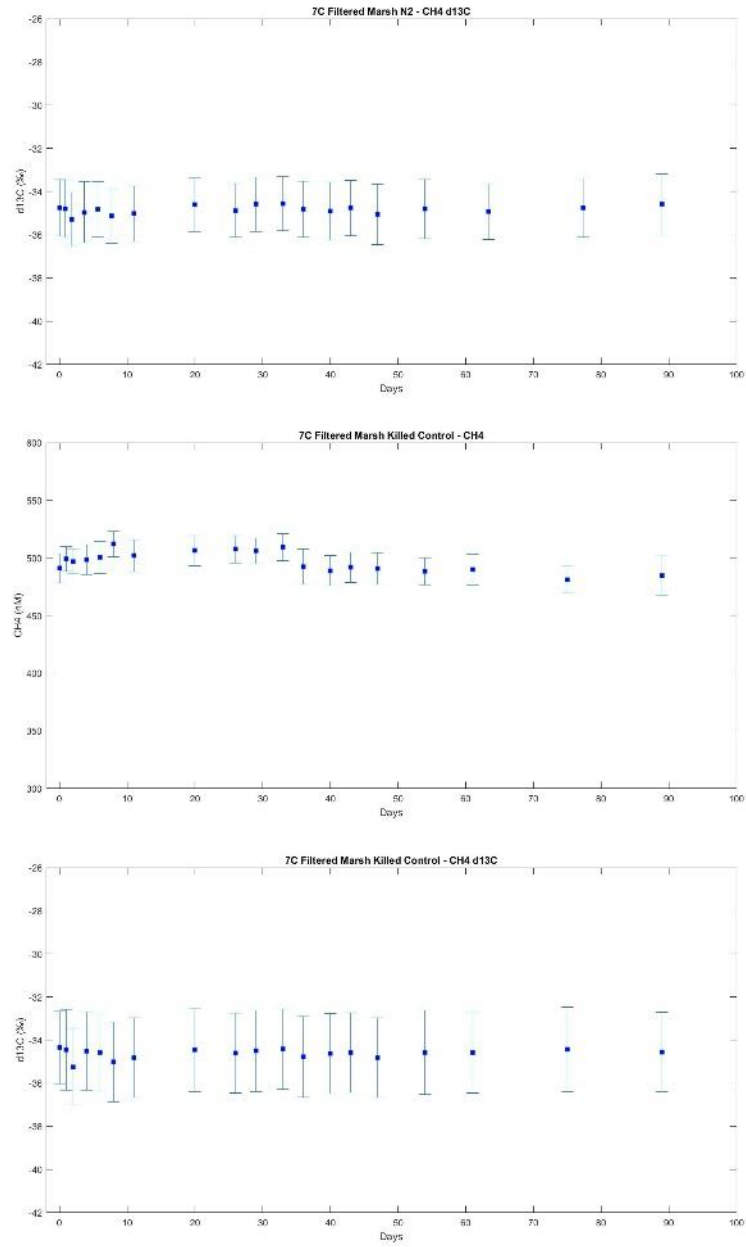


Figure A1. 7°C filtered marsh methane and $\delta^{13}\text{C}$ results for BES (a, b), Nitrogen-headspace (c, d), and killed control samples (e, f).

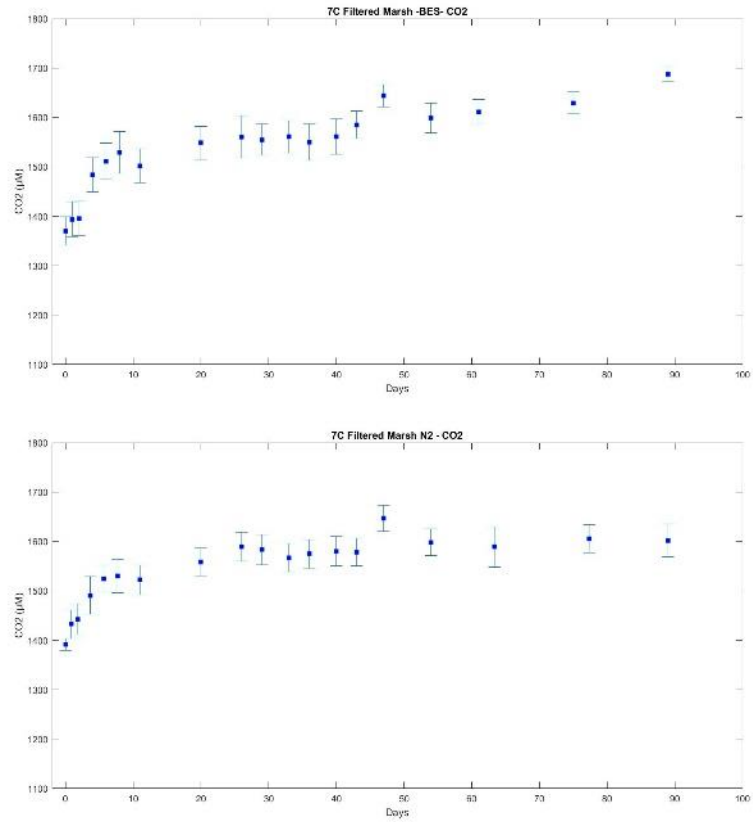
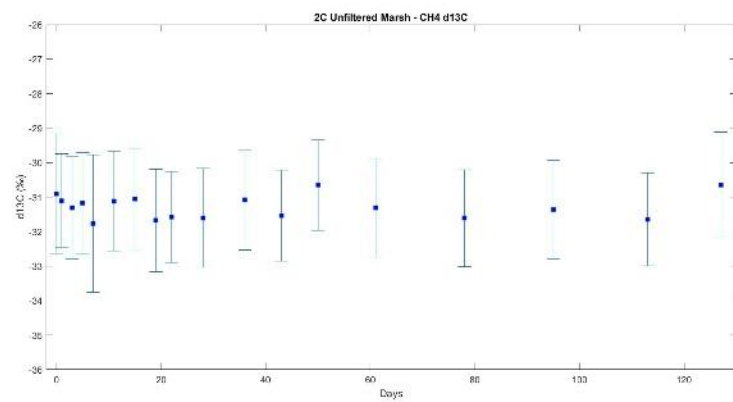
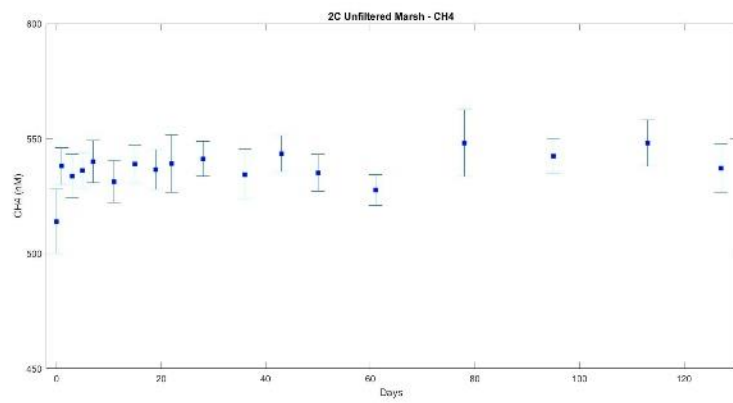
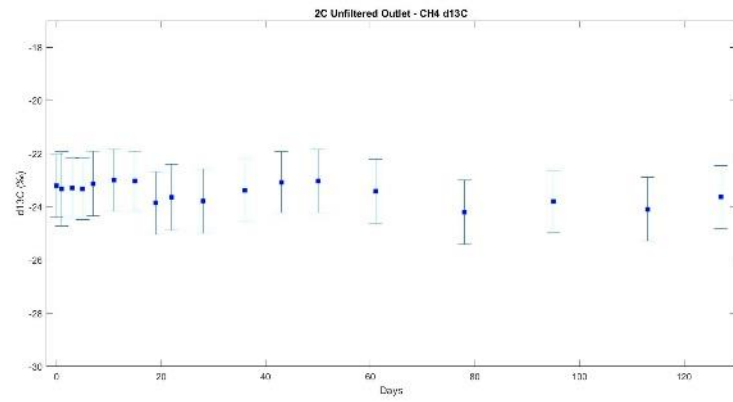
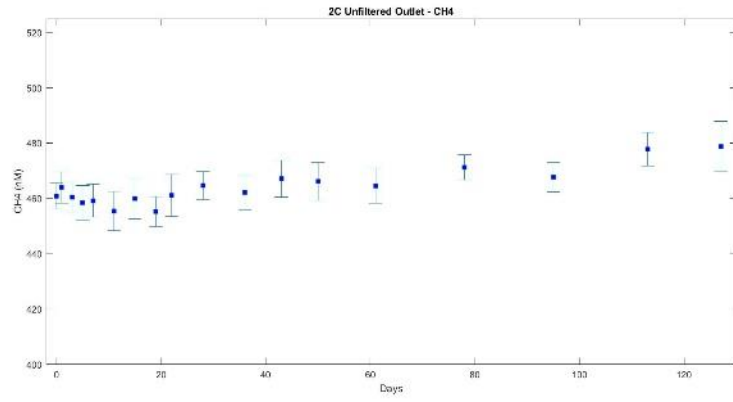
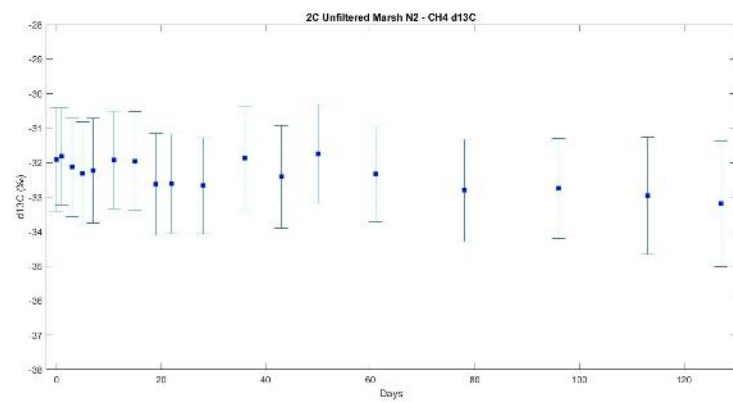
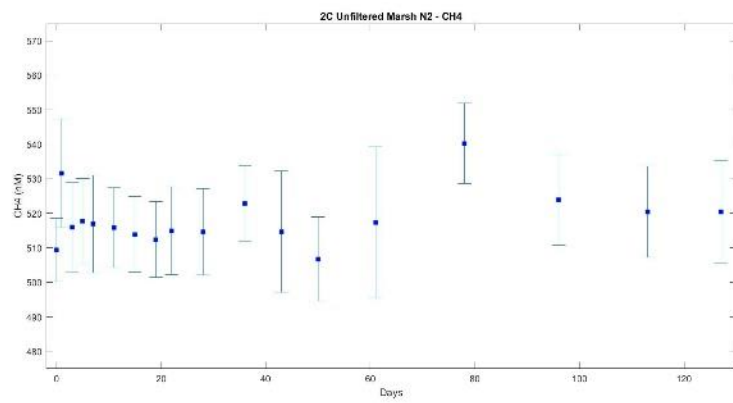
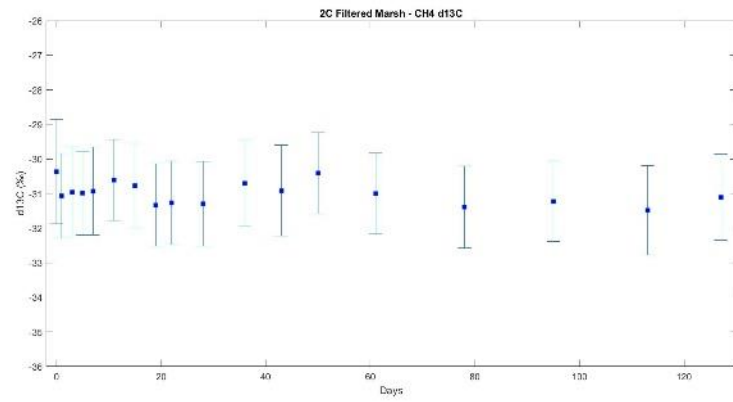
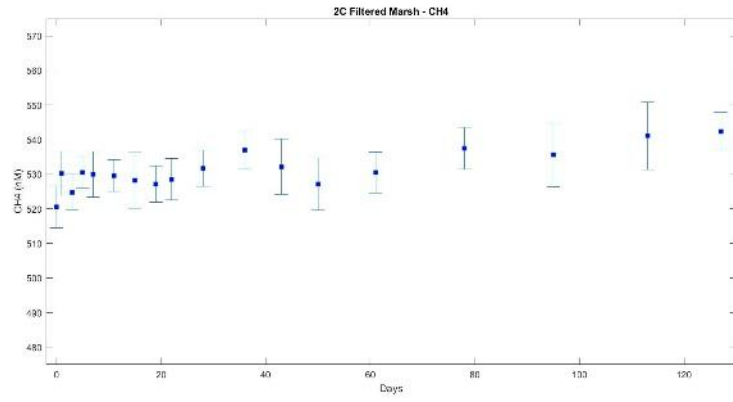


Figure A2. 7°C filtered marsh carbon dioxide results for BES (a) and nitrogen-headspace (b) samples.





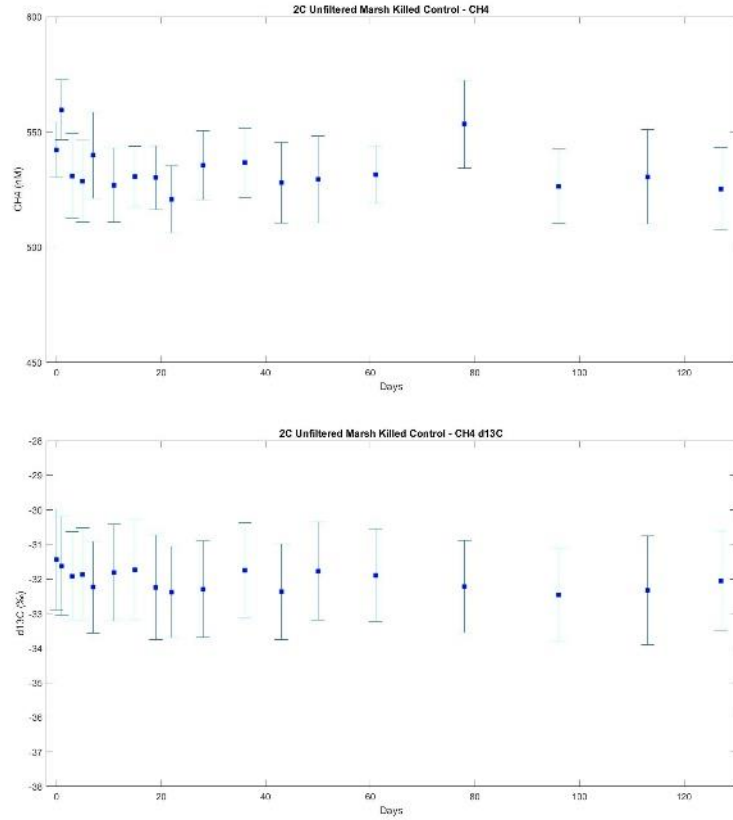
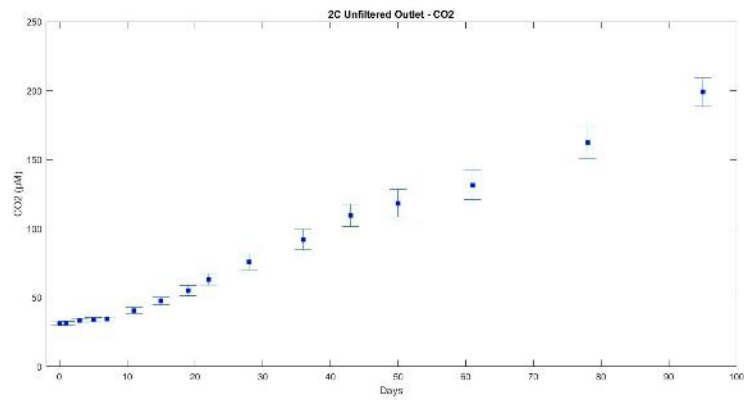


Figure A3. 2°C methane and $\delta^{13}\text{C}$ results for all treatment groups: unfiltered outlet (a, b), unfiltered marsh (c, d), filtered marsh (e, f), unfiltered marsh with nitrogen headspace (g, h), and killed control (i, j).



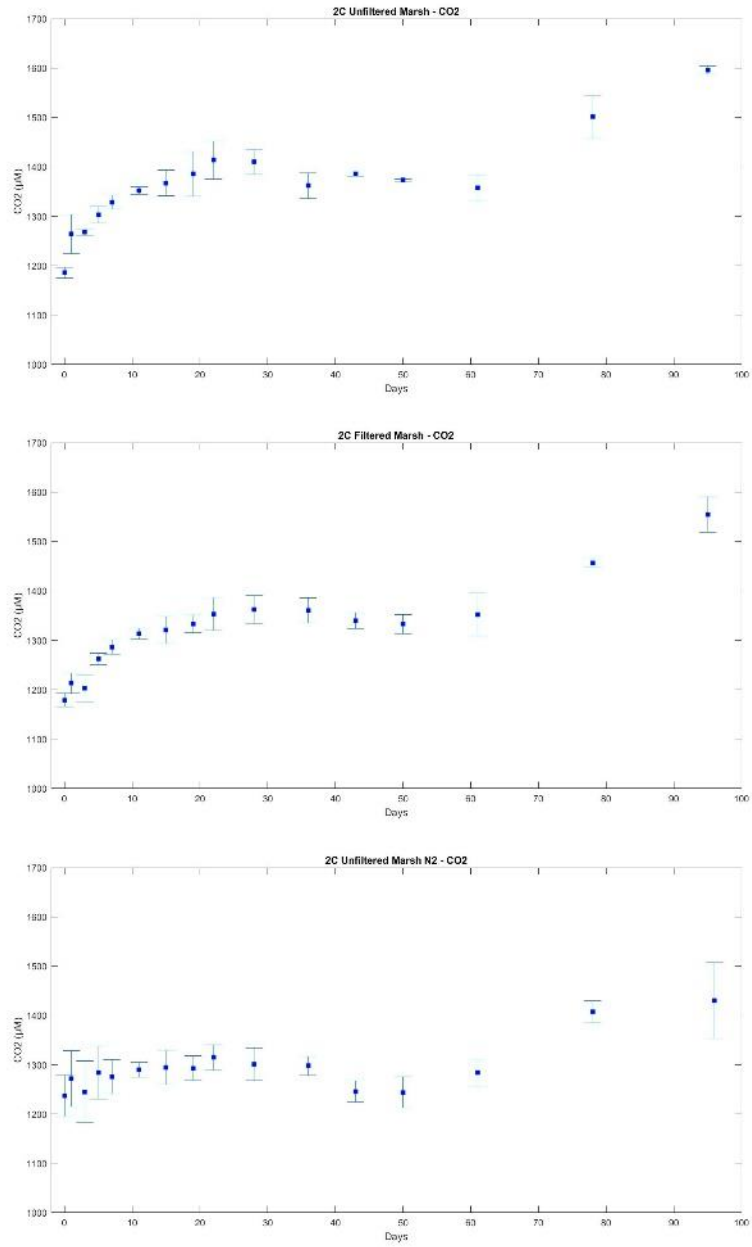


Figure A4. 2°C carbon dioxide results for all treatment groups: unfiltered outlet (a), unfiltered marsh (b), filtered marsh (c), and unfiltered marsh with nitrogen-headspace (d).

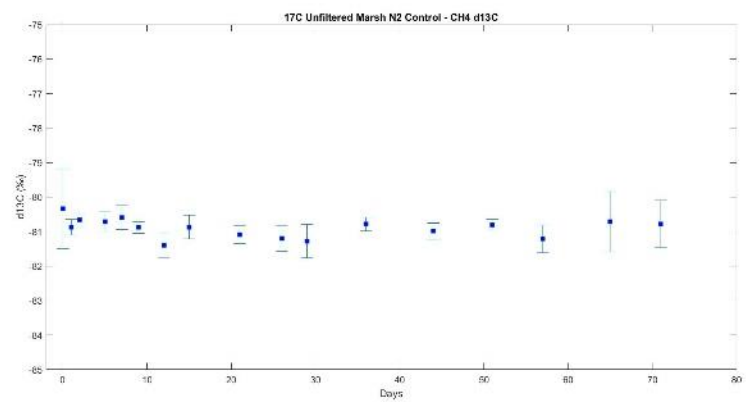
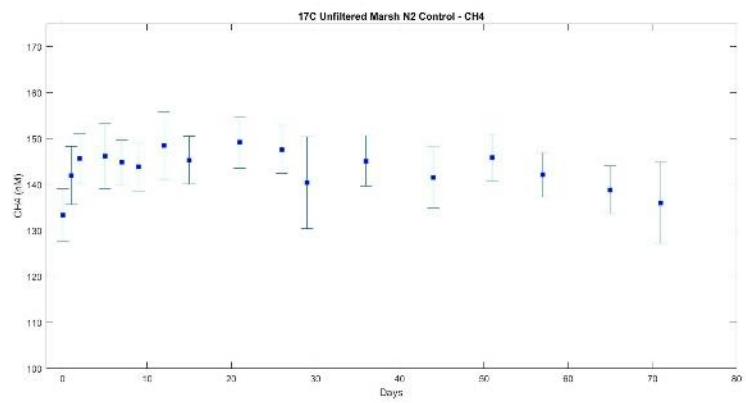
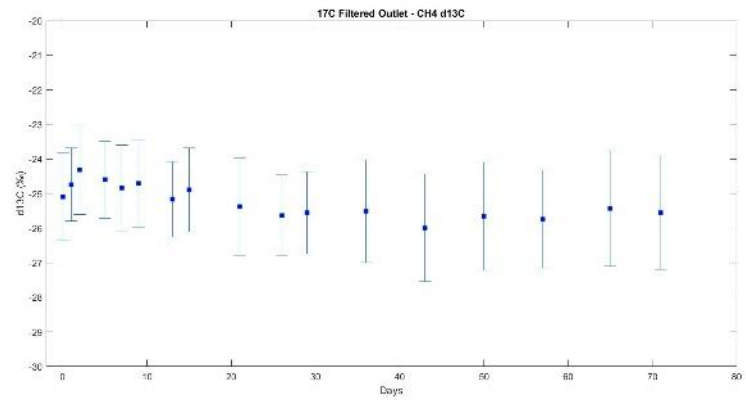
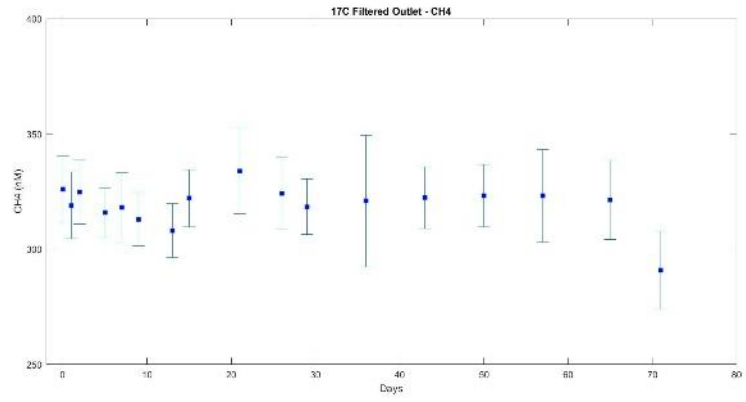
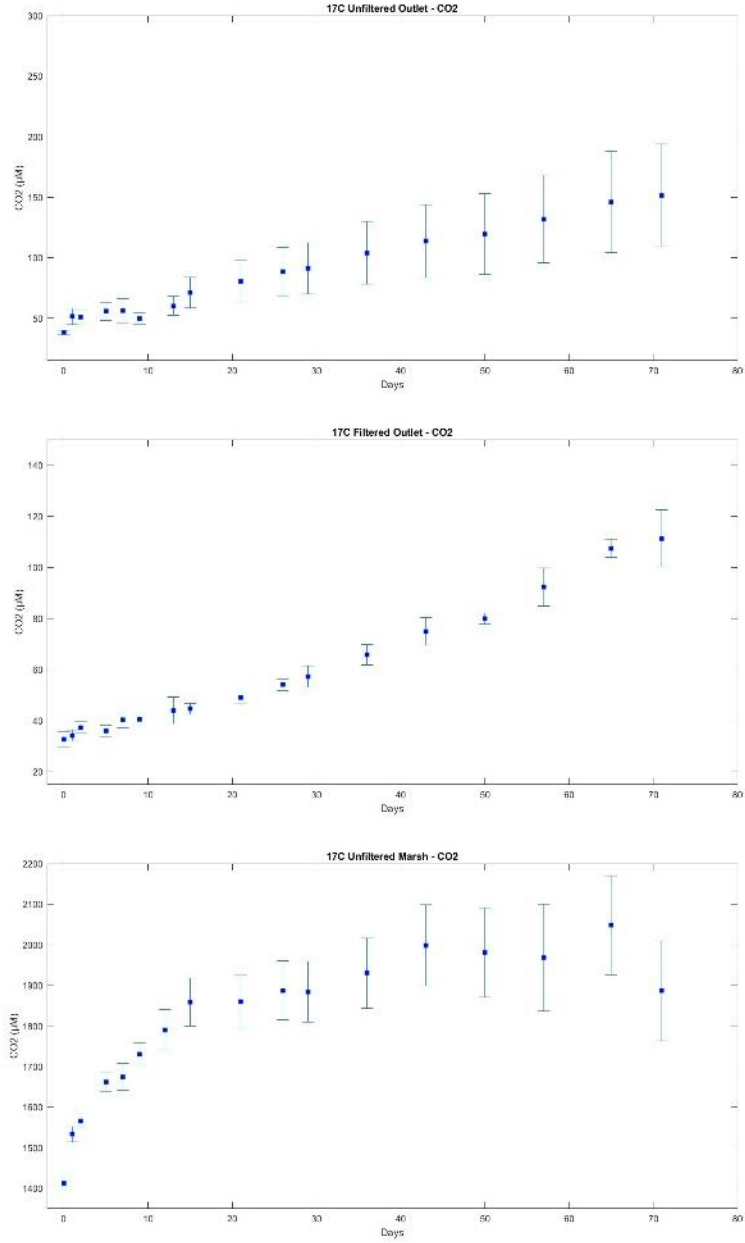


Figure A5. 17°C methane and $\delta^{13}\text{C}$ results for filtered marsh (a, b) and killed control (c, d).



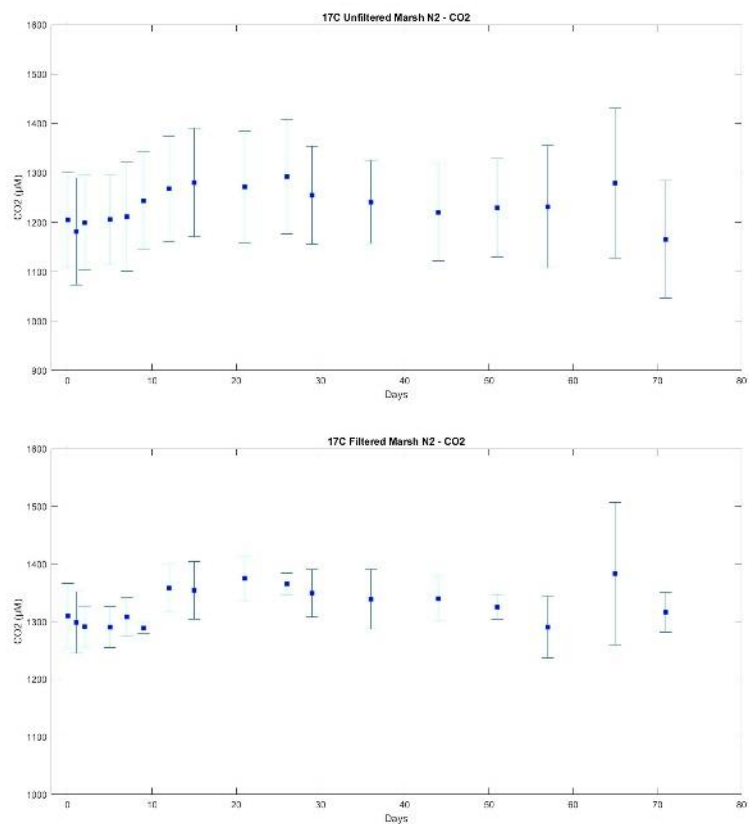


Figure A6. 17°C carbon dioxide results for unfiltered outlet (a), filtered outlet (b), unfiltered marsh (c), unfiltered nitrogen-headspace marsh (d), and filtered nitrogen-headspace marsh samples.

Appendix B

Microbiology Results

Inhibition Tests

Several early PCR runs yielded dissociation peaks in the 76-78°C range. The cleaning up of all DNA samples was successful in removing at least some of the inhibitor compounds, evidenced by PCR amplification plots and gel results. Figures 10 and 11 demonstrate the inhibition tests that were conducted prior to running all samples on qPCR, in which the Ct decreased by roughly 10 cycles following the DNA

clean-up. In turn, this resulted in the majority of samples exhibiting amplification within the range of the dilution curve.

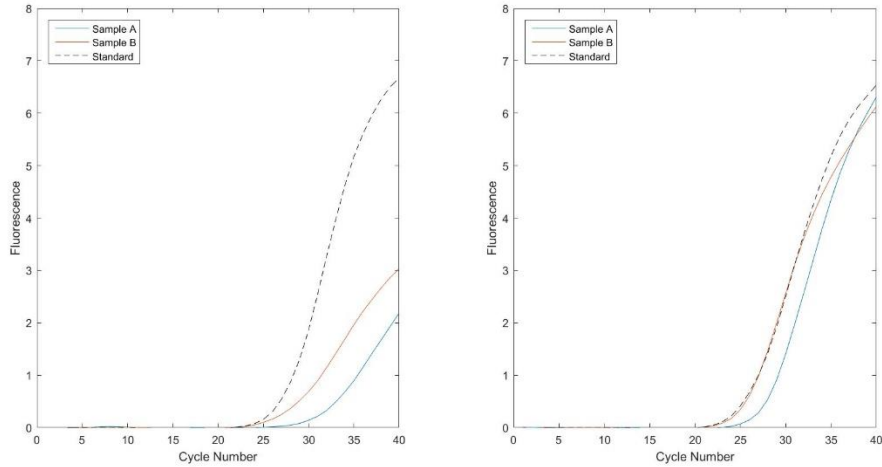


Figure B1. qPCR inhibition test amplification results prior (a) and subsequent (b) to DNA re-purification. Standard DNA is indicated by the dashed line.

qPCR Dissociation Curves

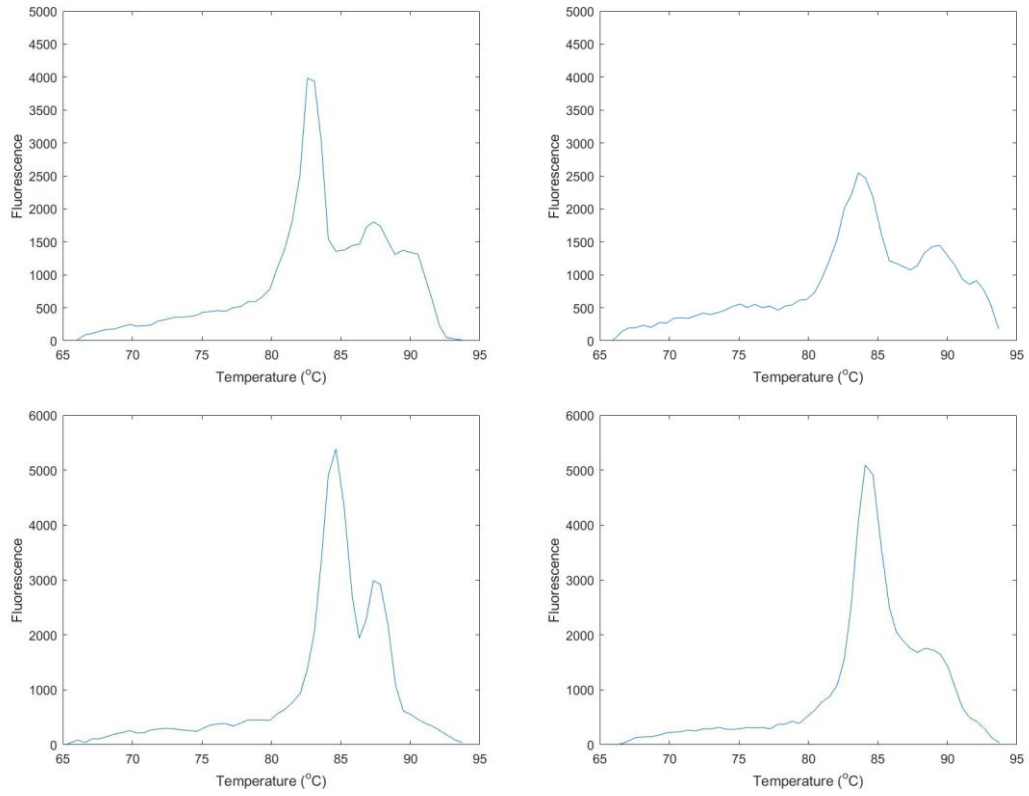


Figure B2. Dissociation curves for 7°C filtered outlet (a), filtered marsh (b), filtered marsh with BES (c), and filtered marsh with nitrogen-headspace (d).

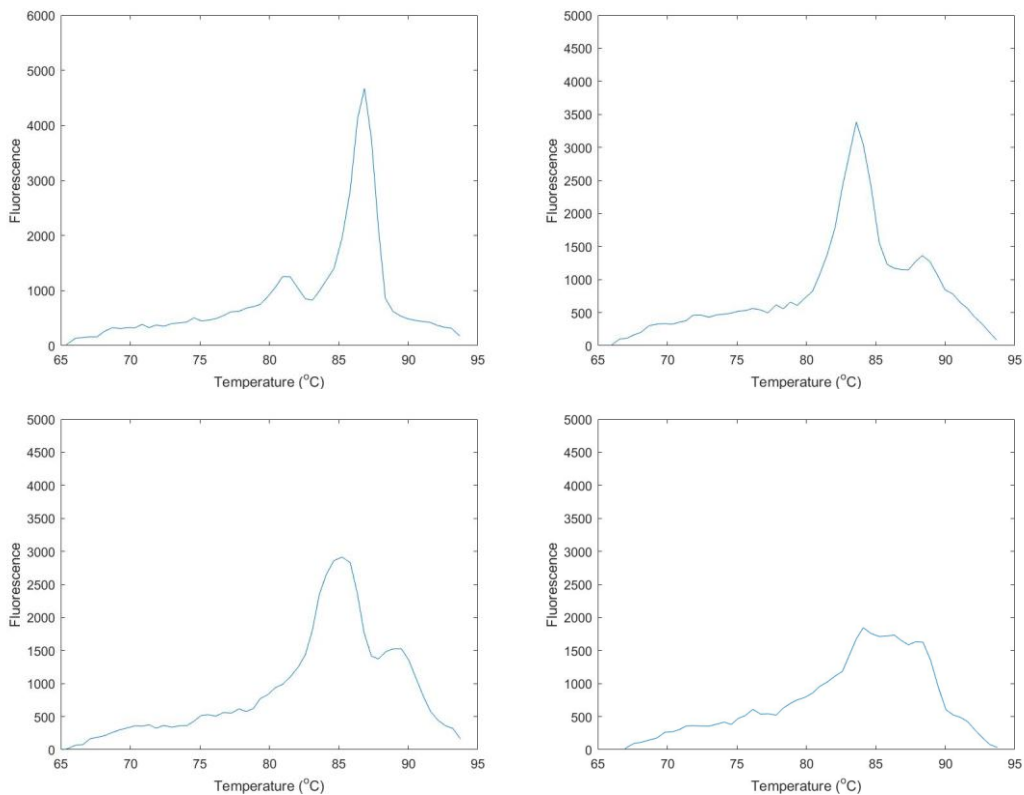


Figure B3. 2°C dissociation curve results for unfiltered outlet (a), unfiltered marsh (b), filtered marsh (c), and unfiltered marsh with nitrogen-headspace (d) samples.

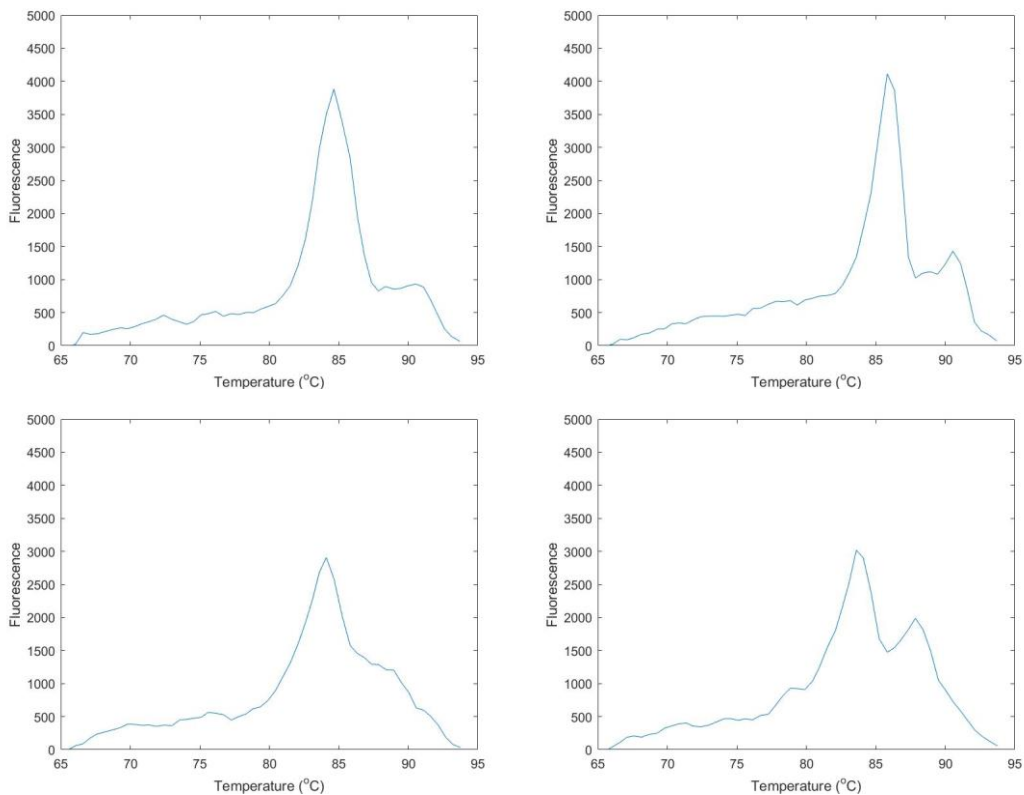


Figure B4. 17°C dissociation curve results for filtered outlet (a), unfiltered marsh with hydrocarbon-free headspace (b), unfiltered marsh with nitrogen-headspace (b), and filtered marsh with nitrogen-headspace (c) samples.

Appendix C Narragansett Bay Time Series Supplemental Figures

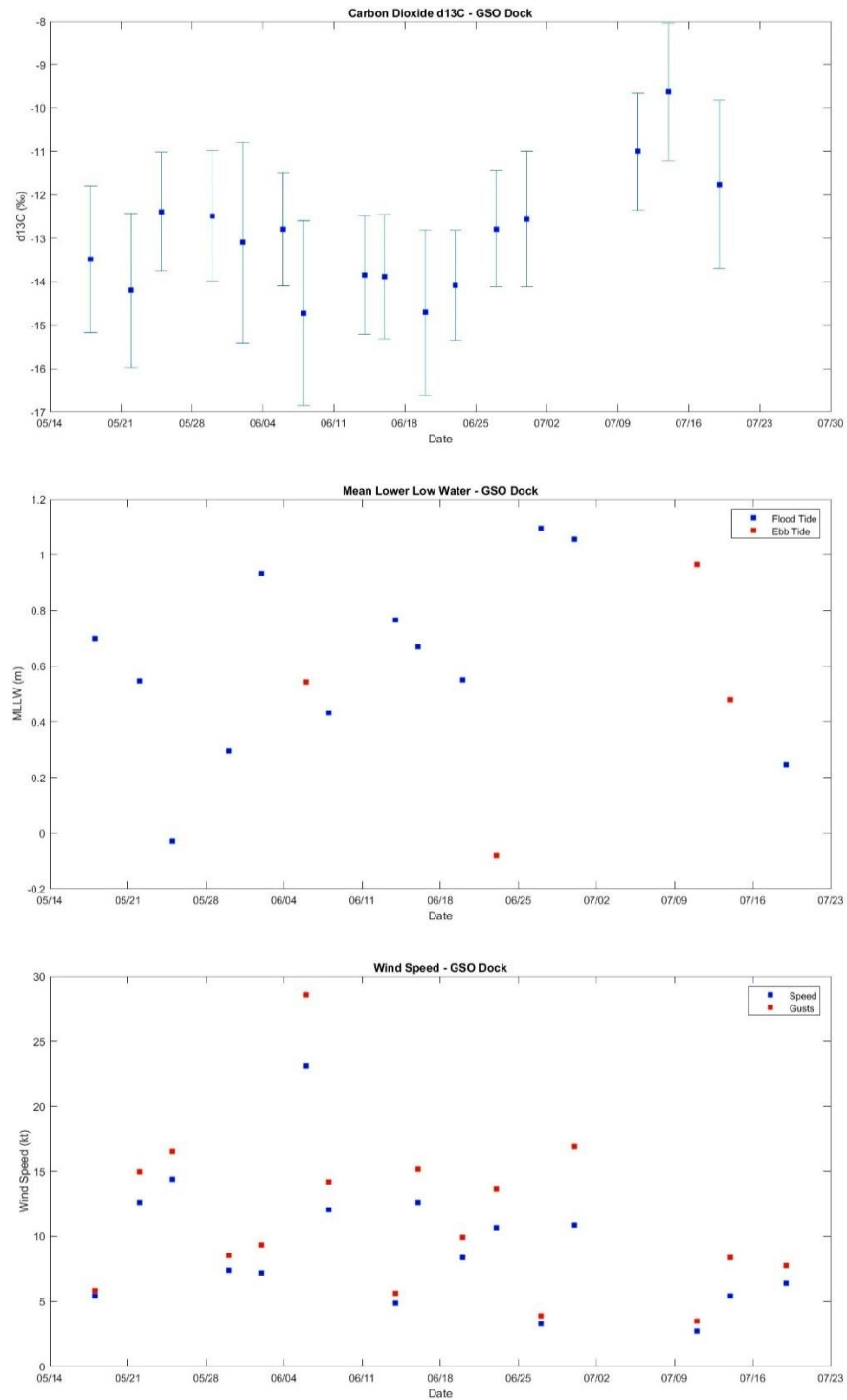


Figure A1. CO_2 $\delta^{13}\text{C}$ measurements (a) and MLLW (b) and wind speed (c) data downloaded from <https://tidesandcurrents.noaa.gov> over the span of May through July 2017.

BIBLIOGRAPHY

- Abdel-Moati, A. R. 1990. "Adsorption of Dissolved Organic Carbon (DOC) on Glass Fibre Filters during Particulate Organic Carbon (POC) Determination." *Water Research* 24 (6): 763–64. [https://doi.org/10.1016/0043-1354\(90\)90033-3](https://doi.org/10.1016/0043-1354(90)90033-3).
- Abril, Gwenaël, Marc-Vincent Commarieu, and Frédéric Guérin. 2007. "Enhanced Methane Oxidation in an Estuarine Turbidity Maximum." *Limnology and Oceanography* 52 (1): 470–75. <https://doi.org/10.4319/lo.2007.52.1.0470>.
- Ahad, Jason M. E., Raja S. Ganeshram, Charlotte L. Bryant, Luz M. Cisneros-Dozal, Philippa L. Ascough, Anthony E. Fallick, and Greg F. Slater. 2011. "Sources of N-Alkanes in an Urbanized Estuary: Insights from Molecular Distributions and Compound-Specific Stable and Radiocarbon Isotopes." *Marine Chemistry* 126 (1): 239–249. <https://doi.org/10.1016/j.marchem.2011.06.002>.
- Alshboul, Alshboul, Jorge Encinas-Fernandex, Hilmar Hofmann, and Andreas Lorke. 2016. "Export of Dissolved Methane and Carbon Dioxide with Effluents from Municipal Wastewater Treatment Plants." *Environmental Science & Technology* 50 (11): 5555–63.
- Anthony, C. 1986. "Bacterial Oxidation of Methane and Methanol." *Advances in Microbial Physiology* 27: 113–210.
- Atkinson, Larry P., and John R. Hall. 1976. "Methane Distribution and Production in the Georgia Salt Marsh." *Estuarine and Coastal Marine Science* 4 (6): 677–686. [https://doi.org/10.1016/0302-3524\(76\)90074-8](https://doi.org/10.1016/0302-3524(76)90074-8).

- Atlas, R., and R. Bartha. 1998. *Microbial Ecology : Fundamentals and Applications*.
Fourth. Menlo Park, CA: Benjamin/Cummings.
- Avery, Gbrooks, Robert Shannon, Jeffrey White, Christopher Martens, and Marc Alperin. 1999. "Effect of Seasonal Changes in the Pathways of Methanogenesis on the $\Delta^{13}\text{C}$ Values of Pore Water Methane in a Michigan Peatland." *Global Biogeochemical Cycles* 13 (2): 475–484.
<https://doi.org/10.1029/1999GB900007>.
- Bange, H.W., U.H Bartell, S. Rapsomanikis, and M.O. Andreae. 1994. "Methane in the Baltic and North Seas and a Reassessment of the Marine Emissions of Methane." *Global Biogeochemical Cycles* 8 (4): 465–480.
<https://doi.org/10.1029/94GB02181>.
- Bauer, J.E., and T.S. Bianchi. 2011. "Dissolved Organic Carbon Cycling and Transformation." In *Biogeochemistry*, 5:7–67. Waltham, MA: Academic.
- Bethke, C. M., R. A. Sanford, M. F. Kirk, Q. Jin, and T. M. Flynn. 2011. "The Thermodynamic Ladder in Geomicrobiology." *American Journal of Science* 311 (3): 183–210. <https://doi.org/10.2475/03.2011.01>.
- Biddanda, B. A., and L. Pomeroy. 1988. "Microbial Aggregation and Degradation of Phytoplankton-Derived Detritus in Seawater. 1. Microbial Succession." *Marine Ecology Progress Series. Oldendorf* 42 (1): 79–88.
- Bornemann, Maren, Ingeborg Bussmann, Lucas Tichy, Jörg Deutzmann, Bernhard Schink, Michael Pester, and Tillmann Lueders. 2016. "Methane Release from Sediment Seeps to the Atmosphere Is Counteracted by Highly Active Methylococcaceae in the Water Column of Deep Oligotrophic Lake

Constance.” *FEMS Microbiology Ecology* 92 (8).

<https://doi.org/10.1093/femsec/fiw123>.

Bourne, David G., Ian R. McDonald, and J. Colin Murrell. 2001. “Comparison of PmoA PCR Primer Sets as Tools for Investigating Methanotroph Diversity in Three Danish Soils.” *Applied and Environmental Microbiology* 67 (9): 3802–9. <https://doi.org/10.1128/AEM.67.9.3802-3809.2001>.

Bridgham, Scott D., Hinsby Cadillo-Quiroz, Jason K. Keller, and Qianlai Zhuang. 2013. “Methane Emissions from Wetlands: Biogeochemical, Microbial, and Modeling Perspectives from Local to Global Scales.” *Global Change Biology* 19 (5): 1325–1346. <https://doi.org/10.1111/gcb.12131>.

Bugna, Glynnis C., Jeffrey P. Chanton, Jaye E. Cable, William C. Burnett, and Peter H. Cable. 1996. “The Importance of Groundwater Discharge to the Methane Budgets of Nearshore and Continental Shelf Waters of the Northeastern Gulf of Mexico.” *Geochimica et Cosmochimica Acta* 60 (23): 4735–4746. [https://doi.org/10.1016/S0016-7037\(96\)00290-6](https://doi.org/10.1016/S0016-7037(96)00290-6).

Canuel, Elizabeth A., Sarah S. Cammer, Hadley A. McIntosh, and Christina R. Pondell. 2012. “Climate Change Impacts on the Organic Carbon Cycle at the Land-Ocean Interface.” *Annual Review of Earth and Planetary Sciences* 40 (1): 685–711. <https://doi.org/10.1146/annurev-earth-042711-105511>.

Canuel, Elizabeth A., Katherine H. Freeman, and Stuart G. Wakeham. 1997. “Isotopic Compositions of Lipid Biomarker Compounds in Estuarine Plants and Surface Sediments.” *Limnology and Oceanography* 42 (7): 1570–1583. <https://doi.org/10.4319/lo.1997.42.7.1570>.

- Canuel, Elizabeth A., and Amber K. Hardison. 2016. "Sources, Ages, and Alteration of Organic Matter in Estuaries." *Annual Review of Marine Science* 8: 409–434. <https://doi.org/10.1146/annurev-marine-122414-034058>.
- Carpenter, Lucy J., Stephen D. Archer, and Rachael Beale. 2012. "Ocean-Atmosphere Trace Gas Exchange." *Chemical Society Reviews* 41 (19): 6473–6506. <https://doi.org/10.1039/c2cs35121h>.
- Chalmers, Alice G., Richard G. Wiegert, and Paul L. Wolf. 1985. "Carbon Balance in a Salt Marsh: Interactions of Diffusive Export, Tidal Deposition and Rainfall-Caused Erosion." *Estuarine, Coastal and Shelf Science* 21 (6): 757–71.
- Chanton, J. P., P. H. Glaser, L. S. Chasar, D. J. Burdige, M. E. Hines, D. I. Siegel, L. B. Tremblay, and W. T. Cooper. 2008. "Radiocarbon Evidence for the Importance of Surface Vegetation on Fermentation and Methanogenesis in Contrasting Types of Boreal Peatlands." *Global Biogeochemical Cycles* 22 (4): n/a–n/a. <https://doi.org/10.1029/2008GB003274>.
- Chen, Si, Miguel A. Goni, and Raymond Torres. 2016. "The Role of Salt Marsh Structure in the Distribution of Surface Sedimentary Organic Matter." *Estuaries and Coasts* 39 (1): 108–22.
- Chinman, Richard A., and Scott W. Nixon. 1985. *Depth-Area Volume Relationships in Narragansett Bay*. Marine Technical Report (University of Rhode Island); 87. Narragansett, R.I.: The University.
- Chowdhury, Taniya Roy, and Richard P. Dick. 2013. "Ecology of Aerobic Methanotrophs in Controlling Methane Fluxes from Wetlands." *Applied Soil Ecology* 65 (March): 8–22. <https://doi.org/10.1016/j.apsoil.2012.12.014>.

- Ciais, P., C. Sabine, L. Bopp, V. Brovkin, J. Canadell, A. Chhabra, P. DeFries, et al. 2013. "Carbon and Other Biogeochemical Cycles." In *Climate Change 2013: The Physical Science Basis. Contribution of Working Group I to the Fifth Assessment Report of the Intergovernmental Panel on Climate Change*. Cambridge, UK; New York, NY, USA: Cambridge University Press.
- Cifuentes, L. A., and G.G. Salata. 2001. "Significance of Carbon Isotope Discrimination between Bulk Carbon and Extracted Phospholipid Fatty Acids in Selected Terrestrial and Marine Environments." *Organic Geochemistry* 32 (4): 613–21.
- Clarke, P. H. 1953. "Hydrogen Sulphide Production by Bacteria." *Journal of General Microbiology* 8 (3): 397–407. <https://doi.org/10.1099/00221287-8-3-397>.
- Conrad, Ralf, Peter Claus, and Peter Casper. 2009. "Characterization of Stable Isotope Fractionation during Methane Production in the Sediment of a Eutrophic Lake, Lake Dagow, Germany." *Limnology and Oceanography* 54 (2): 457–471. <https://doi.org/10.4319/lo.2009.54.2.0457>.
- Craig, Harmon. 1953. "The Geochemistry of the Stable Carbon Isotopes." *Geochimica et Cosmochimica Acta* 3 (2): 53–92. [https://doi.org/10.1016/0016-7037\(53\)90001-5](https://doi.org/10.1016/0016-7037(53)90001-5).
- Dalton, H. 1991. "Structure and Mechanism of Action of the Enzymes Involved in Methane Oxidation." In *Applications of Enzyme Biotechnology*, 55–68. New York: J.W. Kelley (ed.), Plenum Press.
- Dalton, Howard. 1980. "Oxidation of Hydrocarbons by Methane Monooxygenases from a Variety of Microbes." In *Advances in Applied Microbiology*, edited by

- D. Perlman, 26:71–87. Academic Press. [https://doi.org/10.1016/S0065-2164\(08\)70330-7](https://doi.org/10.1016/S0065-2164(08)70330-7).
- Damm, E., R.P. Kiene, J. Schwarz, E. Falck, and G. Dieckmann. 2008. “Methane Cycling in Arctic Shelf Water and Its Relationship with Phytoplankton Biomass and DMSP.” *Marine Chemistry* 109 (1): 45–59. <https://doi.org/10.1016/j.marchem.2007.12.003>.
- Damm, E., S. Thoms, A. Beszczynska-Möller, E. M. Nöthig, and G. Kattner. 2015. “Methane Excess Production in Oxygen-Rich Polar Water and a Model of Cellular Conditions for This Paradox.” *Polar Science* 9 (3): 327–334. <https://doi.org/10.1016/j.polar.2015.05.001>.
- de Angelis, and M.I. Scranton. 1993. “Fate of Methane in the Hudson River and Estuary.” *Global Biogeochemical Cycles* 7 (3): 509–523.
- Dedysh, Svetlana N., Claudia Knief, and Peter F. Dunfield. 2005. “Methylocella Species Are Facultatively Methanotrophic.” *Journal of Bacteriology* 187 (13): 4665–70. <https://doi.org/10.1128/JB.187.13.4665-4670.2005>.
- Ditchfield, Ak, St Wilson, M. C. Hart, Kj Purdy, Dh Green, and A. D. Hatton. 2012. “Identification of Putative Methylophobic and Hydrogenotrophic Methanogens within Sedimenting Material and Copepod Faecal Pellets.” *Aquatic Microbial Ecology* 67 (2): 151–160. <https://doi.org/10.3354/ame01585>.
- Drake, Harold L., Marcus A. Horn, and Pia K. Wüst. 2009. “Intermediary Ecosystem Metabolism as a Main Driver of Methanogenesis in Acidic Wetland Soil.”

Environmental Microbiology Reports 1 (5): 307–18.

<https://doi.org/10.1111/j.1758-2229.2009.00050.x>.

Duc, Nguyen Thanh, Patrick Crill, and David Bastviken. 2010. “Implications of Temperature and Sediment Characteristics on Methane Formation and Oxidation in Lake Sediments.” *Biogeochemistry* 100 (1–3): 185–96.
<https://doi.org/10.1007/s10533-010-9415-8>.

E. Damm, E. Helmke, S. Thoms, U. Schauer, E. Nöthig, K. Bakker, and R. P. Kiene. 2010. “Methane Production in Aerobic Oligotrophic Surface Water in the Central Arctic Ocean.” *Biogeosciences* 7 (3): 1099–1108.

Eischeid, Anne C. 2011. “SYTO Dyes and EvaGreen Outperform SYBR Green in Real-Time PCR.” *BMC Research Notes* 4 (July): 263–263.
<https://doi.org/10.1186/1756-0500-4-263>.

Fritz, Christian, Veronica A. Pancotto, Josephus T. M. Elzenga, Eric J. W. Visser, Ab P. Grootjans, Arjan Pol, Rodolfo Iturraspe, Jan G. M. Roelofs, and Alfons J. P. Smolders. 2011. “Zero Methane Emission Bogs: Extreme Rhizosphere Oxygenation by Cushion Plants in Patagonia.” *The New Phytologist* 190 (2): 398–408. <https://doi.org/10.1111/j.1469-8137.2010.03604.x>.

Gelesh, Lauren, Kathleen Marshall, William Boicourt, and Laura Lapham. 2016. “Methane Concentrations Increase in Bottom Waters during Summertime Anoxia in the Highly Eutrophic Estuary, Chesapeake Bay, U.S.A.” *Limnology and Oceanography* 61 (S1): S253–66. <https://doi.org/10.1002/lno.10272>.

Grunwald, Maik, Olaf Dellwig, Melanie Beck, Joachim W. Dippner, Jan A. Freund, Cora Kohlmeier, Bernhard Schnetger, and Hans-Jürgen Brumsack. 2009.

“Methane in the Southern North Sea: Sources, Spatial Distribution and Budgets.” *Estuarine, Coastal and Shelf Science* 81 (4): 445–456.

<https://doi.org/10.1016/j.ecss.2008.11.021>.

Guo, Yuedong, Changchun Song, Lili Wang, Wenwen Tan, Xianwei Wang, Qian Cui, and Zhongmei Wan. 2016. “Concentrations, Sources, and Export of Dissolved CH₄ and CO₂ in Rivers of the Permafrost Wetlands, Northeast China.”

Ecological Engineering 90 (Supplement C): 491–97.

<https://doi.org/10.1016/j.ecoleng.2015.10.004>.

Hanson, R. S., and T. E. Hanson. 1996. “Methanotrophic Bacteria.” *Microbiology and Molecular Biology Reviews* 60 (2): 439.

Hayes, J. M. 2001. “Fractionation of Carbon and Hydrogen Isotopes in Biosynthetic Processes.” *Reviews in Mineralogy and Geochemistry* 43 (1): 225–277.

<https://doi.org/10.2138/gsrmg.43.1.225>.

Hoefs, Jochen. 2009. *Stable Isotope Geochemistry*. Springer Science & Business Media.

Hoehler, Tori M., Marc J. Alperin, Daniel B. Albert, and Christopher S. Martens.

1994. “Field and Laboratory Studies of Methane Oxidation in an Anoxic Marine Sediment: Evidence for a Methanogen-Sulfate Reducer Consortium.”

Global Biogeochemical Cycles 8 (4): 451–63.

<https://doi.org/10.1029/94GB01800>.

Holmes, M. Elizabeth, Jeffrey P. Chanton, Malak M. Tfaily, and Andrew Ogram.

2015. “CO₂ and CH₄ Isotope Compositions and Production Pathways in a

Tropical Peatland.” *Global Biogeochemical Cycles* 29 (1): 1–18.

<https://doi.org/10.1002/2014GB004951>.

Holmes, M.E., F.J. Sansone, T.M. Rust, and B.N. Popp. 2000. “Methane Production, Consumption, and Air-sea Exchange in the Open Ocean: An Evaluation Based on Carbon Isotopic Ratios.” *Global Biogeochemical Cycles* 14 (1): 1–10.
<https://doi.org/10.1029/1999GB001209>.

Hopkinson, C.S., and E.M. Smith. 2005. “Estuarine Respiration: An Overview of Benthic, Pelagic, and Whole System Respiration.” In *Respiration in Aquatic Ecosystems*, 122–46. Oxford, UK: P.A. del Giorgio, P.J.L.B Williams (ed.), Oxford University Press.

Im, Jeongdae, Sung-Woo Lee, Sukhwan Yoon, Alan A. DiSpirito, and Jeremy D. Semrau. 2011. “Characterization of a Novel Facultative Methylocystis Species Capable of Growth on Methane, Acetate and Ethanol.” *Environmental Microbiology Reports* 3 (2): 174–81. <https://doi.org/10.1111/j.1758-2229.2010.00204.x>.

K. Malowany, J. Stix, A. Van Pelt, and G. Lucic. 2015. “H₂S Interference on CO₂ Isotopic Measurements Using a Picarro G1101-i Cavity Ring-down Spectrometer.” *Atmospheric Measurement Techniques* 8 (10): 4075–4082.
<https://doi.org/10.5194/amt-8-4075-2015>.

Kaplan, Isaac. 2013. *Natural Gases in Marine Sediments*. Springer Science & Business Media.

- Karl, David M., Lucas Beversdorf, Karin M. Bjorkman, Matthew J. Church, Asuncion Martinez, and Edward F. Delong. 2008. "Aerobic Production of Methane in the Sea." *Nature Geosci* 1 (7): 473–78. <https://doi.org/10.1038/ngeo234>.
- Karl, David M., and Bronte D. Tilbrook. 1994. "Production and Transport of Methane in Oceanic Particulate Organic Matter." *Nature* 368 (6473): 732–734. <https://doi.org/10.1038/368732a0>.
- Karstensen, J., and M. Tomczak. 1998. "Age Determination of Mixed Water Masses Using CFC and Oxygen Data." *Journal of Geophysical Research: Oceans* 103 (C9): 18599–18609. <https://doi.org/10.1029/98JC00889>.
- Keir, Robin S., Jens Greinert, Monika Rhein, Gert Petrick, Jürgen Sültenfuß, and Karin Fürhaupter. 2005. "Methane and Methane Carbon Isotope Ratios in the Northeast Atlantic Including the Mid-Atlantic Ridge (50°N)." *Deep-Sea Research Part I* 52 (6): 1043–1070. <https://doi.org/10.1016/j.dsr.2004.12.006>.
- Kincaid, C. 2012. "The Development and Application of the Full Bay ROMS Hydrodynamic Model for Simulations of Chemical Transport with Multiple Freshwater Sources." *Narragansett Bay Commission Final Report*.
- Kincaid, C., D. Bergondo, and K. Rosenburger. 2003. "Spatial and Temporal Variability in Flow at the Mouth of Narragansett Bay." *Journal of Geophysical Research: Oceans* 108 (C7). <https://doi.org/10.1029/2002JC001395>.
- King, J. Y., W. S. Reeburgh, K. K. Thieler, G. W. Kling, W. M. Loya, L. C. Johnson, and K. J. Nadelhoffer. 2002. "Pulse-labeling Studies of Carbon Cycling in Arctic Tundra Ecosystems: The Contribution of Photosynthates to Methane

Emission.” *Global Biogeochemical Cycles* 16 (4): 10–11–10–18.

<https://doi.org/10.1029/2001GB001456>.

Kirschke, Stefanie, Philippe Bousquet, Philippe Ciais, Marielle Saunois, Josep G.

Canadell, Edward J. Dlugokencky, Peter Bergamaschi, et al. 2013. “Three Decades of Global Methane Sources and Sinks.” *Nature Geoscience* 6 (10): 813–823. <https://doi.org/10.1038/ngeo1955>.

Knief, Claudia. 2015. “Diversity and Habitat Preferences of Cultivated and

Uncultivated Aerobic Methanotrophic Bacteria Evaluated Based on PmoA as Molecular Marker.” *Frontiers in Microbiology* 6: 1346.

Kolb, Steffen, Claudia Knief, Stephan Stubner, and Ralf Conrad. 2003. “Quantitative

Detection of Methanotrophs in Soil by Novel PmoA-Targeted Real-Time PCR Assays.” *Applied and Environmental Microbiology* 69 (5): 2423–29. <https://doi.org/10.1128/AEM.69.5.2423-2429.2003>.

Kosiur, David R., and Ann L. Warford. 1979. “Methane Production and Oxidation in

Santa Barbara Basin Sediments.” *Estuarine and Coastal Marine Science* 8 (4): 379–385. [https://doi.org/10.1016/0302-3524\(79\)90054-9](https://doi.org/10.1016/0302-3524(79)90054-9).

Kreader, C. A. 1996. “Relief of Amplification Inhibition in PCR with Bovine Serum

Albumin or T4 Gene 32 Protein.” *Applied and Environmental Microbiology* 62 (3): 1102–6.

Küsel, K., M. Blothe, D. Schulz, M. Reiche, and H.L. Drake. 2008. “Microbial

Reduction of Iron and Porewater Biogeochemistry in Acidic Peatlands.” *Biogeosciences* 5 (6): 1537–49.

- Lake, Samuel J., and Mark J. Brush. 2015. "Contribution of Nutrient and Organic Matter Sources to the Development of Periodic Hypoxia in a Tributary Estuary." *Estuaries and Coasts; Port Republic* 38 (6): 2149–71.
<http://dx.doi.org.uri.idm.oclc.org/10.1007/s12237-015-9954-2>.
- Lapoussière, Amandine, Christine Michel, Michel Starr, Michel Gosselin, and Michel Poulin. 2011. "Role of Free-Living and Particle-Attached Bacteria in the Recycling and Export of Organic Material in the Hudson Bay System." *Journal of Marine Systems* 88 (3): 434–445.
<https://doi.org/10.1016/j.jmarsys.2010.12.003>.
- LaZerte, Bruce D. 1981. "The Relationship between Total Dissolved Carbon Dioxide and Its Stable Carbon Isotope Ratio in Aquatic Sediments." *Geochimica et Cosmochimica Acta* 45 (5): 647–56. [https://doi.org/10.1016/0016-7037\(81\)90039-9](https://doi.org/10.1016/0016-7037(81)90039-9).
- Lee, Dong Y., Michael S. Owens, Mary Doherty, Erin M. Eggleston, Ian Hewson, Byron C. Crump, and Jeffrey C. Cornwell. 2015. "The Effects of Oxygen Transition on Community Respiration and Potential Chemoautotrophic Production in a Seasonally Stratified Anoxic Estuary." *Estuaries and Coasts* 38 (1): 104–17. <https://doi.org/10.1007/s12237-014-9803-8>.
- Liu, Ze-hua, Hua Yin, Zhi Dang, and Yu Liu. 2014. "Dissolved Methane: A Hurdle for Anaerobic Treatment of Municipal Wastewater." *Environmental Science & Technology* 48 (2): 889–90. <https://doi.org/10.1021/es405553j>.
- Lofton, Dendy D., Stephen C. Whalen, and Anne E. Hershey. 2014. "Effect of Temperature on Methane Dynamics and Evaluation of Methane Oxidation

- Kinetics in Shallow Arctic Alaskan Lakes.” *Hydrobiologia* 721 (1): 209–22.
<https://doi.org/10.1007/s10750-013-1663-x>.
- Loh, Ai Ning, James E. Bauer, and Elizabeth A. Canuel. 2006. “Dissolved and Particulate Organic Matter Source-age Characterization in the Upper and Lower Chesapeake Bay: A Combined Isotope and Biochemical Approach.” *Limnology and Oceanography* 51 (3): 1421–1431.
<https://doi.org/10.4319/lo.2006.51.3.1421>.
- Magen, Cédric, Laura L. Lapham, John W. Pohlman, Kathleen Marshall, Samantha Bosman, Michael Casso, and Jeffrey P. Chanton. 2014. “A Simple Headspace Equilibration Method for Measuring Dissolved Methane.” *Limnology and Oceanography: Methods* 12 (9): 637–650.
<https://doi.org/10.4319/lom.2014.12.637>.
- Martin, Rose, and Serena Moseman-Valtierra. 2015. “Greenhouse Gas Fluxes Vary Between Phragmites Australis and Native Vegetation Zones in Coastal Wetlands Along a Salinity Gradient.” *Wetlands* 35 (6): 1021–1031.
<https://doi.org/10.1007/s13157-015-0690-y>.
- Marty, D.G. 1993. “Methanogenic Bacteria in Seawater.” *Limnology and Oceanography* 38 (2): 452–456. <https://doi.org/10.4319/lo.1993.38.2.0452>.
- Matoušů, Anna, Roman Osudar, Karel Šimek, and Ingeborg Bussmann. 2017. “Methane Distribution and Methane Oxidation in the Water Column of the Elbe Estuary, Germany.” *Aquatic Sciences* 79 (3): 443–458.
<https://doi.org/10.1007/s00027-016-0509-9>.

- Melton, J. R., R. Wania, E.L. Hodson, B. Poulter, B. Ringeval, R. Spahni, T. Bohn, et al. 2013. "Present State of Global Wetland Extent and Wetland Methane Modelling: Conclusions from a Model Inter-Comparison Project (WETCHIMP)." *Biogeosciences* 10 (2): 753–88.
- Middelburg, Jack J., and Peter M. J. Herman. 2007. "Organic Matter Processing in Tidal Estuaries." *Marine Chemistry*, Special issue: Dedicated to the memory of Professor Roland Wollast, 106 (1): 127–47.
<https://doi.org/10.1016/j.marchem.2006.02.007>.
- Middelburg, Jack J., Joop Nieuwenhuize, Niels Iversen, Nana Høgh, Hein de Wilde, Wim Helder, Richard Seifert, and Oliver Christof. 2002. "Methane Distribution in European Tidal Estuaries." *Biogeochemistry* 59 (1–2): 95–119.
<https://doi.org/10.1023/A:1015515130419>.
- Moran, S. B., M. A. Charette, S. M. Pike, and C. A. Wicklund. 1999. "Differences in Seawater Particulate Organic Carbon Concentration in Samples Collected Using Small- and Large-Volume Methods: The Importance of DOC Adsorption to the Filter Blank." *Marine Chemistry* 67 (1): 33–42.
[https://doi.org/10.1016/S0304-4203\(99\)00047-X](https://doi.org/10.1016/S0304-4203(99)00047-X).
- Moskalski, Susanne M., and Christopher K. Sommerfield. 2011. "Suspended Sediment Deposition and Trapping Efficiency in a Delaware Salt Marsh." *Geomorphology*.
- Murrell, J.C., and I.R. McDonald. 2000. *The Desk Encyclopedia of Microbiology*. London: M. Schaechter (ed.), Elsevier Ltd.

- Myhre, G., B. H. Samset, M. Schulz, Y. Balkanski, S. Bauer, T. K. Berntsen, H. Bian, et al. 2013. "Radiative Forcing of the Direct Aerosol Effect from AeroCom Phase II Simulations." *Atmos. Chem. Phys.* 13 (4): 1853–77.
<https://doi.org/10.5194/acp-13-1853-2013>.
- Nozoe, Takuhito. 1997. "Effects of Methanogenesis and Sulfate-Reduction on Acetogenic Oxidation of Propionate and Further Decomposition of Acetate in Paddy Soil." *Soil Science and Plant Nutrition* 43 (1): 1–10.
<https://doi.org/10.1080/00380768.1997.10414709>.
- Oremland, Ronald S. 1979. "Methanogenic Activity in Plankton Samples and Fish Intestines A Mechanism for in Situ Methanogenesis in Oceanic Surface Waters." *Limnology and Oceanography* 24 (6): 1136–1141.
<https://doi.org/10.4319/lo.1979.24.6.1136>.
- Oremland, Ronald S., and Sandra Polcin. 1982. "Methanogenesis and Sulfate Reduction: Competitive and Noncompetitive Substrates in Estuarine Sediments." *Applied and Environmental Microbiology* 44 (6): 1270.
- Osudar, Roman, Anna Matoušů, Mashal Alawi, Dirk Wagner, and Ingeborg Bussmann. 2015. "Environmental Factors Affecting Methane Distribution and Bacterial Methane Oxidation in the German Bight (North Sea)." *Estuarine, Coastal and Shelf Science* 160: 10–21.
<https://doi.org/10.1016/j.ecss.2015.03.028>.
- Parkes, John R., Fiona Brock, Natasha Banning, Edward R.C. Hornibrook, Erwan G. Roussel, Andrew J. Weightman, and John C. Fry. 2011. "Changes in Methanogenic Substrate Utilization and Communities with Depth in a Salt-

- Marsh, Creek Sediment in Southern England.” *Estuarine, Coastal and Shelf Science*.
- Pesch, C.G., E.J. Shumchenia, M. Charpentier, and M.C. Pelletier. 2012. “Imprint of the Past: Ecological History of Greenwich Bay, Rhode Island.” U.S. Environmental Protection Agency.
- Pike, S. M., and S. B. Moran. 1997. “Use of Poretics® 0.7 Mm Pore Size Glass Fiber Filters for Determination of Particulate Organic Carbon and Nitrogen in Seawater and Freshwater.” *Marine Chemistry* 57 (3): 355–360.
[https://doi.org/10.1016/S0304-4203\(97\)00020-0](https://doi.org/10.1016/S0304-4203(97)00020-0).
- Ploug, H., M. Kühl, B. Buchholz-Cleven, and Bb Jørgensen. 1997. “Anoxic Aggregates - an Ephemeral Phenomenon in the Pelagic Environment?” *Aquatic Microbial Ecology* 13: 285–294. <https://doi.org/10.3354/ame013285>.
- Pulliam, William M. 1993. “Carbon Dioxide and Methane Exports from a Southeastern Floodplain Swamp.” *Ecological Monographs* 63 (1): 29–53.
<https://doi.org/10.2307/2937122>.
- Quay, Paul, John Stutsman, David Wilbur, Amy Snover, Ed Dlugokencky, and Tom Brown. 1999. “The Isotopic Composition of Atmospheric Methane.” *Global Biogeochemical Cycles* 13 (2): 445–461.
<https://doi.org/10.1029/1998GB900006>.
- Ramaswamy, V., and C.-T. Chen. 1997. “Climate Forcing-Response Relationships for Greenhouse and Shortwave Radiative Perturbations.” *Geophysical Research Letters* 24 (6): 667–70. <https://doi.org/10.1029/97GL00253>.

- Raposa, K.B., and M.L. Schwartz. 2009. *An Ecological Profile of the Narragansett Bay National Estuarine Research Reserve*. Narragansett, RI: Rhode Island Sea Grant.
- Raymond, Peter A., and James E. Bauer. 2001. "Use of ¹⁴C and ¹³C Natural Abundances for Evaluating Riverine, Estuarine, and Coastal DOC and POC Sources and Cycling: A Review and Synthesis." *Organic Geochemistry* 32 (4): 469–485. [https://doi.org/10.1016/S0146-6380\(00\)00190-X](https://doi.org/10.1016/S0146-6380(00)00190-X).
- Reeburgh, William S. 2007. "Oceanic Methane Biogeochemistry." *Chemical Reviews* 107 (2): 486–513.
- Reeburgh, William S., Bess B. Ward, Stephen C. Whalen, Kenneth A. Sandbeck, Katherine A. Kilpatrick, and Lee J. Kerkhof. 1991. "Black Sea Methane Geochemistry." *Deep Sea Research Part A, Oceanographic Research Papers* 38: S1189–S1210. [https://doi.org/10.1016/S0198-0149\(10\)80030-5](https://doi.org/10.1016/S0198-0149(10)80030-5).
- Repeta, Daniel J., Sara Ferrón, Oscar A. Sosa, Carl G. Johnson, Lucas D. Repeta, Marianne Acker, Edward F. Delong, and David M. Karl. 2016. "Marine Methane Paradox Explained by Bacterial Degradation of Dissolved Organic Matter." *Nature Geoscience* 9 (12): 884–87. <https://doi.org/10.1038/ngeo2837>.
- Rudd, John W. M., and R. D. Hamilton. 1978. "Methane Cycling in a Cutrophic Shield Lake and Its Effects on Whole Lake Metabolism 1." *Limnology and Oceanography* 23 (2): 337–48. <https://doi.org/10.4319/lo.1978.23.2.0337>.
- Ruiz-Villalba, Adrián, Elizabeth van Pelt-Verkuil, Quinn D Gunst, Jan M Ruijter, and Maurice JB van den Hoff. 2017. "Amplification of Nonspecific Products in Quantitative Polymerase Chain Reactions (QPCR)." *Biomolecular Detection*

and Quantification 14 (November): 7–18.

<https://doi.org/10.1016/j.bdq.2017.10.001>.

Russell, J.b. 1992. “Another Explanation for the Toxicity of Fermentation Acids at Low PH: Anion Accumulation versus Uncoupling.” *Journal of Applied Bacteriology* 73 (5): 363–70. <https://doi.org/10.1111/j.1365-2672.1992.tb04990.x>.

Salonen, K., T. Kairesalo, and Roger Jones. 2012. *Dissolved Organic Matter in Lacustrine Ecosystems: Energy Source and System Regulator*. Springer Science & Business Media.

Sansone, F.J., M.E. Holmes, and B.N. Popp. 1999. “Methane Stable Isotopic Ratios and Concentrations as Indicators of Methane Dynamics in Estuaries.” *Global Biogeochemical Cycles* 13 (2): 463–474. <https://doi.org/10.1029/1999GB900012>.

Schmidt, Courtney Elizabeth. 2014. *Investigation of Nitrogen Cycling Using Stable Nitrogen and Oxygen Isotopes in Narragansett Bay, RI*. Thesis PhD-- University of Rhode Island. http://digitalcommons.uri.edu/oa_diss/209.

Schulz, K.G., J. Barcelos e Ramos, R.E. Zeebe, and U. Riebesell. 2009. “CO₂ Perturbation Experiments: Similarities and Differences between Dissolved Inorganic Carbon and Total Alkalinity Manipulations.” *Biogeosciences Discussions* 6 (2): 4441–62.

Schutte, Charles A., Alicia M. Wilson, Tyler Evans, Willard S. Moore, and Samantha B. Joye. 2016. “Methanotrophy Controls Groundwater Methane Export from a

- Barrier Island.” *Geochimica et Cosmochimica Acta* 179 (April): 242–56.
<https://doi.org/10.1016/j.gca.2016.01.022>.
- Scranton, Mary I., Patrick Crill, Marie A. de Angelis, Percy L. Donaghay, and John M. Sieburth. 1993. “The Importance of Episodic Events in Controlling the Flux of Methane from an Anoxic Basin.” *Global Biogeochemical Cycles* 7 (3): 491–507. <https://doi.org/10.1029/93GB00869>.
- Scranton, Mary I., Percy Donaghay, and John Mcn Sieburth. 1995. “Nocturnal Methane Accumulation in the Pycnocline of an Anoxic Estuarine Basin.” *Limnology and Oceanography* 40 (4): 666–672.
<https://doi.org/10.4319/lo.1995.40.4.0666>.
- Scranton, Mary I., and K. McShane. 1991. “Methane Fluxes in the Southern North Sea: The Role of European Rivers.” *Continental Shelf Research* 11 (1): 37–52.
[https://doi.org/10.1016/0278-4343\(91\)90033-3](https://doi.org/10.1016/0278-4343(91)90033-3).
- Segers, Reinoud. 1998. “Methane Production and Methane Consumption: A Review of Processes Underlying Wetland Methane Fluxes.” *Biogeochemistry* 41 (1): 23–51. <https://doi.org/10.1023/A:1005929032764>.
- Semrau, Jeremy D., Alan A. DiSpirito, and Sukhwan Yoon. 2010. “Methanotrophs and Copper.” *FEMS Microbiology Reviews* 34 (4): 496–531.
<https://doi.org/10.1111/j.1574-6976.2010.00212.x>.
- Sieburth, Jmcn, and Pl Donaghay. 1993. “Planktonic Methane Production and Oxidation within the Algal Maximum of the Pycnocline: Seasonal Fine-Scale Observations in an Anoxic Estuarine Basin.” *Marine Ecology Progress Series* 100: 3–15. <https://doi.org/10.3354/meps100003>.

- Sowers, Kevin R., and James G. Ferry. 1983. "Isolation and Characterization of a Methylophilic Marine Methanogen, Methanococcoides Methylophilus Gen. Nov., Sp. Nov." *Applied and Environmental Microbiology* 45 (2): 684.
- Stolyar, S., A. M. Costello, T. L. Peeples, and M. E. Lidstrom. 1999. "Role of Multiple Gene Copies in Particulate Methane Monooxygenase Activity in the Methane-Oxidizing Bacterium Methylococcus Capsulatus Bath." *Microbiology (Reading, England)* 145 (Pt 5): 1235–44.
- Stolyar, Sergei, Marion Franke, and Mary E. Lidstrom. 2001. "Expression of Individual Copies of Methylococcus Capsulatus Bath Particulate Methane Monooxygenase Genes." *The Journal of Bacteriology* 183 (5): 1810–12. <https://doi.org/10.1128/JB.183.5.1810-1812.2001>.
- Sullivan, Benjamin W., Paul C. Selmants, and Stephen C. Hart. 2013. "Does Dissolved Organic Carbon Regulate Biological Methane Oxidation in Semiarid Soils?" *Global Change Biology* 19 (7): 2149–2157. <https://doi.org/10.1111/gcb.12201>.
- Tang, Kam W., Daniel F. McGinnis, Katharina Frindte, Volker Brüchert, and Hans-Peter Grossart. 2014. "Paradox Reconsidered: Methane Oversaturation in Well-oxygenated Lake Waters." *Limnology and Oceanography* 59 (1): 275–284. <https://doi.org/10.4319/lo.2014.59.1.0275>.
- Theisen, Andreas R., M. Hanif Ali, Stefan Radajewski, Marc G. Dumont, Peter F. Dunfield, Ian R. McDonald, Svetlana N. Dedysh, Carlos B. Miguez, and J. Colin Murrell. 2005. "Regulation of Methane Oxidation in the Facultative

- Methanotroph *Methylocella Silvestris* BL2.” *Molecular Microbiology* 58 (3): 682–92. <https://doi.org/10.1111/j.1365-2958.2005.04861.x>.
- Trotsenko, Yuri A., and John Colin Murrell. 2008. “Metabolic Aspects of Aerobic Obligate Methanotrophy.” *Advances in Applied Microbiology* 63: 183–229. [https://doi.org/10.1016/S0065-2164\(07\)00005-6](https://doi.org/10.1016/S0065-2164(07)00005-6).
- Uhlig, C., J. B. Kirkpatrick, S. D’Hondt, and B. Loose. 2017. “Methane Oxidizing Seawater Microbial Communities from an Arctic Shelf.” *Biogeosciences Discuss.* 2017 (October): 1–37. <https://doi.org/10.5194/bg-2017-410>.
- Uhlig, Christiane. 2016. “[Narragansett Bay Methanotrophy].” *Unpublished Raw Data*.
- Uhlig, Christiane, and Brice Loose. 2017. “Using Stable Isotopes and Gas Concentrations for Independent Constraints on Microbial Methane Oxidation at Arctic Ocean Temperatures.” *Limnology and Oceanography: Methods* 15 (8): 737–751. <https://doi.org/10.1002/lom3.10199>.
- Uncles, R., and J. Stephens. 1993. “The Freshwater-Saltwater Interface and Its Relationship to the Turbidity Maximum in the Tamar Estuary, United Kingdom.” *Estuaries* 16 (1): 126–141. <https://doi.org/10.2307/1352770>.
- Valentine, David L. 2011. “Emerging Topics in Marine Methane Biogeochemistry.” *Annual Review of Marine Science* 3: 147–171. <https://doi.org/10.1146/annurev-marine-120709-142734>.
- Valentine, David L., Douglas C. Blanton, William S. Reeburgh, and Miriam Kastner. 2001. “Water Column Methane Oxidation Adjacent to an Area of Active

- Hydrate Dissociation, Eel River Basin.” *Geochimica et Cosmochimica Acta* 65 (16): 2633–2640. [https://doi.org/10.1016/S0016-7037\(01\)00625-1](https://doi.org/10.1016/S0016-7037(01)00625-1).
- Vigneron, Adrien, Andrew Bishop, Eric B. Alsop, Kellie Hull, Ileana Rhodes, Robert Hendricks, Ian M. Head, and Nicolas Tsesmetzis. 2017. “Microbial and Isotopic Evidence for Methane Cycling in Hydrocarbon-Containing Groundwater from the Pennsylvania Region.” *Frontiers in Microbiology* 8 (April). <https://doi.org/10.3389/fmicb.2017.00593>.
- Wanninkhof, Rik. 1992. “Relationship between Wind Speed and Gas Exchange over the Ocean.” *Journal of Geophysical Research: Oceans* 97 (C5): 7373–7382. <https://doi.org/10.1029/92JC00188>.
- Weaver, T. L., and P. R. Dugan. 1972. “Enhancement of Bacterial Methane Oxidation by Clay Minerals.” *Nature* 237 (5357): 518. <https://doi.org/10.1038/237518a0>.
- Weiss, R. F. 1974. “Carbon Dioxide in Water and Seawater: The Solubility of a Non-Ideal Gas.” *Marine Chemistry* 2 (3): 203–215. [https://doi.org/10.1016/0304-4203\(74\)90015-2](https://doi.org/10.1016/0304-4203(74)90015-2).
- Whitehead, K. 2008. “Marine Organic Geochemistry.” In *Chemical Oceanography and the Marine Carbon Cycle*, 262–302. Cambridge, UK: SR Emerson, JI Hedges (ed.), Cambridge University Press.
- Whiticar, Michael J. 1999. “Carbon and Hydrogen Isotope Systematics of Bacterial Formation and Oxidation of Methane.” *Chemical Geology* 161 (1–3): 291–314. [https://doi.org/10.1016/S0009-2541\(99\)00092-3](https://doi.org/10.1016/S0009-2541(99)00092-3).

- Whiting, G. J., and J. P. Chanton. 1993. "Primary Production Control of Methane Emission from Wetlands." *Nature* 364 (6440): 794–95.
<https://doi.org/10.1038/364794a0>.
- Wieczorek, Adam S., Harold L. Drake, and Steffen Kolb. 2011. "Organic Acids and Ethanol Inhibit the Oxidation of Methane by Mire Methanotrophs." *FEMS Microbiology Ecology* 77 (1): 28–39.
- Wilmking, M., Y. Kuzyakov, K. -H. Knorr, and M. Dorodnikov. 2011. "Plant-Mediated CH₄ Transport and Contribution of Photosynthates to Methanogenesis at a Boreal Mire: A ¹⁴C Pulse-Labeling Study." *Biogeosciences* 8 (8): 2365–2375. <https://doi.org/10.5194/bg-8-2365-2011>.
- Wüst, Pia K., Marcus A. Horn, and Harold L. Drake. 2009. "Trophic Links between Fermenters and Methanogens in a Moderately Acidic Fen Soil." *Environmental Microbiology* 11 (6): 1395–1409.
<https://doi.org/10.1111/j.1462-2920.2009.01867.x>.
- Yamamoto, Sachio, James B. Alcauskas, and Thomas E. Crozier. 1976. "Solubility of Methane in Distilled Water and Seawater." *Journal of Chemical & Engineering Data* 21 (1): 78–80. <https://doi.org/10.1021/je60068a029>.
- Yang, Wen-Bin, Chung-Shin Yuan, Chuan Tong, Pin Yang, Lei Yang, and Bang-Qin Huang. 2017. "Diurnal Variation of CO₂, CH₄, and N₂O Emission Fluxes Continuously Monitored in-Situ in Three Environmental Habitats in a Subtropical Estuarine Wetland." *Marine Pollution Bulletin* 119 (1): 289–98.
<https://doi.org/10.1016/j.marpolbul.2017.04.005>.

Yu, Juan, Zhouqing Xie, Liguang Sun, Hui Kang, Pengzhen He, and Guangxi Xing.

2015. “ $\Delta^{13}\text{C}$ -CH₄ Reveals CH₄ Variations over Oceans from Mid-Latitudes to the Arctic.” *Scientific Reports* 5 (1): 13760.

<https://doi.org/10.1038/srep13760>.